

Flow over and around submerged groynes

Numerical modelling and analysis of a groyne flume experiment

L.R. (Lindert) Ambagts

Flow over and around submerged groynes

Numerical modelling and analysis of a groyne
flume experiment

by

L.R. (Lindert) Ambagts

in partial fulfilment of the requirements for the degree of

Master of Science
in Civil Engineering

at the Delft University of Technology,
to be defended publicly on Wednesday June 5th 2019 at 15:45

Thesis committee:	Prof. dr. ir. W.S.J. Uijtewaal,	Delft University of Technology
	Dr. ir. E. Mosselman,	Delft University of Technology & Deltares
	Dr. ir. R. J. Labeur,	Delft University of Technology
	Dr. ir. C. J. Sloff,	Delft University of Technology & Deltares
	Dr. ir. M.F.M. Yossef,	Deltares

An electronic version of this thesis is available at <http://repository.tudelft.nl/>.

Cover: Aerial photo of the River IJssel near Doesburg. Source: <https://beeldbank.rws.nl>, Rijkswaterstaat / Joop van Houdt

Preface

Before I was one year old the flood of January 1995 made an island of my home. I lived with my parents on a small farm in the countryside near the village Wilp which is located near the River IJssel. The farm is situated on a terp and my parents chose not to evacuate together with 250.000 people but stay on the farm. For the rest of my youth I lived on that beautiful place close to the River IJssel, cycling over the summer dike every day to Deventer to my primary school. My high school was in Zutphen so I still cycled along the IJssel every day albeit in the other direction. On windy or long school days my appreciation for the cycling along the river might not have been so large. But in retrospect I really appreciate this and it must have had a strong influence on my choices looking at what I have been studying during my time in Delft. So for me to study rivers and groynes for my thesis was a beautiful opportunity. Therefore I am very glad that I can contribute to the field of River Engineering.

I want to express my gratitude to my thesis committee for their feedback and suggestions which made it possible for me to conclude my Master of Science in Civil Engineering with the specialisation 'Hydraulic Engineering' at the Delft University of Technology. Also I want to thank Harmen Talstra for his support and very bright ideas concerning Finel. And Frank Platzek for his hard work to make the experimental data from BAW available for my thesis. I am also very thankful to my father who helped me a lot. Also my fellow students at Deltares and especially my friends were of great help during this process.

Finally I want to Thank the BAW for providing me with the valuable data and Deltares and Svašek for the working place and support.

*L.R. (Lindert) Ambagts
Delft, May 2019*

Summary

Groynes are used in river training with the goal of minimising bank erosion, preventing ice jamming and increasing navigable depth. During a flood the groynes become submerged and add resistance, thereby increasing the water level for a particular discharge. To predict the water levels during a design flood numerical models are used. Groynes can be modelled in different ways, either they are included in the bed topography when the resolution is sufficiently high or, with a sub-grid parametrisation when the grid cell-size is larger than the geometry of the groyne. For the Dutch branches of the River Rhine a two-dimensional model with sub-grid weir formulations as parametrisations for groynes is used to evaluate river training measures such as lowering, streamlining or shortening groynes. The research questions of this study are: "how does the flow structure over and around a submerged groyne look like and to what extent is this analogous to a weir?", Thereafter the question is: "how is this implemented in numerical models and how accurate are groyne adaptations modelled?"

In this research valuable data from a flume experiment with groynes provided by the BAW is analysed and the experimental set-up is subsequently modelled with Delft3D and Finel. The data is analysed to investigate how the flow structure over and around groynes is and to see how it compares to a weir. Numerical models are used to simulate the experiment both in 2DH with sub-grid weirs and in 3D non-hydrostatic with groynes included in the bed topography. The BAW data is used to carefully calibrate the models.

From the data analysis it becomes clear that the stronger the submergence the more lateral influence there is over the groyne, so the less it behaves as a single weir. More discharge is going over the groyne near the tip and less near the side wall of the flume. The flow over the smooth concrete groynes, as used in the BAW experiment, separates at the leading edge of the crest, leading to a separation zone that is higher than the groyne height.

The results of the numerical models show that both the 3D non-hydrostatic and 2DH sub-grid weir models underestimate the resistance of the submerged groynes compared to the measurements. The 3D model performs better than the 2DH model, especially concerning the discharge distribution between the main channel and the groyne field. The underestimation of the resistance leads to lower water levels or larger discharge capacity. Because the energy losses over the groynes are underestimated the flow velocity in the groyne field is too high. This decreases the resistance due to the horizontal mixing layer that forms between the higher flow velocities in the main channel and the lower flow velocities in the groyne fields. The 3D Delft3D model does not resolve the leading edge flow separation and the flow velocity in the groyne field does not decelerate as much as measured. In Finel local refinement of the grid showed better leading-edge flow separation. To improve the accuracy of the modelled acceleration due to leading-edge separation and deceleration downstream of the groyne, the flux limiter provided by Finel (suppressing overshoots around steep gradients) is adapted to allow for some local overshoots near the bed level (on behalf of slightly steeper bottom boundary layer gradients). The sub-grid weirs have the same problem as the 3D non-hydrostatic Delft3D model, as the height of the weir is used to calculate the deceleration losses and not the actual height of the separation zone.

The comparison of the influence of groyne adaptations (lowering or streamlining) between the 2DH and 3D model shows that the 2DH model including sub-grid weirs results in a larger effect on the upstream water level. The underestimation of the energy losses due to the sub-grid weirs leads to a larger fraction of the discharge affected by the lowering. Streamlining is modelled in the Delft3D 3D non-hydrostatic model only and shows a similar effect on the upstream water level as the lowering of the groynes by 1/8 of their height.

The implications of these findings on a full-scale river reach, including sloping and sedimented groyne fields, floodplains, rough groynes, smaller relative length of the groynes and bends, are difficult to estimate. In this experiment the effects of the groynes are larger than in reality, so they provide an upper boundary.

Contents

1	Introduction	1
1.1	Research context: Groyne modelling and Room for the River	1
1.2	Problem statement: Uncertainties in groyne modelling.	3
1.3	Objective and research questions: Insight in flow over groynes	3
1.4	Methodology: Laboratory data analysis and numerical modelling	3
2	Literature study of groynes and river modelling	4
2.1	River training and groynes	4
2.2	Flow around emerged groynes	5
2.3	Flow over and around submerged groynes	6
2.4	Analogy between groynes and weirs.	7
2.5	Groyne resistance	8
2.6	Groynes in numerical models	9
2.6.1	Numerical modelling	9
2.6.2	Groyne modelling	10
2.6.3	Conclusion.	11
3	Data Analysis of the BAW groyne flume experiment	12
3.1	BAW groyne flume experiment	12
3.2	Experimental set-up: A 70 m long 2.5 m wide flume.	12
3.3	Approach: Flow patterns over a groyne	13
3.4	Results: Data analysis of the groyne experiment	13
3.5	Water levels	13
3.6	Velocity	17
3.6.1	Mixing layer	20
3.6.2	Vertical velocity profiles	21
3.7	Discharge distribution	22
3.8	Conclusion: Is the flow over a groyne weir like?	23
4	Numerical modelling of the groyne flume experiment	25
4.1	Numerical model setup	25
4.2	Approach: Steps to compare model performance.	26
4.3	Results: Delft3D Numerical modelling of groyne experiment	27
4.3.1	Uniform flow: V00 case	27
4.3.2	Flow around and over groynes: V01 case	27
4.3.3	Discharge boundary: Upstream water levels compared	28
4.3.4	Water level boundary: Total discharge compared	29
4.3.5	Water level boundary: Discharge distribution	29
4.4	2DH Modelling: Delft3D	30
4.4.1	2DH Coarse grid: sub-grid weirs	30
4.4.2	2DH Fine grid	30
4.4.3	Conclusions 2DH models	32
4.5	3D and 2DV modelling	33
4.5.1	3D Non-hydrostatic: Delft3D	33
4.5.2	3D Hydrostatic: Delft3D	38
4.5.3	3D Non-hydrostatic: Finel	39
4.5.4	2DV and 1D: Delft3D: Groyne vs. weir comparison.	41
4.5.5	Conclusions 3D models	43
4.6	Conclusions on numerical models	45

5	Groyne adaptations	47
5.1	Lowering	47
5.2	Streamlining	49
5.3	Conclusions on groyne adaptations.	51
6	Discussion	54
6.1	BAW groyne experiment: Materials and geometry.	54
6.2	Numerical models: Limitations and modelling choices	55
6.3	Scale effects and real geometry	56
7	Conclusions and recommendations	58
7.1	Conclusions.	58
7.2	Recommendations	60
	Bibliography	61
A	Theoretical roughness	65
B	Discharge coefficient analysis	68

Introduction

The background from which this research originates is described in the first section. In Section 1.2 the problem is stated. Thereafter in section 1.3 the research questions are presented. Finally a brief description of the methodology is shown in Section 1.4.



Figure 1.1: Groynes in the River IJssel near Deventer (Photo: Lindert Ambagts)

1.1. Research context: Groyne modelling and Room for the River

Groynes are structures transverse to the principal flow direction of a river. They protrude into the main channel, blocking part of the wet cross-section and confining the flow. Groynes, among other measures (Przedwojski et al., 1995), are used widely for river training. The main objectives of river training are: flood protection, minimising bank erosion, aligning the river channel, decrease the risk of ice jamming and improving the navigable depth (Yossef, 2002). Groynes decrease the cross-sectional area, therefore the flow velocity and specific discharge increase for a given discharge. This increased flow velocity erodes the bed which increases the navigable depth. During average discharge conditions the groyne crests are emerged and the groyne fields do not contribute to the conveyance of water. This is because the flow separates from the groyne tip and the separation zone covers the whole groyne field. In the separation zone the flow recirculates because momentum is exchanged by the eddies that shed off from the groyne tip and the mixing layer.

When the discharge and consequently the water level are increased the groynes become submerged. The horizontal separation zone, and the accompanying recirculation cell vanish (Uijttewaal, 2005; Yossef, 2005; Sukhodolov, 2014). The groyne fields start contributing to the conveyance of water. When the streamlines cannot follow the downstream slope of the groyne the flow separates from the groyne crest. A vertical separation zone behind the groyne is formed in which the water recirculates. Still there is a mixing layer between the flow in groyne fields with a low velocity and the faster flow velocity in the main channel. In this mixing layer momentum is transferred laterally. In the submerged situation the groynes act as an unwanted obstruction to the flow. They exert a drag force on the flow and therefore lead to an increase in water level (Azinfar and Kells, 2009). This leads to higher water levels in the situation with groynes compared to a situation without groynes. To mitigate this negative effect measures such as lowering, shortening and streamlining of groynes can be implemented. Energy is lost for both emerged and submerged groynes. Energy loss means irreversible transfer from kinetic energy to heat. Energy is dissipated by turbulent mixing due to velocity gradients and deceleration of the flow.

In the Dutch Room for the River programme various river training measures have been implemented to decrease the water levels during a design flood (Sijmons et al., 2017). This is done by literally giving the river more room. For example: floodplains have been excavated, dikes have been relocated, obstacles have been removed and side channels have been constructed. Also adaptations to groynes have been made, they have been lowered and directed slightly downstream. In the past a lot of changes to groynes have been investigated. For example: changing the layout, lowering, as well as streamlining groynes (e.g. Ogink and Driegen 1984; Mosselman and Struiksma 1992; Bloemberg 2001; van der Wal 2004; van der Wal et al. 2006; Anlauf and Hentschel 2007; van Broekhoven 2007; Zagonjoli et al. 2017; Zagonjoli 2017; Yossef 2017). An example of the measures from Room for the River and innovative groyne design is visible in Figure 1.2. This design was chosen as the winner of a design competition 'Kribben van de Toekomst' (Groynes of the Future) in 2006 (Klaassen et al., 2006).



Figure 1.2: Innovative island groynes in the River IJssel at Deventer during extreme low water levels in July of 2018. In the background, under the railway bridge and at the left the excavated floodplains, constructed for Room for the River, are visible (Photo: Lindert Ambagts)

In earlier days physical modelling was necessary to evaluate the effect and performance of this kind of river training measures and computing power was limited. Today numerical models are used to quantify the effect of the proposed measures and changes to the river system. The branches of the River Rhine are modelled depth averaged (2DH) with a grid resolution of 40 m in flow direction and 20 m over the width (RWS-WVL, 2017). The groynes in the Dutch rivers typically have a length between 50 and 80 m, a crest width of 2 m and a crest height with respect to the main channel bed level of 6 m. This means that the grid is too coarse to include the groynes in the bed topography. In order to overcome this limitation a sub-grid parametrisation of the effect of groynes on the flow is necessary. This is done by adding the parameterised energy losses, calculated with the weir formulas, to the momentum equations. The accuracy of the numerical models depends on various parameters:

- Schematisation of the geometry
- Main channel roughness
- Roughness of the floodplains
- Roughness of the groyne fields
- Energy losses due to deceleration
- Turbulent momentum exchange (turbulent viscosity coefficient)
- Extrapolation to extreme water levels

The performance and predictive power of the models depend on the accuracy of the above mentioned parameters. Thus the assumptions made with respect to these parameters have to be accurate and valid for the situations they are applied to (Warmink et al., 2013). Especially the roughness is important, because the models are calibrated to fit a measured water level for a given discharge by adjusting the roughness parameters (Straatsma and Huthoff, 2011). Warmink et al. (2010) found that the calibrated roughness is smaller than the roughness predicted using formulas that relate the bed form height to hydraulic roughness. This might imply that roughness due to vegetation and groynes is overestimated. If the roughness of the main channel is underestimated the effect of shortening, lowering or removing groynes is overestimated. This would result in an optimistic estimate of the discharge capacity or water level. This means that it is important to know how much energy is dissipated by the groynes and which fraction of the discharge flows through over the groynes. In order to understand this, the flow over and around submerged groynes has to be understood. This in order to evaluate how the flow can be modelled to improve the certainty and accuracy of groynes in numerical models.

1.2. Problem statement: Uncertainties in groyne modelling

The qualitative effects of groyne adaptations, such as lowering, streamlining or removing, are known. However, quantifying the effects with high accuracy in numerical models is uncertain. Especially in river models that cover a large area with groynes as sub-grid weirs when extrapolating to extreme discharges. When the goal is to determine design flood levels.

1.3. Objective and research questions: Insight in flow over groynes

The goal of this research is to gain insight in the flow over and around strongly submerged groynes. In order to determine the processes that influence the resistance of groynes to flow during floods. And subsequently to evaluate whether the effects of essential physics are captured in 2DH numerical models in which groynes are parameterised as sub-grid weirs.

Data from a laboratory experiment carried out by the Bundesanstalt für Wasserbau (BAW) are analysed and the experiment is modelled with different numerical models in order to answer the following research questions:

- What is the 3D flow structure over and around the groyne in highly submerged conditions?
To what extent does a groyne behave as a weir?
- What processes influence energy losses over a groyne?
And how do these losses differ from a weir?
- How well are these processes represented on a 2DH coarse-grid model where groynes are represented by sub-grid weir formulas and in 3D non-hydrostatic models?
- How well are groyne adaptations modelled by the numerical models?

1.4. Methodology: Laboratory data analysis and numerical modelling

- What needs to be done in order to answer the research questions and complete the objective?

First literature is studied to gain insight in:

- The flow over and around groynes.
- The state of the art in the numerical modelling of groynes.
- Problems in determining the resistance of groynes.

Next, data from the physical experiment of the BAW are analysed in order to compare the behaviour of a groyne to a weir.

Thereafter the experimental set-up of the BAW is modelled to gain insight in the performance of numerical models. This is done by comparing the model results with the data and comparing the sub-grid modelled groynes with groynes that are represented in the bed topography. After that the groynes in the numerical models are lowered (2DH and 3D) and stream lined (3D)

Finally conclusions are drawn by answering the research questions and recommendations for further research are given.

Literature study of groynes and river modelling

In this chapter additional background on groynes and the modelling of groynes in river model is presented. The literature on hydrodynamics in rivers with groynes is studied and the theoretical background is highlighted and important physical processes that influence the resistance are presented.

2.1. River training and groynes

Lowland rivers are trained with the objective to stabilise the main channel and maintain a sufficient depth for navigation. Other purposes are: to increase safety against flooding, minimise bank erosion and prevent ice jamming. For a more complete description of river training see Mamak 1964; Jansen et al. 1979; Przedwojski et al. 1995. During the recent centuries dikes have been reinforced and relocated and groynes have been constructed. After the flood waves at the end of the 20th century the notion was formed that possibly the river was being constricted too much. In order to increase the safety against flooding and stimulate flora and fauna habitats, the Room for the River Programme was initiated in the Dutch branches of the Rhine River. This programme includes a variety of river training measures, see fig 2.1.

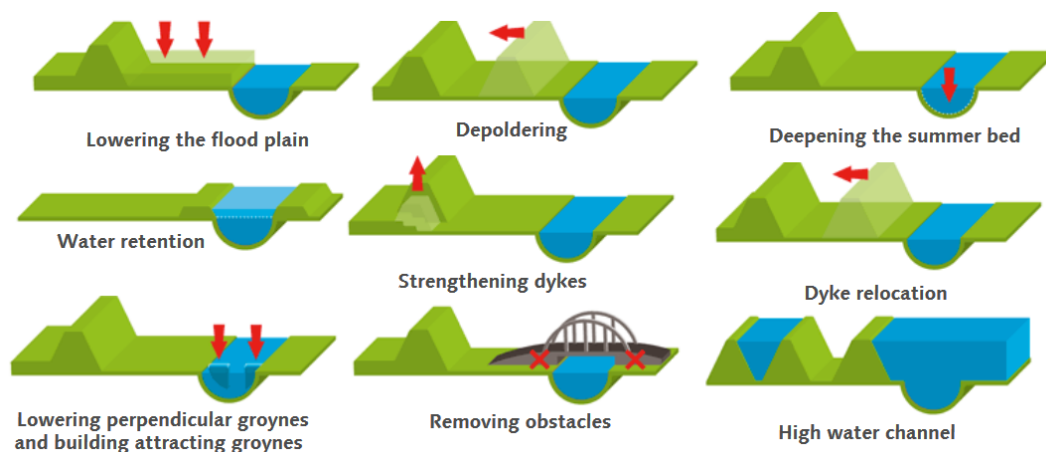


Figure 2.1: Measures implemented for Room for the River (Sijmons et al., 2017)

These interventions have in common that they provide the river more space and decrease flow resistance. The less resistance the flow experiences the lower the water level for a particular discharge. The two interventions involving groynes are the most important for this research. Concerning these interventions a couple of questions arise (Yossef, 2016):

- What is the effect of lowering groynes?
- What is the effect of streamlining groynes?
- How can this be modelled?

The essence of the current research lies in these questions. That is because the factors that influence the resistance of groynes are difficult to isolate and quantify in the complex flow situation of a river reach including groynes and floodplains.

Groynes are transverse structures that protrude from the river bank into the main channel. They create a constriction that leads to smaller flow carrying cross-section. This in turn leads to higher flow velocities that increase the erosion capacity of the flow. Groynes are made of gravel, (natural) rock or prefabricated concrete elements, sand and sometimes geotextile. Groynes are made of piles when it is not feasible to use rock, for instance in very large rivers or when transport of rock is too expensive.

There are various types of groynes, permeable or non-permeable, submerged or emerged, attracting, deflecting or repelling. The geometries are varied in practice: T-shaped, L-shaped, curved, etc. These types have similar purposes but they serve different local goals. Permeable groynes are used to decrease the blocking effect, attracting groynes are directed downstream in order to attract the flow towards the river bank. Repelling groynes point upstream to divert the flow to the other bank. The shape of the groyne tip is most often adjusted to prevent the adverse effects locally. An L-groyne or island groyne deflects the local sedimentation area (groyne flame) that forms downstream of the local erosion pit more to the banks (Sieben, 2009; Albers, 2016).

Besides the orientation and layout more design parameters can be altered. The length of the groyne is determined by the required cross-section, the spacing, and desired length that has to protrude into the bank to prevent outflanking. The spacing between subsequent groynes depends on the river width, groyne length, flow velocity and angle with the bank. Groynes have a typical length between 50 m and 80 m, the distance between groynes is around 200 m. The crest height is on the same level as the floodplains sloping down towards the main channel in order to save construction material (Bouwmeester, 1987). See Figure 2.2 for an example of the layout of a typical Dutch river groyne.

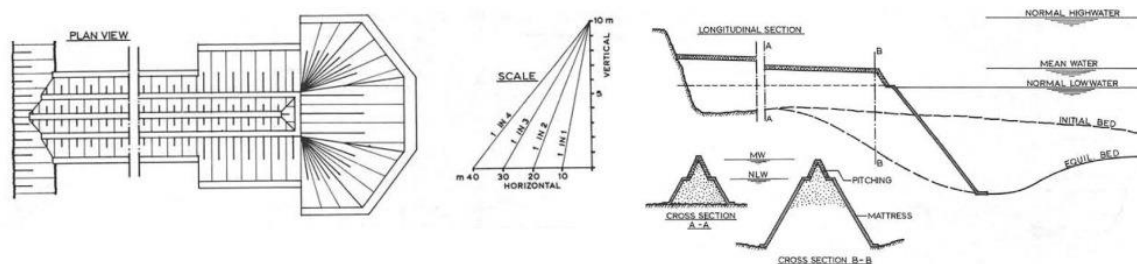


Figure 2.2: Example groyne layout (Jansen et al., 1979)

The cross-section of a groyne is characterised by the crest width and slope angles. A minimum crest width of 1 m is used for construction purposes and the slope angles range from 1:1.5 to 1:5 (V:H). A final design consideration is the expected scour depth. The base of the groyne should be deep enough to guarantee stability.

2.2. Flow around emerged groynes

To understand what processes influence the resistance of a groyne it is important to understand the characteristics of flow around groynes. Groynes are emerged except during floods. When emerged the discharge is conveyed through the main channel and momentum is exchanged between the main channel and the groyne fields. Much research has been done to investigate the emerging hydrodynamic flow patterns around groynes. The following flow patterns are the most important:

- Separation zone
- Vortex street
- Horizontal recirculation zone (primary eddy)
- Dynamic eddies
- Secondary eddy

This is visualised in Figure 2.3

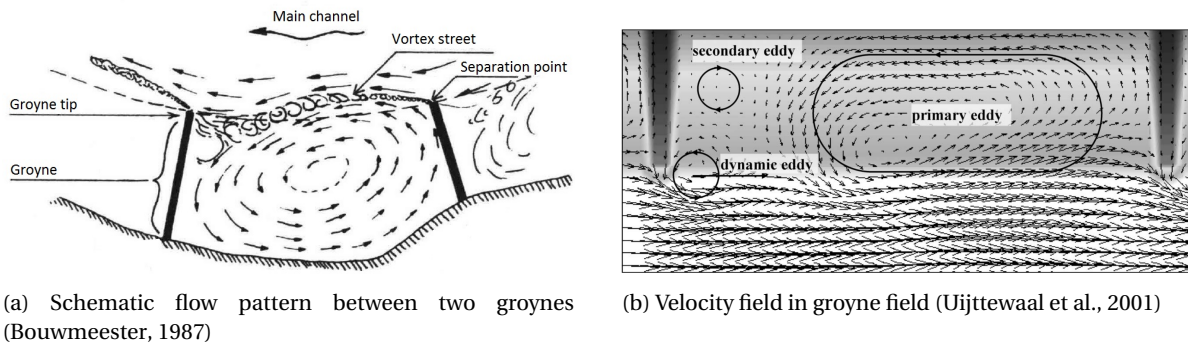


Figure 2.3: Flow around emerged groynes in (2.3a) a schematic drawing and (2.3b) results from Particle Tracking Velocimetry (PTV) in a laboratory experiment.

In a case with one groyne in a straight channel the groyne confines the flow, increasing the velocity and specific discharge. At the groyne tip the flow velocity is increased due to the constriction. The flow separates from the groyne tip creating a vortex street from which eddies shed and a separation zone behind downstream of the groyne is formed. At the separation point the flow deflects towards the centre axis of the river. Downstream, where the influence of the groyne decreases the flow is directed towards the bank. In the separation zone, one or two eddies are formed. The primary and largest eddy stretches downstream up to 5 or 6 times the groyne length depending on the flow velocity and geometry of the groyne (Francis et al., 1968; Rajaratnam and Nwachukwu, 1983). The smaller secondary eddy is located in the corner near the bank and the groyne just downstream of the groyne (Uijttewaal et al., 2001). The velocity gradient between the main channel and the groyne field induces to a turbulent mixing layer in which free turbulence exchanges momentum (Nieuwstadt et al., 2016). This layer gets closer to the side wall and hits the wall in the reattachment point.

These flow patterns depend on the geometry of the groyne, the orientation and geometry of the channel. But also the discharge and subsequent flow velocity have an influence on the location of the reattachment point and formation of secondary eddies. The mixing layer that exchanges mass and momentum has been researched extensively (e.g. Uijttewaal and Tukker 1998; van Prooijen 2004; Talstra 2011).

The distance between groynes (spacing) is in general too small for the flow to reattach to the banks. Therefore the flow is concentrated at a distance from the banks at moderate and low discharges. The velocity gradient between the main channel and groyne fields drives a recirculation cell in the separation zone analogous to the single groyne case. Depending on the groyne layout one or two horizontal eddies develop. If the groyne field is longer, i.e. the groyne spacing is larger, a secondary eddy is formed. Between the main channel and the groyne field exchange of momentum takes place due to the dynamic eddies in the vortex street. This adds to the resistance and therefore influences the water level in the river. In the groyne fields the water level slope is smaller than that of the main channel. Uijttewaal et al. (2001) found that these dynamic eddies contribute more to the momentum exchange compared to a stable mixing layer formed in a velocity gradient.

2.3. Flow over and around submerged groynes

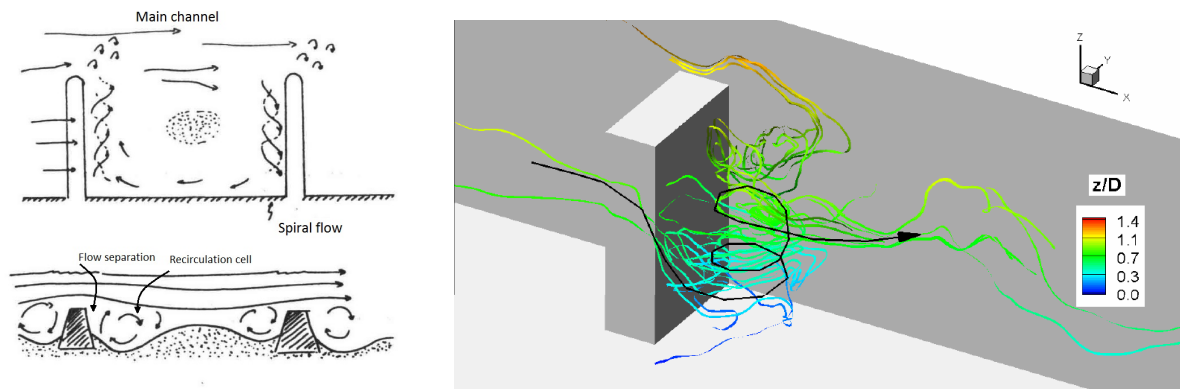
During increasing discharge the water level in the river rises. At a particular discharge the groynes become submerged, consequently the flow patterns in the groyne fields will change. This changes the exchange of momentum and mass between the groyne field and the main channel (Yossef, 2004; Uijttewaal, 2007). The submerged groynes constrict the flow not only in the horizontal direction but they also block part of the cross-sectional area in the vertical direction. This blocking of the flow results in energy losses and resistance to the flow leading to an increase in water level. So during high discharges the groynes should be as low and short as possible in order to minimise their resistance.

In the vicinity of the crest the flow velocity is highest. Due to the short crest of a groyne the streamlines are directed upwards leading to an area of decreased pressure just above the crest. Therefore the flow velocity in the vertical is highest just above the crest (Jongeling, 2005; Baron and Patzwahl, 2013). The water that flows over the crest has two possible modes. In the first the streamlines follow the downstream slope. The expansion of the flow and advection of momentum occur over the whole water depth. At a particular downstream water level and sufficient discharge a hydraulic jump occurs (Wols, 2005). In the second mode the flow separates from the crest forming a separation zone behind the groyne (Heijer et al., 1997). In this separation zone

the flow recirculates around a horizontal axis. See Figure 2.4 for a schematic drawing and an example of a numerical simulation of this recirculation zone. In this recirculation cell the pressure is lower compared to the hydrostatic pressure distribution.

The first mode would result in a lower resistance compared to the second mode because more energy is dissipated in a separation zone. The velocity gradient between the eddy and the flow in the groyne field deforms streamlines and induces vortices. These vortices grow, are advected by the flow, merge and finally damp out. During this damping the kinetic energy is transformed into heat and pressure head. They contribute to the redistribution of kinetic energy. They decrease the velocity differences by momentum exchange.

The underpressure in the vertical recirculation cell also attracts water from the main channel. The water that flows around the groyne tip experiences a suction towards the groyne field over the height of the recirculation cell according to Jongeling et al. (2010).



(a) Schematised flow pattern between two groynes (Bouwmeester, 1987)

(b) Instantaneous streamlines in 3D behind a single groyne (McCoy, 2006)

Figure 2.4: Flow around submerged groynes in (2.4a) a schematic drawing and (2.4b) results from 3D LES simulations with 2 rectangular submerged groynes.

2.4. Analogy between groynes and weirs

The flow patterns over submerged groynes resemble flow over a drowned weir. The same processes influence the energy loss in the case of a weir, namely: deceleration losses. However, fundamental differences exist. The most important one is that the groyne fields are connected with the main channel and the floodplains. Therefore the discharge and water level in the groyne fields depend on the combined effect of flow over and around the groyne. The flow in the main channel and the floodplains has a different velocity than the flow through the groyne fields leading to mixing layers that contribute to the dissipation of energy.

For weirs numerous laboratory experiments have been carried out during the last century (e.g. Villemonte 1947; Fritz and Hager 1998; Bloembergen 2001; Wirken and Bladel 2004; Stolker 2005; Ali and Uijtewaal 2013). Based on these experiments formulas are found that describe the discharge over a groyne with given water levels. The influence of the slope, crest length and height, vegetation, orientation, etc. is quantified in various formulas (Kruijt, 2013). Changing the downstream slope or submergence level of the weirs influences the energy losses over a weir. That results in different water levels for the same discharge. The characteristics of flow over a weir are that the flow is two dimensional (2DV). See Figure 2.5 for a schematic representation of a weir with the parameters that are needed to analytically calculate the energy loss over a weir. So if groynes have a uniform distribution of discharge, velocity and water level over the crest that would indicate that there is a part that behaves as a weir.

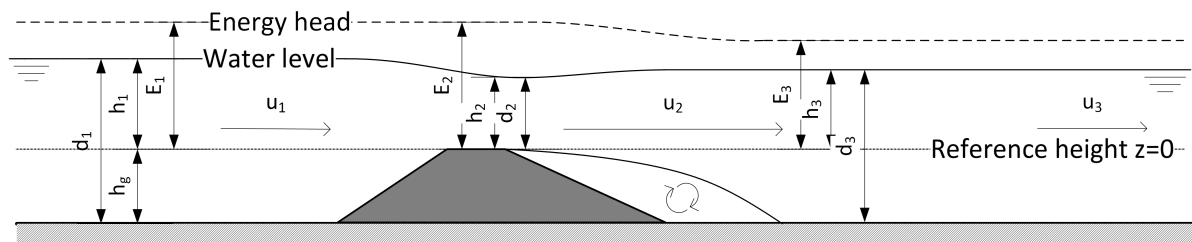


Figure 2.5: Schematic drawing of a weir and the relevant parameters.

Fundamental differences between a weir and a groyne are:

- Water can flow around a groyne
- Momentum can be exchanged between the flow through the groyne fields and the main channel and floodplains
- Groyne crests are not horizontal (crest slopes down towards main channel) and the bed in groyne fields is not horizontal
- Near the groyne tip underpressure could attract flow from main channel
- In bends groynes are at an oblique angle with the flow direction

The geometry of groynes influences the streamlines over and around the groyne, and subsequently the discharge head loss relation. River groynes are constructed with side slopes that are steep enough for the flow to separate and form a vertical recirculation cell. Due to the underpressure (compared to hydrostatic pressure) in that cell water from the main channel is attracted. The 'inflow' of water decreases the underpressure compared to a weir with the same geometry properties, especially near the groyne tip. The area of influence of the tip depends on the groyne geometry. It is thought that downstream of a groyne the underpressure is weaker than the underpressure downstream of a weir. Therefore the streamlines are less curved than in the situation of a weir (Jongeling et al., 2010). In general the larger a recirculation cell and the higher the velocities the more energy it dissipates (Han, 2015). This would indicate that a groyne would have less energy dissipation than a weir with the same geometry.

2.5. Groyne resistance

Because groynes are obstacles to the flow they increase the water level during high discharges. The resistance of a groyne depends on various parameters. Energy is dissipated at several locations. This is visualised in Figure 2.6. The dissipation of energy is the transfer from kinetic energy into heat and potential energy. This happens when turbulent eddies are formed, for instance when flows expand and a separation zone is formed. This happens due to the following processes:

- 1) Deceleration losses due to flow expansion over the recirculation cell downstream of the groyne.
- 2) Momentum and mass exchange between main channel and groyne field.
- 3) Eddies shedding from tip in vortex street.
- 4) Water flows around groyne tip.
- 5) Momentum exchange between groyne field and flood plain (not in BAW experiment).
- 6) Geometry of the groyne (Constant in BAW experiment).
- 7) Roughness of the groyne material/vegetation (not in BAW experiment).
- 8) Roughness of groyne field (Constant in BAW experiment).
- 9) Roughness of floodplain.

The horizontal mass and momentum exchange between the main channel and groyne field is what distinguishes groynes from weirs. The horizontal exchange is governed by the turbulent mixing layer that emerges between flows with different flow velocities. The mixing decreases the gradient in the velocity and thereby energy is dissipated. Dissipation is characterised with a certain mixing length. The mixing length depends on the width of the mixing layer and a proportionality constant (van Prooijen, 2004). The width of the mixing layer is defined as the distance between two regions of different velocity divided by the maximum velocity gradient (Uijtewaal and Booij, 2000). In the vertical separation zone energy is dissipated downstream of the groyne where the flow expands as described in Section 2.3.

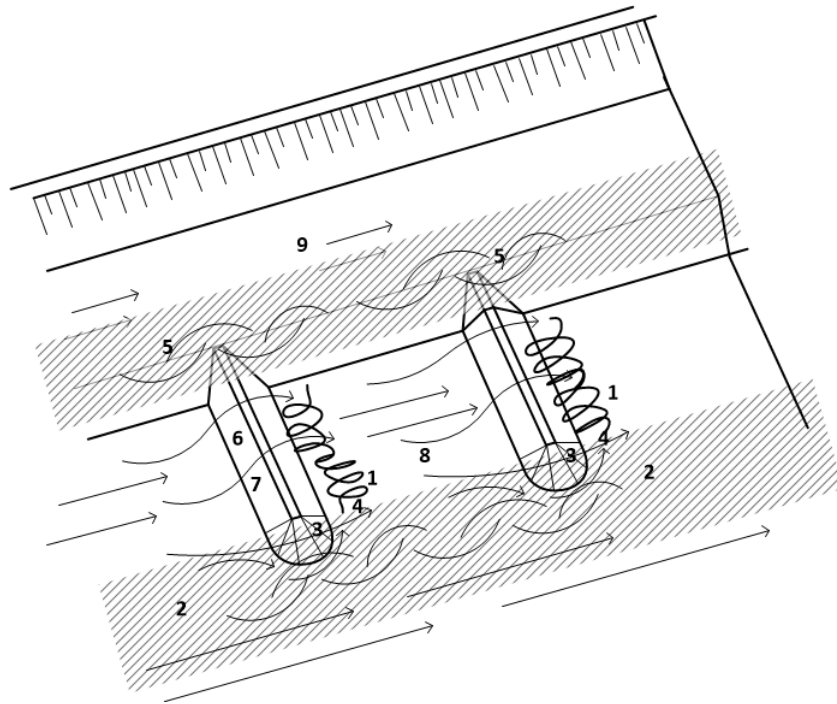


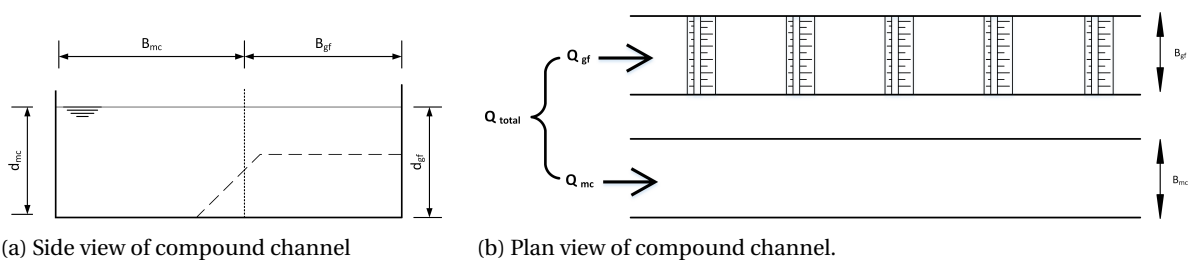
Figure 2.6: Schematic drawing of flow structures for submerged groyne flow

2.6. Groynes in numerical models

2.6.1. Numerical modelling

Traditionally laboratory experiments were used to investigate the effect of river training measures on a scale where numerical models were not feasible or did not even exist. Nowadays rivers are modelled numerically in 1D, 2DH, and 3D. Occasionally laboratory experiments are used to validate numerical models or when particular flow situations are of interest. The way groynes are incorporated in numerical models differs between the model types.

To calculate the water levels and flow velocities for a given discharge in one dimension (1D), the river is characterised with a bed level, width and a roughness. The groynes can be included in this roughness but it is also possible to separate the groyne fields and main channel (see Figure 2.7) and assign different values for the aforementioned parameters. This method is called a 1D compound channel and can be used only in the situation when groynes are submerged (van Leeuwen, 2006). This is the least computationally intensive method. The groynes in the groyne field channel can be modelled in two ways: as roughness elements or as weirs (Yossef, 2005). There are many formulas that describe the discharge head loss relation over a weir as well as for groynes as roughness elements. These formulas are summarised by van Leeuwen (2006) and Kruijt (2013). These formulas have a slightly different range for which they have been validated and different sensitivity to used parameters. This gives a variety in results and Kruijt (2013) raises doubts on the validity of the formulations for groynes because the formulas have unwanted scaling with certain parameters, especially in strongly submerged conditions.



(a) Side view of compound channel

(b) Plan view of compound channel.

Figure 2.7: Side and plan view of a schematic 1D compound channel. The main channel and groyne field can have different roughness parameters

In depth averaged two dimensional (2DH) models groynes can be modelled in two ways. Groynes can be represented in the bed topography when the grid resolution is sufficiently high. When coarser computational grids are used the resulting energy loss can be parameterised and added to the momentum equations on grid cell interfaces. In 2D models variations in velocities and water levels in the horizontal plane are accounted for. In the vertical only the depth averaged velocity is computed. This means that the influence of non-hydrostatic pressure effects is not taken into account. Therefore the effect of the geometry, the recirculation in the vertical, and subsequently the energy loss, cannot be resolved. The energy loss depends also on the numerical discretisation of the advection terms. Schemes can be energy or momentum conservative for contracting or expanding flows. In the case of decelerating flow momentum should be conserved while for accelerating flows energy is conserved (Stelling and Duinmeijer, 2003). In 2DH simulations the horizontal viscosity is of large importance because it determines the horizontal mixing of momentum. Some models have the option to compute the eddy viscosity dynamically. This is called horizontal large eddy simulation (HLES) and takes into account the local grid sizes and local gradients of the flow. (Deltares, 2014). 2DH models are widely used for river modelling in the Netherlands, see Figure 2.8 for an example of a 2DH river model.

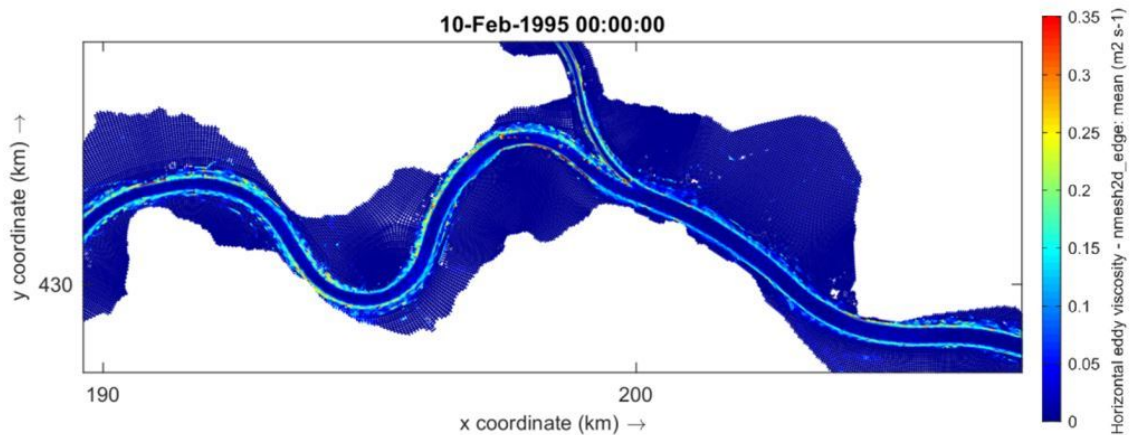


Figure 2.8: Horizontal eddy viscosity as simulated with a 2DH Delft3D model for a section of the River Waal

Three dimensional (3D) models are the most computationally expensive. The flow properties are resolved in all three dimensions. This means that there can be variation of the flow velocity, pressure, turbulent kinetic energy etc. in the vertical. This is useful in problems where the vertical accelerations of the flow are not negligible compared to the horizontal accelerations. In 3D non-hydrostatic models no assumptions about the pressure distribution are made which makes it possible to simulate the underpressure mentioned in Section 2.3 that influences the separation zone length. The grid size is usually too coarse to resolve the smallest length scales of turbulent motion. This means that the velocities are separated into a mean and a fluctuating component. This resulting extra term needs an additional equation to be solved. Therefore a turbulence closure model is used. These models are based on empirical relationships between the turbulent fluctuations and the mean flow properties. The $k-\epsilon$ closure model is the most widely used. In this model k is the turbulent kinetic energy and ϵ is the dissipation of the energy. Ali (2013) found that the $k-\epsilon$ model is suitable to model the discharge and energy losses for flow over weir-like obstacles.

2.6.2. Groyne modelling

The increase in computer power over the past decades made it possible to get more and more accurate models of rivers and groynes. Numerical models are used to predict the effect of river training measures and optimise the design (Huthoff et al., 2013). Groynes are studied extensively in numerical models (e.g. Ouilon and Dartus 1997; van Banning 2002; Busnelli 2002; Yossef 2005; McCoy et al. 2008; Yossef and Zagonjoli 2010; de Goede 2012; Hüsener et al. 2012; Baron and Patzwahl 2013; Kruijt 2013; Platzek 2017; Yossef 2017; Zagonjoli et al. 2017; Yan Toe 2018). Most numerical experiments are focused on emerged groynes. The cases where submerged groynes are modelled are aimed to understand the effect of adaptations to groynes on the water levels. Detailed 3D non-hydrostatic numerical simulations are able to reproduce the flow patterns as

described in Sections 2.3 and 2.2 to a large extent (van Broekhoven, 2007; Huthoff et al., 2013). This gives confidence in the understanding of the effects of groyne adaptation and optimising design. However, when modelling large river reaches such as the branches of the River Rhine (RWS-WVL, 2017) 3D models are not attractive. The required computational time would become very large when all the flow details near groynes and small geometric details would be represented. Especially when three-dimensional non-hydrostatic effects would be taken into account. Besides 3D models have limitations and uncertainties as well (Baron and Patzwahl, 2013) which would lengthen the calibration process substantially.

The Dutch Ministry of Public Works (Rijkswaterstaat) uses 2DH models with a grid resolution of 40 m in flow direction and 20 m over the width to model the flow through the Dutch branches of the River Rhine. Because the groynes are smaller than the grid cells and no vertical gradients in velocity are possible, sub-grid parametrisations of the effects of groynes on the flow are necessary. This has been implemented in the 2DH numerical models with weir formulations. The energy losses over groynes are calculated based on the upstream energy head and the downstream water level (Sieben, 2011). The energy loss is then added to the momentum equation. This approach is refined by adding parameters for vegetation, slope angle and crest width. These formulations are verified based on weir tests (Sieben, 2011). This was tested by de Goede (2012) with data from a measurement campaign during floods in 2010 and 2011. The measured depth averaged flow velocity, water depth and discharge distribution in the main channel were compared with calibrated model results and found good correspondence.

2.6.3. Conclusion

The fundamental difference between a 2DH model with a sub-grid parametrisation of the groyne and a 3D model is that the relation between the energy losses and the discharge over a groyne has to account for the 3D flow patterns that emerge around the groyne. So in the sub-grid parametrisation it is most important that a formulation is used that induces the correct energy head losses. In a 3D model it is important that the 3D flow patterns are captured accurately

Comparisons have been made between fine non-hydrostatic 3D simulations and 2DH models to gain insight in the influence of groynes on the resistance and the effect of streamlining and lowering (Busnelli, 2002; van Banning, 2002; van Broekhoven, 2007; Zagonjoli et al., 2017; Zagonjoli, 2017; Yossef, 2017; Yossef and Visser, 2018). It is concluded that there are differences between the resistance of groynes and of sub-grid weirs for the same set up. The effect of an extrapolated water level and lowering or streamlining groynes is thus uncertain. In order to verify if groynes can be modelled as weirs laboratory or field data should be used. However, it is difficult to obtain reliable velocities, water levels and discharge measurements during a flood. It is even next to impossible to get field data from a design flood. Therefore laboratory tests are necessary with accurate measurements. Thereafter a well calibrated numerical model can give accurate and reliable predictions of the water levels, flow velocities and discharge distributions.

Data Analysis of the BAW groyne flume experiment

The method and results of the data analysis are discussed in this chapter. The first part of this chapter is concerning the contents of the data that is provided by the Bundesanstalt für Wasserbau (BAW). The details of the measurements carried by the BAW in Karlsruhe in 2011 are described. After that the results of this analysis are presented.

3.1. BAW groyne flume experiment

The BAW advises and supports the German ministry of Transport and Digital Infrastructure (BMVI) with regard to operation and maintenance of Germany's federal waterways. A flume experiment was carried out by the BAW to investigate the effect of innovative river training measures and to validate various numerical models between 2011 and 2013. The goal was see what the effect of filling up of groyne fields or increasing groyne spacing was. A large data set including extensive measurements of velocities and water levels was collected to calibrate numerical models and look into their predictive ability.

3.2. Experimental set-up: A 70 m long 2.5 m wide flume

The experimental set-up consists of a flume with a total length of 70 m and a width of 2,5 m of which 63 m is effectively used for measurements. The following situations were considered:

- V00: Flume with graded gravel bed
- V01: Flume with 40 groynes (groyne spacing (S) is 1.50 m)
- V02: Flume with groynes and an embankment of 12 m (8 groyne fields filled)

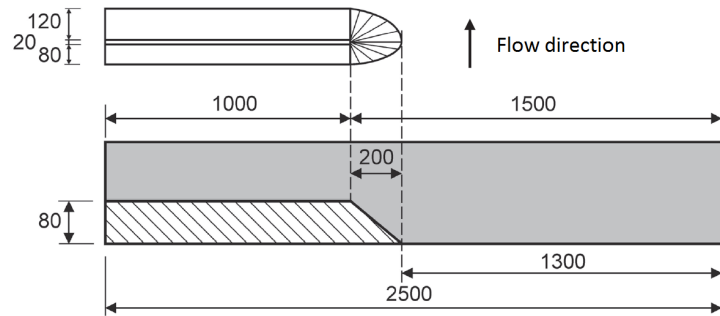
The groynes are 1.20 m long (including the tip of 0.2 m) and have a height of 0.08 m. The surface of the groynes is smooth concrete. The upstream slope angle of the groynes is 1:1 and the downstream slope angle is 1:1.5 (V:H). The flume has glass walls and the bottom is made hydraulically rough with fixed gravel with a grain size between 4 mm and 8 mm. This can be seen in Figure 3.1. The bed slope is $6.0 \cdot 10^{-4}$ m/m (6 mm/m). The discharge was controlled to acquire a desired water level so different submergence levels could be investigated. The flow in the flume including the groynes therefore was steady and non-uniform. In Table 3.1 the measured discharges and target water depths are presented.

Table 3.1: Measured discharges and target depths in experiment cases V00 and V01 (Hüsener et al., 2012).

Water depth (mm)	40	50	60	70	80	85	90	100	120	160	200
Discharge V00 (l/s)	17.7	25	33	42	52	57.5		74.5	100	157.8	222
Discharge V01 (l/s)			16	21	26	29	33	40.5	56	92	128



(a) Empty BAW flume with groynes.



(b) Groyne dimensions with values in mm (after Hüsener (2015)).

Figure 3.1: Dimensions of the groynes and overview of the flume with groynes (V01).

The data is measured using multiple instruments in order to measure water levels, discharge and flow velocities. The instruments used are:

- Magnetic Induction Discharge (MID)
 - Discharge
- Ultrasonic sensors type: Deltares P-EMS E30, (Deltares, 2018)
 - Water levels at fixed locations
- Photogrammetric 3 camera system for 3D-particle tracking velocimetry (3D-PTV) (Henning et al., 2007)
 - Water levels
 - Surface flow velocities
- Acoustic Doppler velocimetry (ADV) type: Nortek Vectrino (down and side looking)
 - Flow velocities in three spatial directions.

3.3. Approach: Flow patterns over a groyne

The data will be used to find if a part of the groyne behaves as a weir, i.e. has a 2DV character. This means that there should be no variation in the water level and flow velocity over the length of the groyne. In order to visualise this the PTV data is projected on a grid to make visualisation and comparison possible.

To conclude on the similarity between the groynes from the experiment and a weir the water level, velocity profiles and discharge distribution over the groyne and in the main channel are analysed.

3.4. Results: Data analysis of the groyne experiment

In this section the results of the data analysis will be presented. The PTV data provide the water level and surface velocity field. The ADV and P-EMS data are used to look at the cross-sectional velocity profile and discharge distribution.

3.5. Water levels

The water levels for the cases with groynes (V01) with a depth of 12 cm and 16 cm are measured with PTV. This gives high density data along a lot of particle tracks. In order to interpret and visualise this data the scattered data is projected on the same 5 cm by 5 cm grid that is used for the numerical models to allow easy comparison. This means that the average value for each cell is calculated based on the measurement points that lie within that cell. See 3.2 for an overview of the water measurements from the PTV. Also an ultrasonic water level gauge was used to measure the water level at fixed locations along the flume. Therefore only the average water level slope can be visualised.

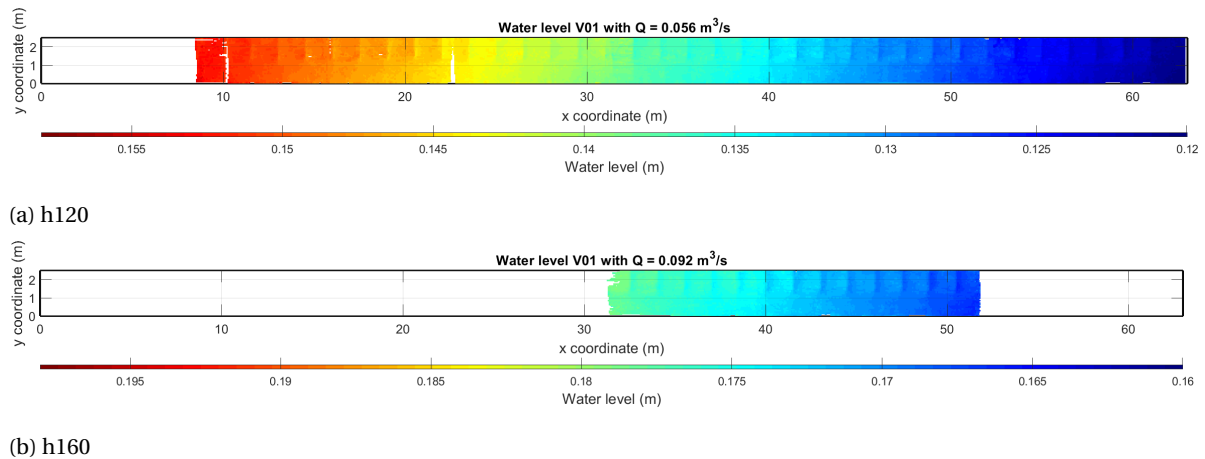


Figure 3.2: PTV measurements of the water level for the V01 case with $Q = 0.056 \text{ m}^3/\text{s}$ (3.2a) and $Q = 0.092 \text{ m}^3/\text{s}$ (3.2b). What can be seen is that the water level in the groyne fields show a distinct drop over each groyne. This is visualised in the next section.

Longitudinal section

The BAW experiment was set up to get a steady flow for various discharges. This was done for both the no groynes case (V00) and the groynes case (V01). The results of that are shown in Table 3.1 and the rating curve as shown in Appendix A in Figure A.2. In the V00 case the flow is uniform and turbulent with Reynolds numbers varying between $7 \cdot 10^3$ and $9 \cdot 10^4$. Together with the rough bottom this means that hydraulic rough conditions apply.

The detailed PTV measurements of the water level show that there is a difference in the water level setup in the groyne fields. With a water depth of 12 cm (h120) the groynes are 4 cm submerged. This leads to a more horizontal water level in the groyne fields. With a submergence of 8 cm, i.e. a water depth of 16 cm (h160) the water level is slightly raised (recovers a little bit) in the groyne field before dropping over the groyne again. See Figure 3.3

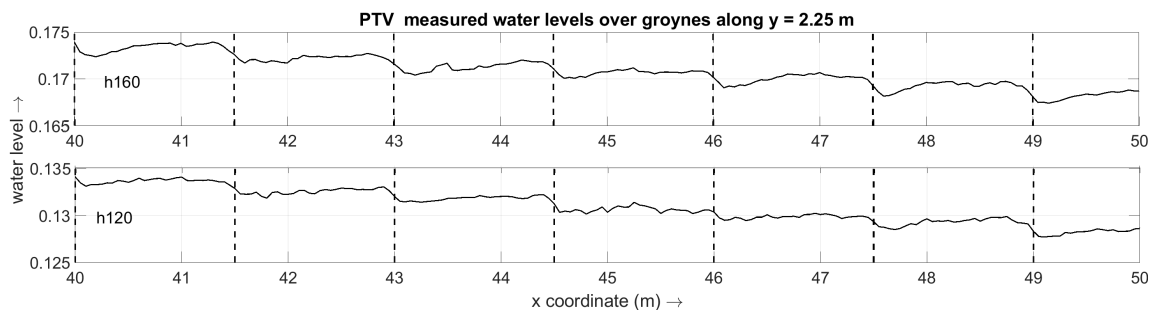


Figure 3.3: Measured water levels in longitudinal section over the groynes at $y = 2.25 \text{ m}$ for $Q = 0.056$ and $0.092 \text{ m}^3/\text{s}$

Besides the PTV measurements the water levels are measured with ultrasonic sensors at multiple locations along the flume to determine if the water level is steady and no variations along the length of the flume exist. These measurements show a constant water level slope that is equal to the bed slope. This is of importance for the water level at the upstream inflow boundary. Because the upstream water level (or head) is the indication of the total resistance induced by the bed, side walls and the groynes. For an overview of the PTV and ultrasonic data see Figure 3.4

Cross-section

Perpendicular to the flow direction the water level can be studied because the water level is measured over a large area. So over many groynes water level measurements are available. This gives the possibility to derive an average water level over a groyne and groyne field. This is done by normalising the water level by subtracting the bed level from the measured water levels. Thereafter a water level cross-section is taken at three constant distances with respect to the groynes. These results are averaged over the PTV measured

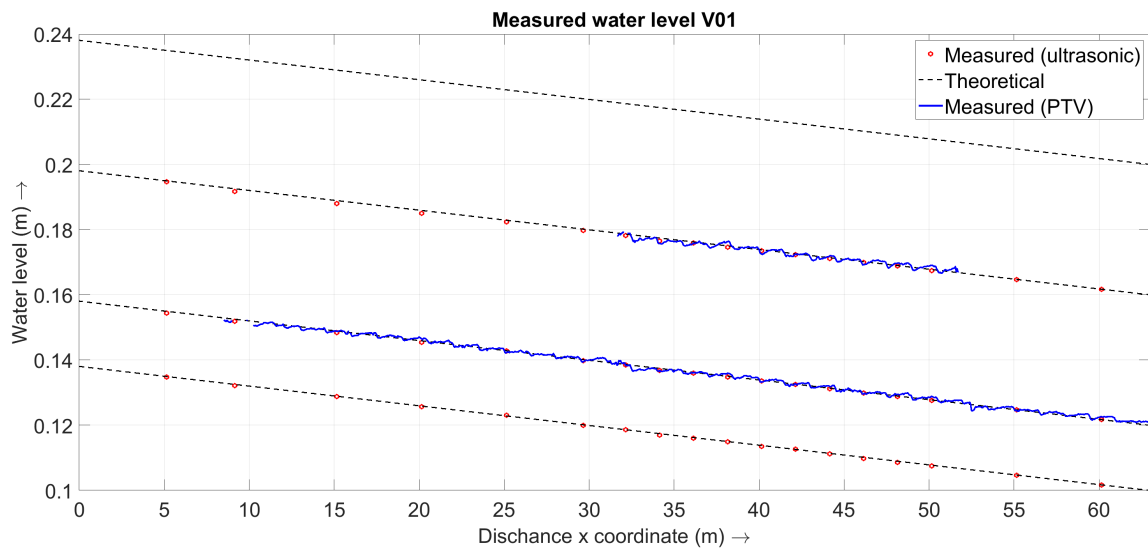


Figure 3.4: Measured and theoretical (target water level of the experiment) water levels in longitudinal section over the groynes for the different water depth conditions (h100, h120, h160 and h200)

groynes. The first section is taken 15 cm upstream of the groyne crest, the second 5 cm downstream of the crest and the third cross-section is 45 cm downstream of the groyne crest. See Figure 3.5

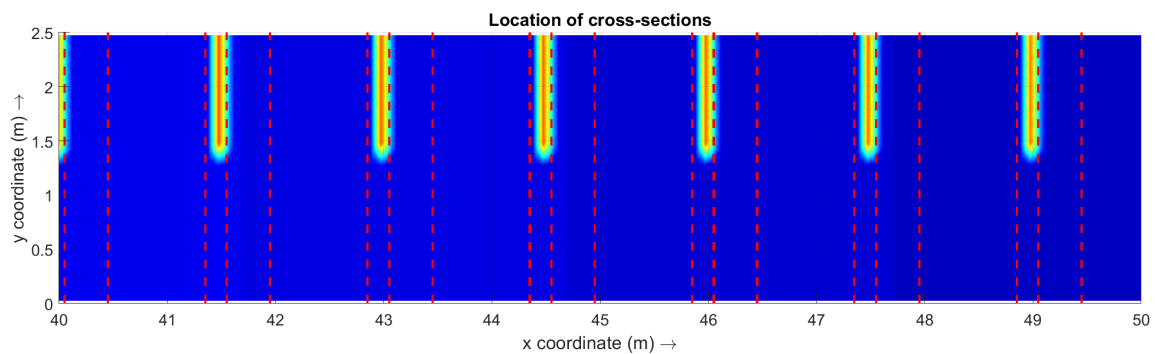
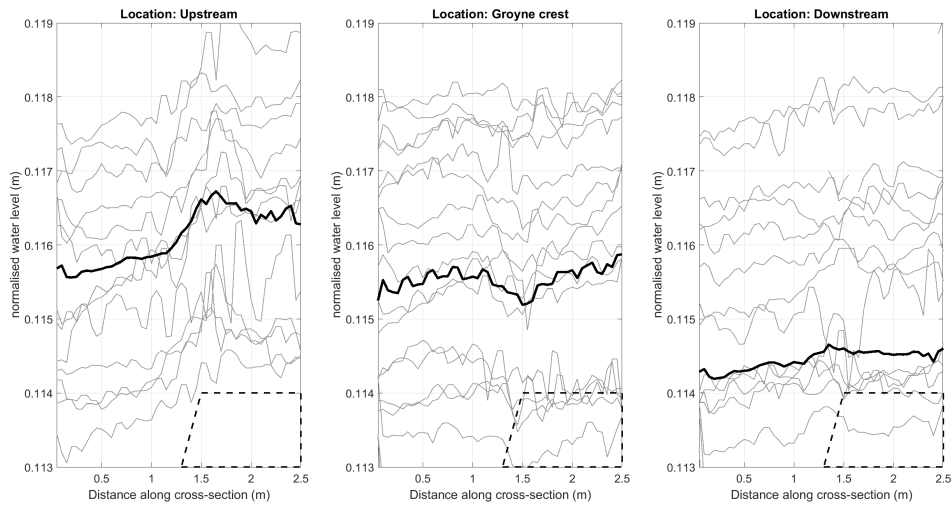
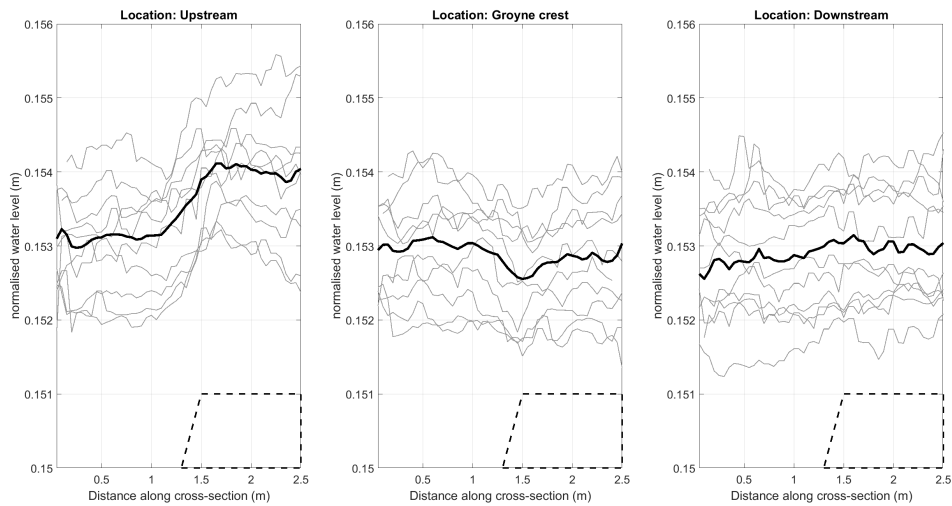


Figure 3.5: Location of the cross-sections used for averaging for cross-sectional water levels

From this analysis the water level setup just upstream of the groyne in the h160 case is clearly visible. What can be seen in Figure 3.6 is that there is a dip in the water level at the location of the groyne tip. This indicates that there is a local velocity maximum. This is visible for both the h120 and h160 case. Due to the larger number of groynes scanned in the h120 case the data is more scattered. For the h160 case 12 groyne fields are scanned with PTV.



(a) h120



(b) h160

Figure 3.6: Per groyne averaged cross-sectional water levels. Upstream = 15 cm upstream, downstream is 45 cm downstream with respect to the groyne crest. The groyne stretches from 1.3 m to the edge at 2.5 m

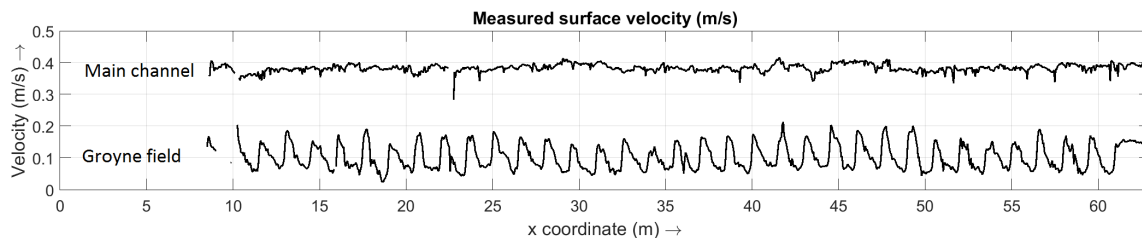
At the groyne tip a dip in the water level is visible. The water setup upstream of the groyne is visible as well. In the h120 case there is a lot more spreading in results, because a larger area was measured leading to more samples. A distinct setup is evident nonetheless. The water level is setup before the groyne, this separates the water level in three parts, a near horizontal part in the main channel, then a gradient towards the higher water level in the groyne field. The water level in a cross-section on top of the groyne can be characterised by three parts as well. The first part is the near horizontal water level in the main channel. Then a dip over a width of around 0.5 m on the groyne tip and finally a near horizontal water level at the location of the groyne. In the groyne field the water level is horizontal.

3.6. Velocity

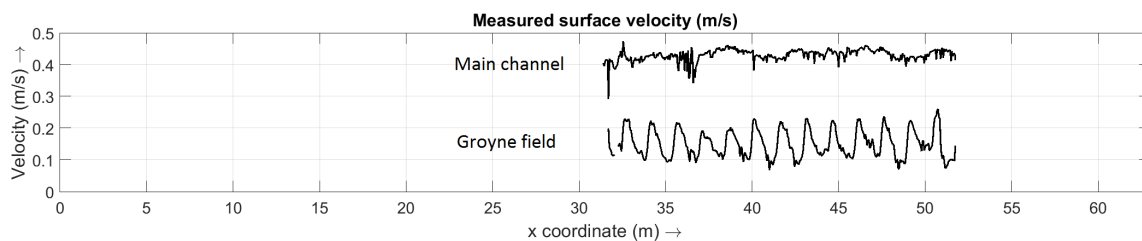
For the flow velocity at the surface an analysis similar to that of the cross-sectional water levels is done. This gives insight in the width of the mixing layer and if the velocity is uniformly over the groyne crest. This, together with the water level can give an indication of the discharge distribution over the groyne. Even more insight in the discharge distribution over the cross-section is gained by the P-EMS measurements. With P-EMS a vertical velocity profile is measured in a cross-section with a groyne (at $x = 44.5$ m). In the groyne field between $x = 44.5$ m and $x = 46$ m some vertical velocity profiles are measured as well. Together with the surface velocity this gives valuable data to calibrate the 3D non-hydrostatic model.

Surface velocity

At the surface the velocity is measured with PTV. This gives high density data points that can be projected on a grid to visualise the measurements. In the main channel the velocity is the highest, with values around 0.38 m/s for h120 and 0.44 m/s for h160. In the groyne fields the velocity accelerates and decelerates. For h120 the surface flow velocity in the groyne fields varies between 0.05 m/s and 0.18 m/s. In the h160 situation the surface velocity in the groyne fields lies between 0.1 m/s and 0.22 m/s. Noteworthy is that the maximum surface velocity in the groyne fields is not positioned directly above the groyne crest but occurs some 2 - 3 times the groyne height (15-20 cm) downstream of the groyne crest. This is also noticed by Baron and Patzwahl (2013). This indicates that the flow velocity of the groyne is strongly non logarithmic. The flow separates from the leading edge with upward directed streamlines. The smallest flow carrying area (vena contracta) is situated some distance downstream of the groyne crest.



(a) h120

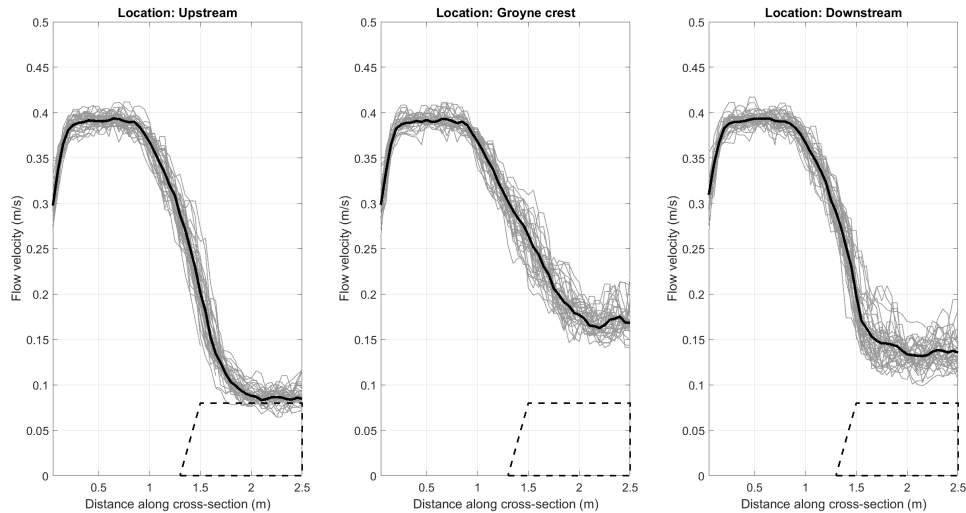


(b) h160

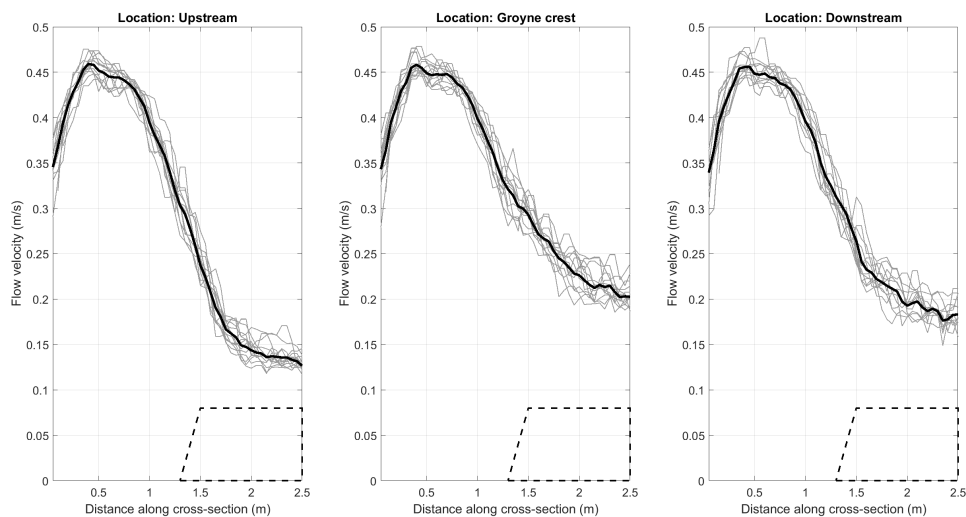
Figure 3.7: Magnitude of the surface velocities in the middle of the main channel ($y = 0.75$ m) and surface velocities in the groyne field ($y = 2.25$ m). For $Q = 0.056$ m³/s (3.7a) and $Q = 0.092$ m³/s (3.7b)

Flow velocity (x component)

In the cross-sectional direction the velocity distribution are visualised in the same way as the water levels in Section 3.5. To give a good insight in the velocity distribution the x- and y-components of the velocity are shown in Figure 3.8. Both the h120 and h160 case show similar lateral surface velocity profiles. A difference is that the flow velocities in the h120 case are smaller than in the 160 case. The difference in flow velocity between the main channel and groyne field are practically the same, see Table 3.2. The gradients in the flow velocity vary however. In the h120 case the width is smaller than in the h160 case. This can be explained because the water level is lower so the groyne blocks a larger fraction of the cross-sectional area. In the h120 case there is a portion of the groyne length, (i.e. cross-sectional width) where the flow velocity is more or less constant. For the h160 case that length is zero, because there is still a gradient in the velocity near the wall.



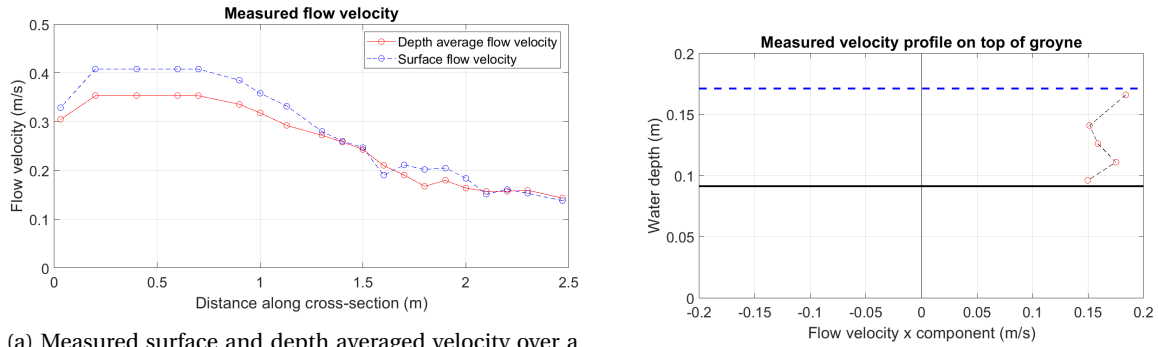
(a) h120



(b) h160

Figure 3.8: Average surface velocities (x component) just upstream, on top and downstream of the groynes. For $Q = 0.056 \text{ m}^3/\text{s}$ (3.8a) and $Q = 0.092 \text{ m}^3/\text{s}$ (3.8b)

From the P-EMS velocity measurements one depth averaged cross-sectional velocity profile can be derived. This is measured with the P-EMS on top of the groyne at $x = 44.5 \text{ m}$. In the vertical between 4 (on top of the groyne) and 10 points (in the main channel) are measured giving the opportunity to derive a depth averaged flow velocity profile, see Figure 3.9a. Measurements are taken at lateral intervals of 10 cm over the groyne and 20 cm in the main channel. However no measurements are taken in the centre of the main channel so the measurement closest to the main channel centre is duplicated. Possibly introducing a small underestimation of the maximum velocity in the main channel. It can be seen that the depth averaged velocity has a wider mixing layer. By comparing the surface velocity with the depth averaged velocity for the h160 case it can be seen that in the main channel the velocity at the surface is higher. Close to the groyne crest the velocity is larger than at the surface for some vertical velocity profiles. So the vertical velocity profile on top of the groyne has a maximum close to the groyne crest, see Figure 3.9b for a typical profile.



(a) Measured surface and depth averaged velocity over a groyne and trough the main channel along cross-section $x = 44.5$ m derived from ADV measurements of vertical velocity profiles

(b) Vertical velocity profile on top of the groyne at $x = 44.5$ m and $y = 2.0$ m. The black line represents the groyne crest and the dashed blue line the water level.

Figure 3.9: ADV measured flow surface and depth average velocity along cross-section at $x = 44.5$ m and ADV measured vertical velocity profile at $x = 44.5$ m and $y = 2.0$ m.

Lateral flow velocity (y component)

In the y direction the flow velocity at the surface is an order of magnitude smaller than the x component, see Figure 3.11. The magnitude of the velocity is again smaller for the h120 case than the h160 case. However the shape of the distribution is very similar. Both cases show that just upstream and on top of the groyne, in the middle of the flume (i.e. at the groyne tip) the y component is negative. This means that near the surface the flow is directed out of the groyne field into the main channel. On average the flow is at every location above zero. This means that at the surface the average flux of mass is directed into the groyne field. This implies that at some depth below the surface the flow must be directed from groyne field to main channel. For an overview of the y component of the surface velocity based on the PTV data see Figure 3.10

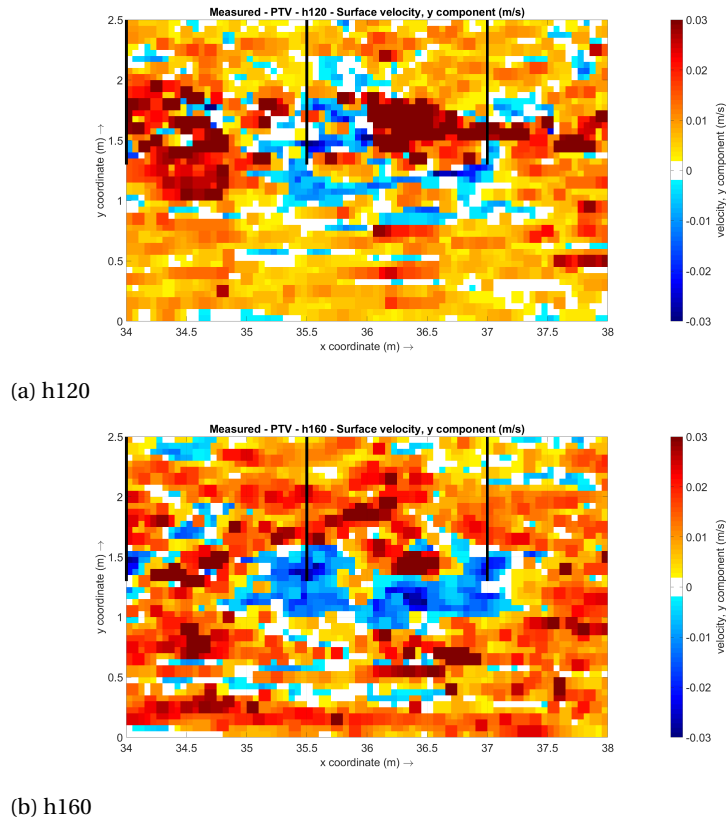
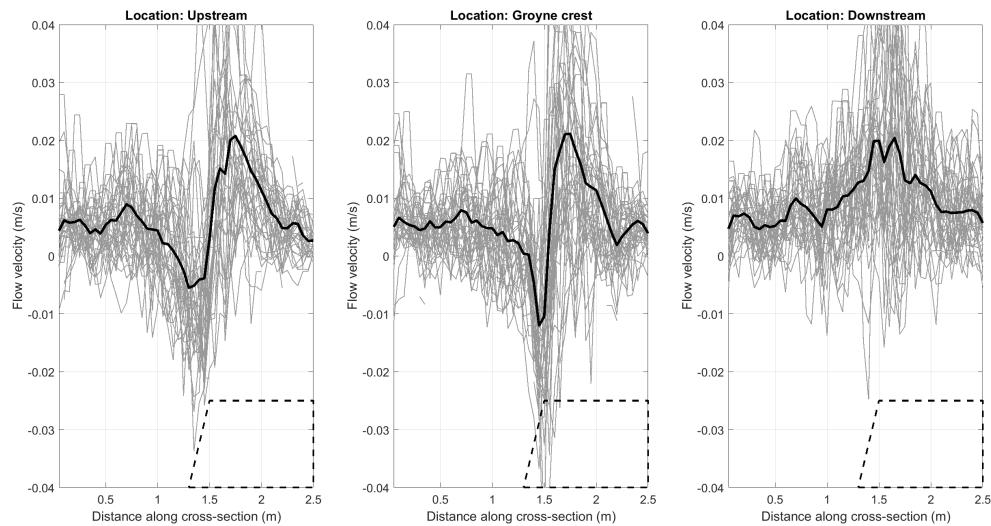
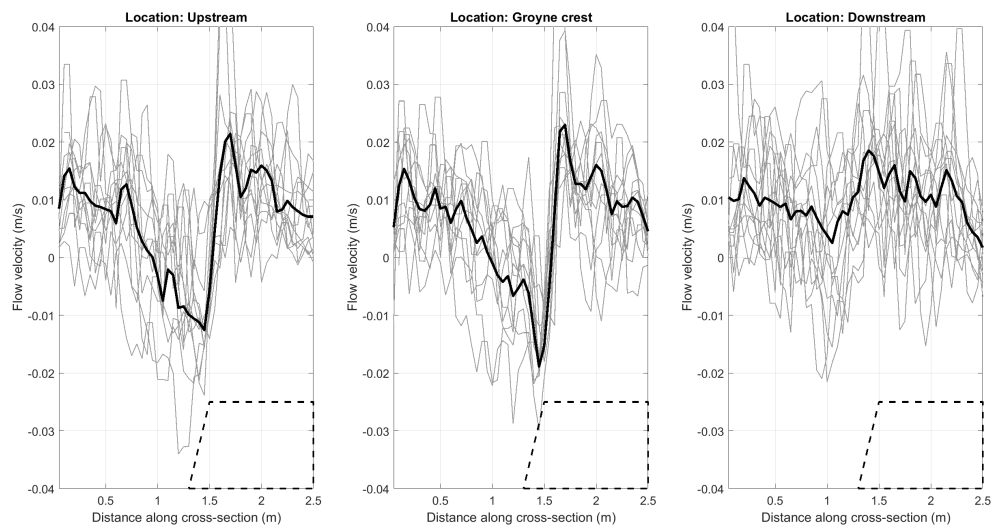


Figure 3.10: Surface velocities (y component). For $Q = 0.056 \text{ m}^3/\text{s}$ (3.10a) and $Q = 0.092 \text{ m}^3/\text{s}$ (3.10b)



(a) h120



(b) h160

Figure 3.11: Average surface velocities (y component) just upstream, on top and downstream of the groynes. For $Q = 0.056 \text{ m}^3/\text{s}$ (3.11a) and $Q = 0.092 \text{ m}^3/\text{s}$ (3.11b)

3.6.1. Mixing layer

From the analysis of the flow velocities at the surface the mixing layer can be characterised. In the mixing layer the momentum is exchanged between the slow flowing water in the groyne field and the fast moving water in the main channel. Due to this lateral momentum exchange the resistance of the flume will increase which reduces the discharge capacity of a channel. As noted in the section about the components of the surface velocities there are differences over the vertical velocity profile, including a recirculation cell and significant lateral velocities, this means that the mixing layer is not uniform over the vertical. The width is also fluctuating in the longitudinal direction, see Table 3.2. See Figure 3.12

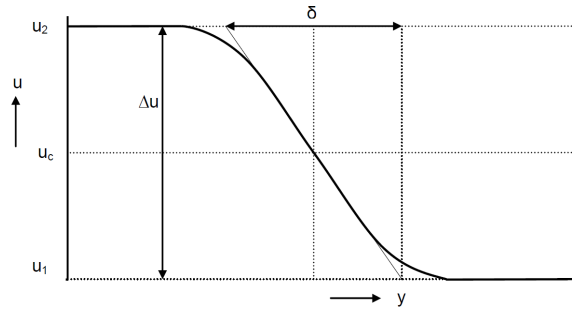


Figure 3.12: Schematic drawing of a mixing layer

Location w.r.t. groyne	h120			h160		
	δ (m)	Δu (m/s)	$\frac{du}{dy}_{max}$ (m/s/m)	dy (m)	Δu (m/s)	$\frac{du}{dy}_{max}$ (m/s/m)
Upstream	0.75	0.315	0.513	1	0.32	0.3516
On top	1.0	0.22	0.208	1.5	0.23	0.28
Downstream	0.7	0.265	0.478	1.2	0.265	0.27

Table 3.2: Mixing layer width and flow velocity gradients derived from Figure 3.8

The difference between the h120 and h160 case can be explained by the discharge distribution. When the discharge is increased the discharge in both the main channel and the groyne fields increase. However in the main channel the discharge increases more than in the groyne field. So the gradient between the two becomes larger, leading to more lateral influence in the h160 case and thus a wider mixing layer.

The width of the mixing layer is an important calibration parameter for the numerical simulations because if it is not correctly modelled, the discharge distribution between the main channel and groyne field is not correct. Thus lateral mass and momentum exchange that influence the resistance induced are off, leading to either an over- or underestimation of the resistance. In rivers with floodplain an additional mixing layer between the groyne fields and floodplains will be formed.

3.6.2. Vertical velocity profiles

A vertical recirculation cell is present due to the steep downstream slope of the groynes in the separation zone behind the groynes. The separation zone starts at the upstream edge of the groyne crest. The recirculation cell has a horizontal axis of rotation, starts at the side wall and ends near the beginning of the downward sloping groyne tip. The velocities in the recirculation cell are measured only in the case with a water depth of 16 cm. But also in the other cases recirculation cells are likely to be formed due to the steep downstream slope angle. The measured flow velocities 25 cm downstream of the groyne crest and 20 cm from the side wall are shown in Figure 3.13.

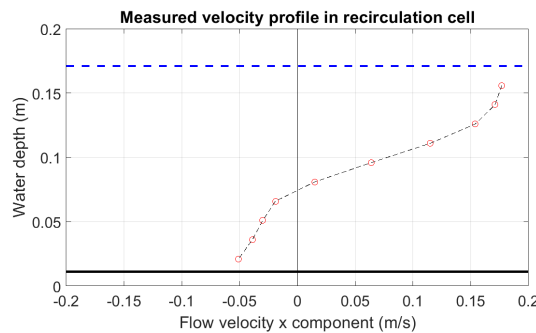


Figure 3.13: Vertical velocity profile in the recirculation cell at $x = 44.75$ m and $y = 2.3$ m. The black line represents the bottom and the dashed blue line the water level at the location of measurement point.

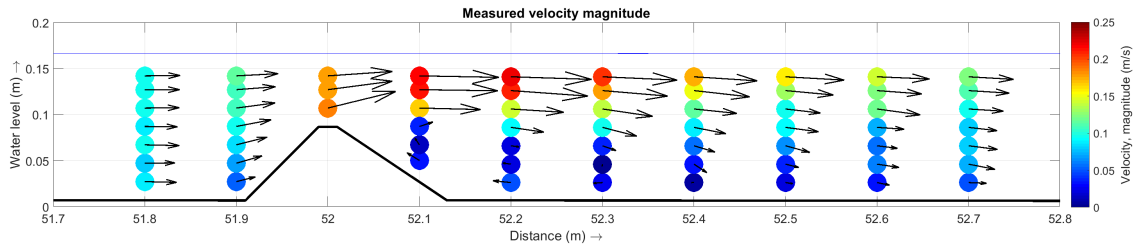


Figure 3.14: Measured vertical velocity profiles over a groyne along a not specified distance from the side wall for the h160 case (Baron and Patzwahl, 2013). The recirculation cell is clearly visible and stretches from 52.0 m to around 52.6 m

Detailed vertical velocity profiles are measured along the cross-section at $x = 44.5$ m. Some vertical profiles are taken at 44.75 m, 45.5 m and 45.75 m. An overview of these measurement are shown in Figure 3.15. This data is used to derive the depth average flow velocity as shown in Figure 3.9a. This data is used by the BAW to derive the discharge distribution.

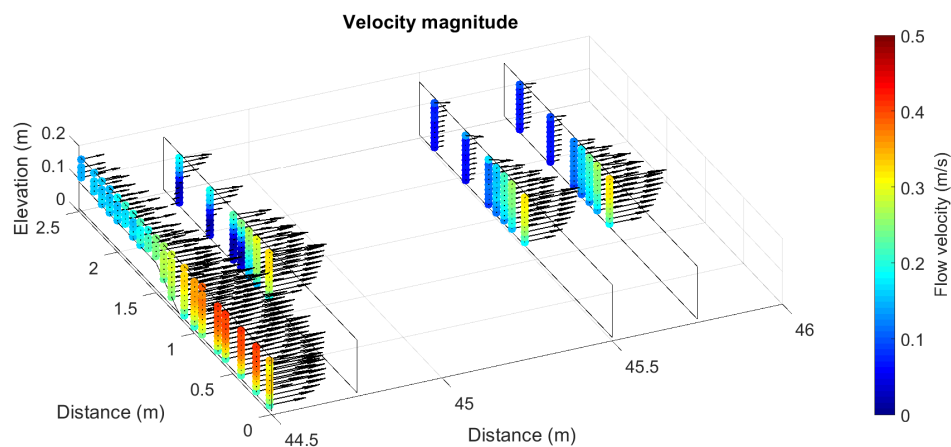


Figure 3.15: Overview of the measured vertical velocity profiles

3.7. Discharge distribution

The extensive ADV measurements of vertical velocity profiles in a cross-section with a groyne (at $x = 44.5$ m) have been used by the BAW to derive an instantaneous discharge distribution over the groyne and in the main channel. The FLIEGE software (Hentschel, 2007) was used to interpolate between the measurement points and generate a velocity field. However problems are encountered due to uncertain boundary velocities at the walls, bottom and free surface. For the analysis some vertical profiles are used on several locations because it was assumed that away from the groyne tip, both in the main channel and at the groyne the velocity profiles would be very similar. This analysis resulted in a total discharge of $0.0886 \text{ m}^3/\text{s}$. This value is 3.7 % lower than the actual measured inflow discharge of $0.092 \text{ m}^3/\text{s}$. In Figure 3.16 the results from the discharge distribution of the BAW are presented.

The discharge distribution shows that over the groyne only 15 % of the total discharge occurs along the horizontal part of the groyne. Including the tip this number goes up to: 22 % of the total discharge. This indicates that over the groyne tip the specific discharge is larger than the horizontal part of the groyne. The effect of different tip geometries is tested by Uijtewaal (2005). In Figure 3.16 the influence of the tip further along the groyne crest is visible. From the calculated specific discharge (Table 3.3) it can be seen that over the groyne tip significantly more discharge flows than over the horizontal part of the groyne. But also in the main channel there is significant variation between the section near the groyne tip and wall.

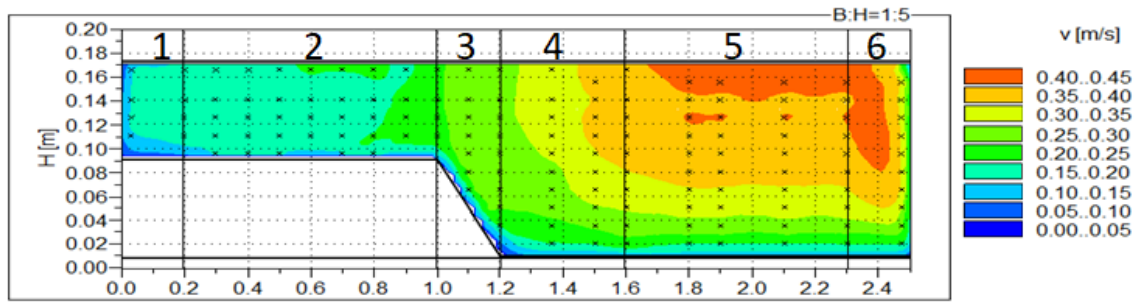


Figure 3.16: V01 0.16 m Cross-sectional discharge distribution at $x = 44.5$ m by the BAW. Notice that the cross-sectional coordinates are flipped. The labels correspond to the discharge distribution analysis by the BAW (See Figure 3.16).

Section	Groyne Field		Main Channel				Total
	1	2	3	4	5	6	
Discharge Q (m^3/s)	0.0023	0.00112	0.0061	0.0185	0.0397	0.0109	0.0886
Area A (m^2)	0.0161	0.0636	0.0245	0.0631	0.115	0.0329	0.3153
Width B (m)	0.2	0.8	0.2	0.4	0.7	0.2	2.5
Specific discharge q (m^2/s)	0.01166	0.01396	0.03029	0.0462	0.0567	0.0544	0.03545
	Q_{GF} (m^3/s)		Q_{MC} (m^3/s)				$Total$ (m^3/s)
	0.0135		0.0751				0.0886

Table 3.3: Calculated discharge distribution based on vertical velocity profiles

3.8. Conclusion: Is the flow over a groyne weir like?

The deceleration losses in the separation zone are likely to be analogous to an imperfect weir. The velocity gradient between the groyne field and the main channel induces a mixing layer that adds to the resistance. This is a fundamental difference between a weir and a groyne.

Based on the water level, velocity and discharge analysis, qualitative comparisons between weirs can be made. In this section the cross-section over the groyne is discussed. The water level is horizontal over the length of the groyne. For both h120 and h160 this is the case. In the direction of flow the water levels show a distinct drop over the groyne. For the h120 case the water level in the groyne fields is horizontal, whereas for the larger water depth the water level drop is a little larger but the water surface rises more towards the next groyne. Concerning the surface velocity there is more variation over the groyne. Only for the h120 case approximately over half of the groyne crest length the flow velocity can be considered constant. For h160 the surface velocity starts sloping at the side wall already. This is also visible in Figure 3.16 where variations along the groyne crest are visible as well. At the groyne tip the similarities with a weir diminish. There is a local drop in the water level (see Figure 3.2). Also lateral surface velocities peak near the tip which indicates momentum and mass exchange. The non-logarithmic vertical velocity profile and the recirculation cell are found for flows over weirs as well. Based on the ADV data it can be seen that the recirculation cell with a negative velocity in x direction extends to up to 90 % of the groyne crest length.

These factors indicate that similarities exist for a part of the groyne. However the similarities decrease for increasing water levels. And completely diminish towards the groyne tip. So a single weir could not replace a groyne, especially for strongly submerged groynes. Near the tip the analogy with a weir does not hold. But this part is essential as it influences the gradient of the mixing layer. So lateral uniformity indicates where the groyne behaves as a weir. As the losses in that area are not influenced directly by the mixing layer.

This experiment does not consider the flood plains. The implication is that there is no mixing layer between the groyne field and the wall. In practice at design flood levels the flood plains are inundated but flow velocities are much lower than in the groyne fields. This could lead to an even further decrease of the part of a groyne that behaves as a weir. Also the bed level in the groyne fields is the same as in the main channel in the BAW experiment. In reality however the groyne fields are silted up and have significantly sloping beds that lie higher than the main channel bed (See for example Figure 1.2). This effects the velocity and discharge distribution between the groyne fields and main channel by making it less uniform.

It is clear the flow over the groyne is not laterally uniform over the whole groyne. Near the tip the discharge is larger than near the wall, see Figure 3.16. Based on the PTV data it also becomes clear that the larger the submergence the larger this area of non-uniformity due to the increased lateral influence, see Figure 3.6 and Figure 3.8. So to be able to model groynes the lateral variation of the groyne has to be captured correctly by the numerical model.

4

Numerical modelling of the groyne flume experiment

The experiment set-up as described in Section 3.2 is modelled in 2DH and 3D (non-hydrostatic) using Delft3D and in 3D (non-hydrostatic) using Finel. In the 2DH model the groynes are either modelled as sub-grid weirs or are included in the bottom topography. The models are calibrated to fit the measured water level by altering the bottom roughness based on the case without groynes (V00). Subsequently the groynes are added and the water level is calibrated to fit the measured water level for emerged groynes by altering the horizontal eddy viscosity. After that, the water levels, velocity profiles and discharge distribution over the groynes and in the groyne fields are compared with the data. The difference between the models is identified subsequently by looking in what is gained by using a 3D or 3D non-hydrostatic simulation compared to a 2DH coarse grid or fine grid simulation.

4.1. Numerical model setup

The hydrodynamics of the BAW experiment are modelled in Delft3D with a grid resolution of 5 cm by 5 cm for the fine grid and 0.25 m by 0.25 m for the coarse grid (see Figure 4.1). In the fine grid the groynes are included in the bottom topography. In the coarse grid only the sub-grid weirs are possible. At the upstream boundary the measured discharge or water level is given and at the downstream boundary the corresponding water level. The modelled cases are shown in Table 4.1.

Table 4.1: Available models in Delft3D. On behalf of the 3D non-hydrostatic mode, the model Finel is applied as well.

Model		Grid	Grid size: x,y,z (m)	Groyne representation
Delft3D	1D	coarse	0.25	sub-grid weir
Delft3D	2DH	coarse	0.25 x 0.25	sub-grid weir
Delft3D	2DH	fine	0.05 x 0.05	sub-grid weir
Delft3D	2DH	fine	0.05 x 0.05	bed topography
Delft3D	2DV	fine	0.05 x 1 x 0.01	bed topography
Delft3D	2DV	super fine	0.01 x 1 x 0.005	bed topography
Delft3D & Finel	3D Non-hydrostatic	fine	0.05 x 0.05 x 0.01	bed topography
Delft3D	3D Hydrostatic	fine	0.05 x 0.05 x 0.01	bed topography

This gives the possibility to investigate the resistance of each case by comparing the modelled water levels to the measured water levels. The resulting velocities can be compared with measurements to indicate if the models reproduce the correct flow patterns over and around the groynes.

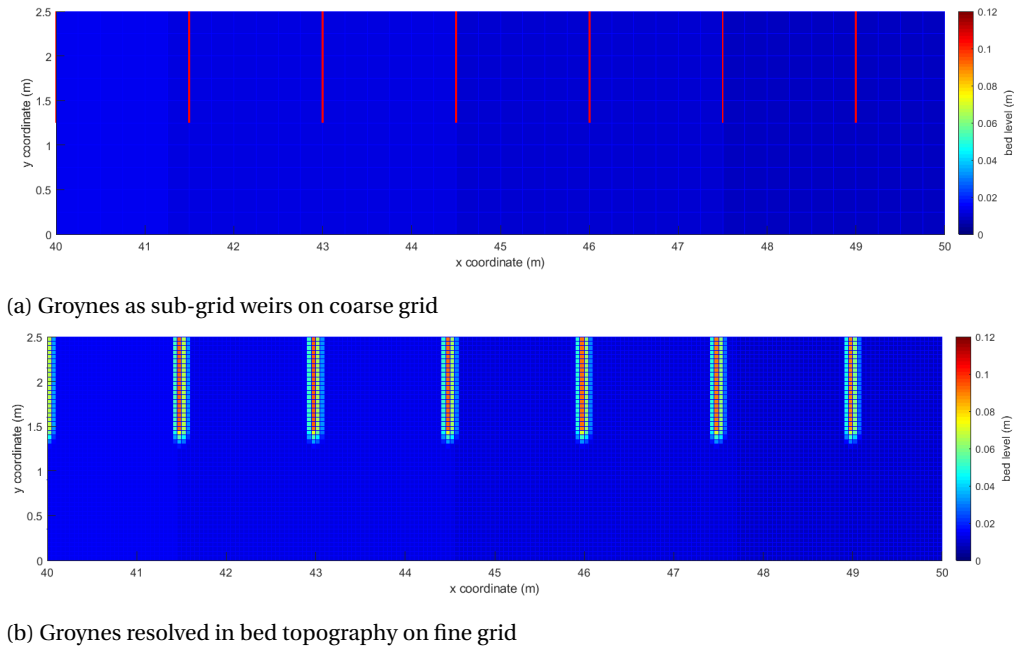


Figure 4.1: Part of the coarse and fine grid and the groyne representations in Delft3D

Both Delft3D and Finel are applied within this study. Delft3D is used as it allows for a direct comparison between 2DH and 3D results using the same structured grid; furthermore, Delft3D contains sub-grid weir implementations similar to WAQUA (the Dutch standard model for evaluation of policy decisions). Finel is applied because of the unstructured mesh that allows for easy local grid refinement in the region of interest, as well as the flexibility in terms of numerical code adaptations supported by Svasek Hydraulics.

Specifically, Finel is used for the full 3D non-hydrostatic simulation of submerged groyne cases. The applied grid in Finel is unstructured (triangular) with an average horizontal element size of 3.5 cm and a maximum of 10 cm (locally). Near the groynes the horizontal resolution is refined down to 2.0 cm, which is necessary to induce flow separation at the correct location along the groyne crest.

4.2. Approach: Steps to compare model performance

The resistance of groynes in the models is compared with the data by looking at the water level and the discharge capacity. The upstream water level indicates if the total resistance within the system corresponds with the data. When the upstream water level is lower than found in the data the resistance added by the groynes is too low. This implies an underestimation of the resistance. And vice versa for higher water levels indicating to higher resistance. Furthermore the characteristics such as surface velocity, depth averaged velocity, water level and discharge distribution are compared to the data to draw conclusions on the performance of the models. This makes it possible to determine which model is the most suitable for groyne modelling.

Table 4.2: Numerical modelling steps

Step	Description	Parameter
Step 1	Calibrate water level for V00 case without groynes	Bottom and wall roughness
Step 2	Calibrate water level and mixing layer width for V01 case	
Step 3a	Compare water levels at upstream boundary	Discharge boundary condition upstream
Step 3b	Compare discharge for given water levels	
Step 4	Compare water levels, discharge capacities and velocities with data from BAW	Water level boundary conditions
Step 5	Check influence of grid size (in 2DV) and reduction factor for sub-grid weir formula (in 2DH coarse grid)	

Both a water level and discharge boundary conditions at the upstream inflow boundary will yield the same conclusions in terms of over- or underestimation of the resistance. However when the models over- or underpredict the resistance added by groynes and a discharge boundary is used the water depth will not be uniform. Because the model is in the influence area of the backwater that is introduced between the fixed downstream water level and the non-equilibrium water depth throughout the flume. This means that the velocities are affected by the backwater and the velocity profile will not differ for every groyne. Conclusions can still be drawn on the over- or underprediction of the resistance.

In the 3D model the groyne geometry will be changed. Both lowered and streamlined groynes will be modelled. With the Delft3D 2DH model also groyne lowering can be simulated. The effects of the lowering in the two models can thereafter be compared. The discharge that flows over the groynes in 3D is used as upstream boundary condition for the 2DV simulations in which the groyne geometry is changed as well.

4.3. Results: Delft3D Numerical modelling of groyne experiment

First the numerical models are calibrated to gain confidence in the model results and know where and in which situations the model deviates from the measurements. After the calibration the parameter settings of the model will not be altered. Subsequently the boundary conditions and bed topography will be changed to include groynes in order to see how well the model performs.

4.3.1. Uniform flow: V00 case

The numerical models are calibrated on 4 water depths of the uniform flow case (V00) by altering bottom and side wall roughness. At the upstream boundary the measured discharge is imposed and at the downstream boundary the measured water level. The calibrated water depths are: 10, 12, 16 and 20 cm. The roughness is calculated analytically (see Appendix A). The calculated values are used in the numerical model. For the 2DH simulation a bottom roughness of 7.5 mm is used and at the side walls a partial slip condition ($z_0 = 2.0 \cdot 10^{-4}$ m). For the 3D simulations a bottom roughness of 10 mm and a partial slip wall roughness value of $3.33 \cdot 10^{-4}$ m were needed. These settings resulted in uniform flow with water depths that match the measurements. The differences in upstream water levels between the model and target values are between -1.3 mm and +1.4 mm. This corresponds to a maximum water level slope error of approximately 3.5 %, see Figure 4.2.

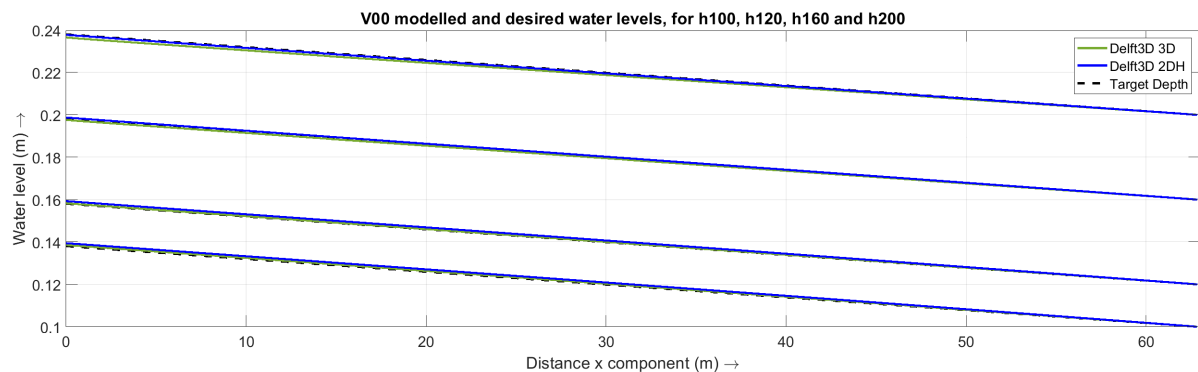


Figure 4.2: Delft3D modelled and target (measured) water levels for the uniform flow case V00 with target water depths of 10, 12, 16 and 20 cm.

4.3.2. Flow around and over groynes: V01 case

The roughness values that are found with the V00 case calibration are used for the V01 case. Only at the location of the groynes the roughness will be decreased because in the BAW experiment smooth concrete is used there (see Figure 3.1a). A Nikuradse roughness height (k_s) of 1 mm is used because the flow velocity near the groyne crest then closely matches the ADV measured flow velocity. A sensitivity analysis showed that the influence of changing the k_s value of the groynes (within a range of 0.1 cm - 5 cm) locally did not significantly affect the water level slope and the upstream water level.

For the V01 case the upstream boundary conditions are varied. In one series of simulations the measured discharge is imposed. The model then calculates the water levels based on this discharge. When the added

resistance of the groynes or sub-grid weirs is not sufficient the model is affected by the backwater because the downstream water level is fixed and does not match the equilibrium water depth. This means that the water level is not parallel to the bed and therefore the flow depth is not uniform. This leads to differences in the cross-sectional velocity profiles at different locations along the x direction. Still conclusions on the over- or underestimation of resistance can be made.

When upstream and downstream the measured water levels are imposed the model calculates the discharge for which the required water levels are reached. The water level is parallel to the bed level. Then the performance of the model can then be determined by comparing the measured discharge with the modelled discharge.

However, neither of these methods are perfect, the first few groynes introduce more losses for both boundary types than the subsequent groynes because the discharge distribution between the main channel and the groyne fields is then in equilibrium. The effect is that the water level at the upstream boundary is correct but the water depth further downstream is a little bit too low. A higher upstream water level could counter this but the calculated discharge at the inflow boundary would increase. So the variation over the first few groynes is accepted. Figure 4.3 shows the Delft3D model results of the 2DH and 3D models with the measured discharge as upstream boundary condition.

4.3.3. Discharge boundary: Upstream water levels compared

In the V01 case, with emerged groynes, only the horizontal eddy viscosity is used as calibration parameter (Deltares, 2014). The eddy viscosity is altered to get a correct mixing layer width and sufficient lateral momentum exchange. The horizontal eddy viscosity is altered to get a correct water level slope in 2DH coarse model for the water levels where the groynes are emerged. These are the following cases: h60, h70 and h80. Because in emerged case the resistance added by the groynes is only due to lateral exchange of momentum and mass between the groyne fields and the main channel. The resulting water levels in a longitudinal section through the groyne fields ($y = 2.25$ m) are shown in Figure 4.3.

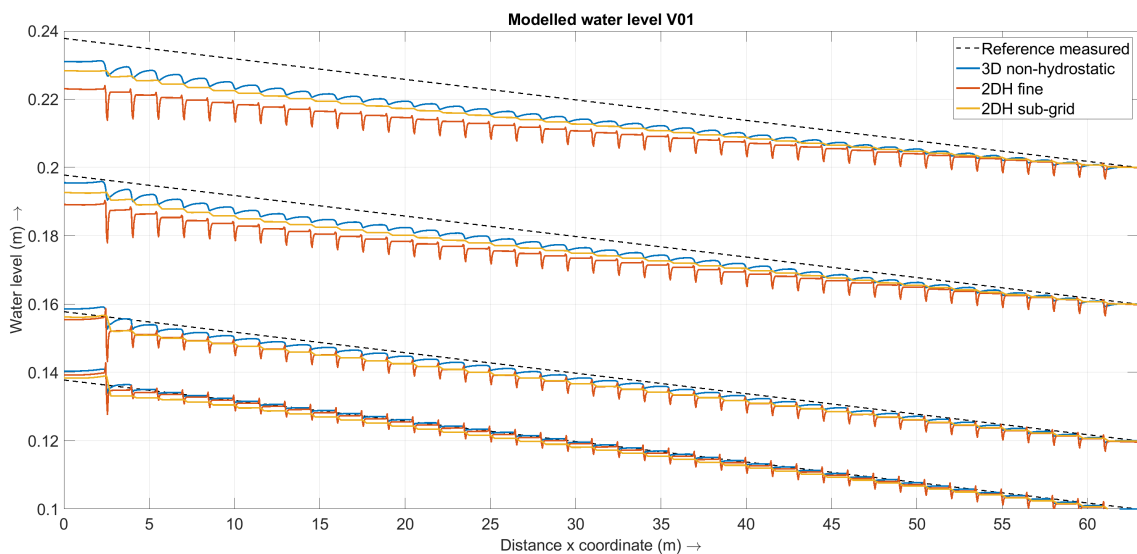
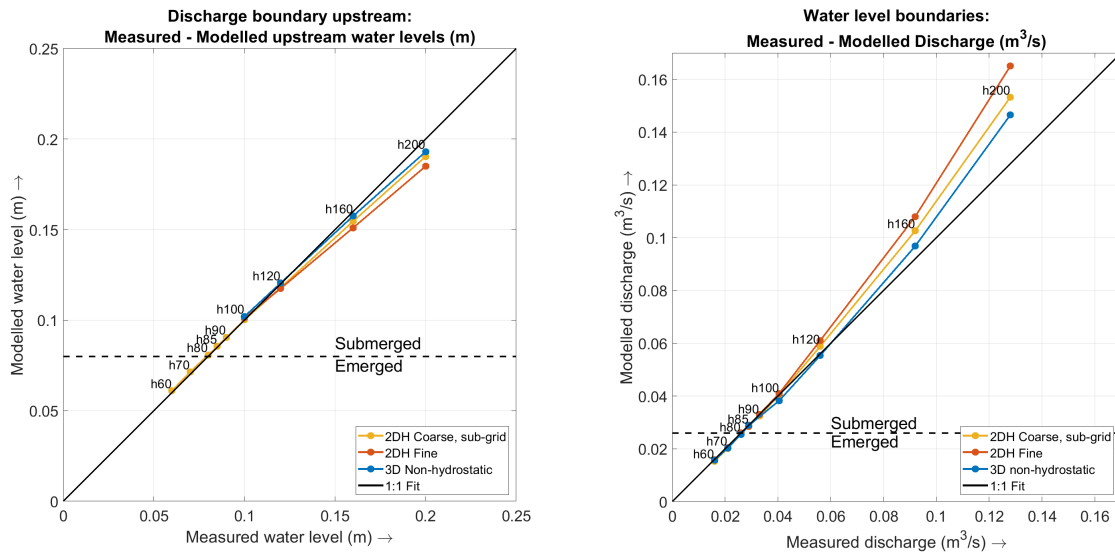


Figure 4.3: Modelled (discharge boundary) and experimental water level in longitudinal section over the groynes for the different water depth conditions (h100, h120, h160 and h200). In the 2DH fine model the groyne are resolved in the bed topography, while for the 2DH coarse model sub-grid weirs are used.

What becomes clear is that neither model produces sufficient energy losses to get a matching water level slope for h160 and h200. Only for the h100 and h120 cases the 2DH coarse and 3D non-hydrostatic model have sufficient resistance. The 2DH fine model already has too little resistance for h120. This means that for increasing submergence the energy losses due to the groynes are underestimated by the models. This is visible in the upstream water levels where the modelled water level is lower than the measured and theoretical values, see Figure 4.4a

4.3.4. Water level boundary: Total discharge compared

The same effects are visible when the upstream boundary is set to the measured water level. Then the discharge needed to get the required water depth is more than the measured discharge. This is visible in the modelled discharges that are larger than the measured discharges, see Figure 4.4b. To understand why the models underestimate the resistance induced by the submerged groynes the results will be compared to data from the BAW experiment as described in Chapter 3.4.



(a) Measured versus modelled upstream water levels

(b) Measured versus modelled discharges

Figure 4.4: Measured versus modelled water levels (4.4a) and discharges (4.4b). Based on simulations with measured discharges and measured water levels as upstream boundary conditions respectively.

4.3.5. Water level boundary: Discharge distribution

Besides the water levels and the total discharge the discharge distribution between the main channel and groyne fields is important as well. Measurements are available only for the h160 case, as described in Section 3.7. For the 2DH fine, 2DH coarse and the 3D non-hydrostatic models the distribution is presented in Table 4.3. The 3D non-hydrostatic model performs best but overestimates the discharge through the groyne field slightly. In this calculation the groyne fields are defined as the part over which the groyne crest is horizontal ($1.5 < y < 2.5$ m). So the main channel consists of the groyne tip and main part with the flat bed ($0 < y < 1.5$ m). This is chosen to make it possible to compare the fine grid with the coarse grid.

Discharge Distribution	Total (m ³ /s)	Main Channel (m ³ /s)	Groyne Field (m ³ /s)	Q_{GF}/Q_{MC} (-)
Measured (ADV derived)	0.0886	0.0751	0.0135	0.18
2DH coarse sub-grid	0.1025	0.07336	0.0292	0.40
2DH fine	0.108	0.0831	0.0249	0.30
3D non-hydrostatic	0.0968	0.08075	0.0161	0.20
3D hydrostatic	0.093	0.0758	0.0171	0.225

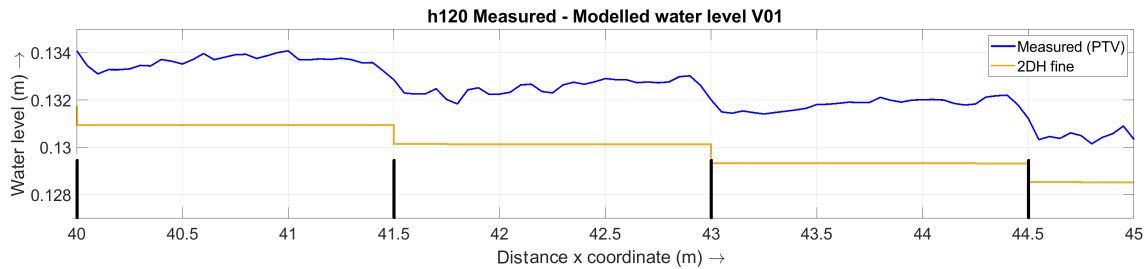
Table 4.3: Discharge distribution for the h160 case. Based on the ADV measurements, see Section 3.7. In this case the groyne field is only the area over which the groyne is horizontal ($1.5 < y < 2.5$ m). The rest is considered the main channel ($0 < y < 1.5$ m).

4.4. 2DH Modelling: Delft3D

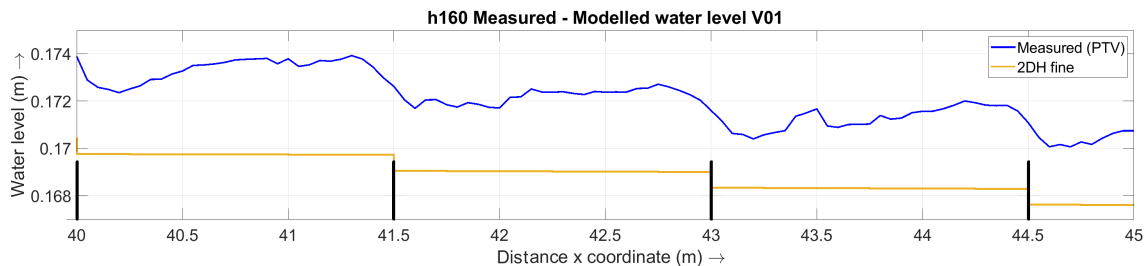
The two models in 2DH perform differently, the fine grid model where the groynes are part of the bed topography underestimates the resistance even more than the coarse-grid model with sub-grid weirs as groynes. In this section the results are based on the model which uses the measured discharge as upstream boundary condition.

4.4.1. 2DH Coarse grid: sub-grid weirs

On the coarse grid (25 cm by 25 cm) the bed topography can not include the geometry of the groynes. So groynes are included as sub-grid energy losses on the cell interfaces. Consequently the water level in the groyne fields is horizontal, see Figure 4.5, so additional set up upstream of the groyne is modelled.



(a) h120 Measured and 2DH coarse grid with sub-grid weirs modelled water level detail



(b) h160 Measured and 2DH coarse with sub-grid weirs grid modelled water level detail

Figure 4.5: Water level detail through groyne fields at $y = 2.25$ m. In the PTV data it is visible that the water level set up is larger for a larger water depth. And that in the 2DH fine model the water level set up only happens at the downstream slope of the groyne.

There is no increase in flow velocity in the groyne field because the acceleration and deceleration is resolved sub-grid. The consequence is that in the groyne field the velocity is virtually constant, both in longitudinal direction and cross-sectional direction. This leads to an overestimation of the discharge over the groynes and through the groyne fields when the groynes are strongly submerged. Analogous to the fine grid 2DH simulation the cross-sectional gradient of the flow velocities is smaller than in reality. The resistance the mixing layer introduces is therefore smaller than in reality.

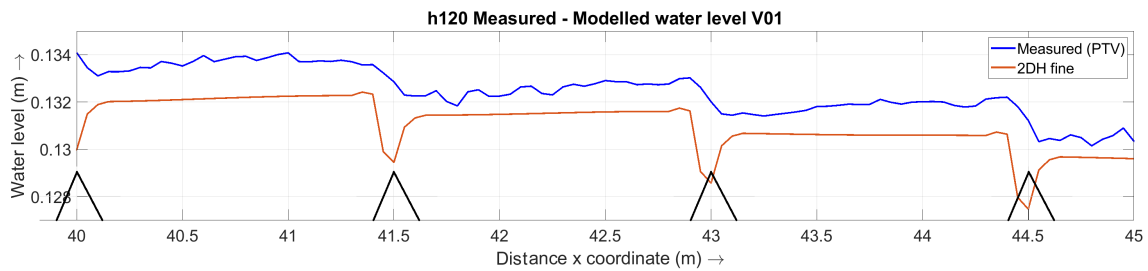
As described in Section 2.6.2 the discharge over a sub-grid weir is based on the upstream energy head and downstream water level. The energy loss is subsequently iteratively calculated based on the deceleration losses between the upstream and downstream flow velocity. But when the streamlines separate from the leading edge the effective momentum carrying cross-section is smaller than the water depth on top of the sub-grid weir. This is analogous to an upside down submerged sluice gate (onderspuier).

4.4.2. 2DH Fine grid

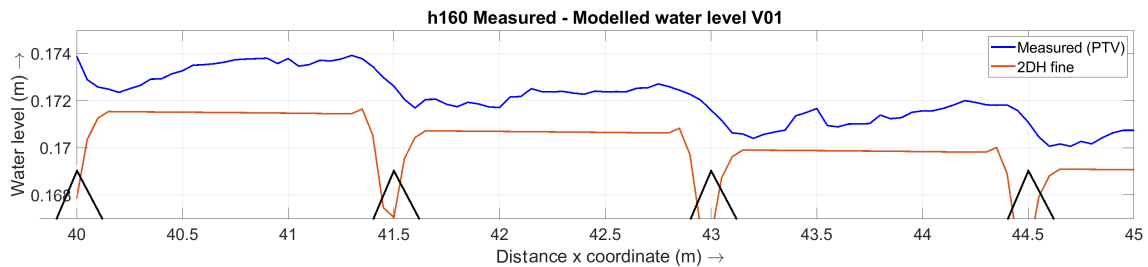
When the groynes are included in the bed topography (on the 5 cm by 5 cm grid) the energy losses introduced by the groynes can only be due to the lateral momentum exchange and deceleration of the depth averaged flow velocity downstream of a groyne. With a depth averaged model no vertical separation zone can be resolved downstream of the groynes, so the more significant this vertical separation zone becomes the worse the model is capable of capturing the correct energy losses. The used advection scheme is the second order accurate Flood scheme (Deltares, 2014) with a MINMOD flux limiter (Stelling and Duijnmeijer, 2003). This is designed for rapidly varying flow over steep obstacles by applying energy conservation for contractions and momentum conservation for expanding flow.

In the data analysis it is shown that for the h160 case the water level in the groyne field sets up more compared to the h120 case (see Figure 3.3). When comparing the PTV measured water levels in the groyne fields with the modelled water levels from the 2DH fine grid model it is visible that the water level is virtually horizontal, while over the groyne the drop in water level is too big, see Figure 4.6. So the water level drop happens only over the upstream slope of the groyne and set up of the water level only at the downstream slope where the flow decelerates. This is because no separation zone is resolved that increases the length over which the flow widens.

Therefore the model can only be correct when the water level is more or less horizontal in the groyne fields and the net water level drop (drop - set up) is correct. This happens for lower water depths and can explain why the h100 case is modelled accurately in terms of calculated water level and discharge.



(a) h120 Measured and 2DH fine grid modelled water level detail



(b) h160 Measured and 2DH fine grid modelled water level detail

Figure 4.6: Water level detail through groyne fields at $y = 2.25$ m. In the PTV data it is visible that the water level set up is larger for a larger water depth. And that in the 2DH fine model the water level set up only happens at the downstream slope of the groyne.

The modelled depth averaged velocity is difficult to compare with the data because from the PTV data only surface velocities are known. At $x = 44.5$ m the ADV measurements give a possibility to compare the depth average velocities in a cross-section on top of a groyne. What is clear is that the modelled depth averaged velocity on top of the groyne is higher than the measured velocity, see Figure 4.7. As the model conserves the energy head for contracting flows the modelled head corresponds well with the measured head. In order to have a correct energy head the water level drops too much while the depth averaged velocity increases too much, see Figure 4.7.

Because the energy losses by the groynes are underestimated a larger fraction of discharge flows over the groynes and a smaller fraction flows through the main channel. Due to this overestimation of the discharge through the groyne fields the flow velocity is higher than when a correct discharge would be modelled. The higher flow velocity in the groyne fields and lower flow velocity in the main channel lead to a smaller gradient in the mixing layer that therefore generates insufficient energy dissipation.

A 2DH fine model does not capture sufficient energy losses for submerged groynes. This is because the energy losses in the separation zone are not resolved. Even an advection scheme which is energy conserving for accelerating flows and momentum conservative for decelerating flows even does not include sufficient losses. Therefore modelling of groynes as part of the bed topography would not yield correct results for the water level and discharge distribution between groyne fields and the main channel.

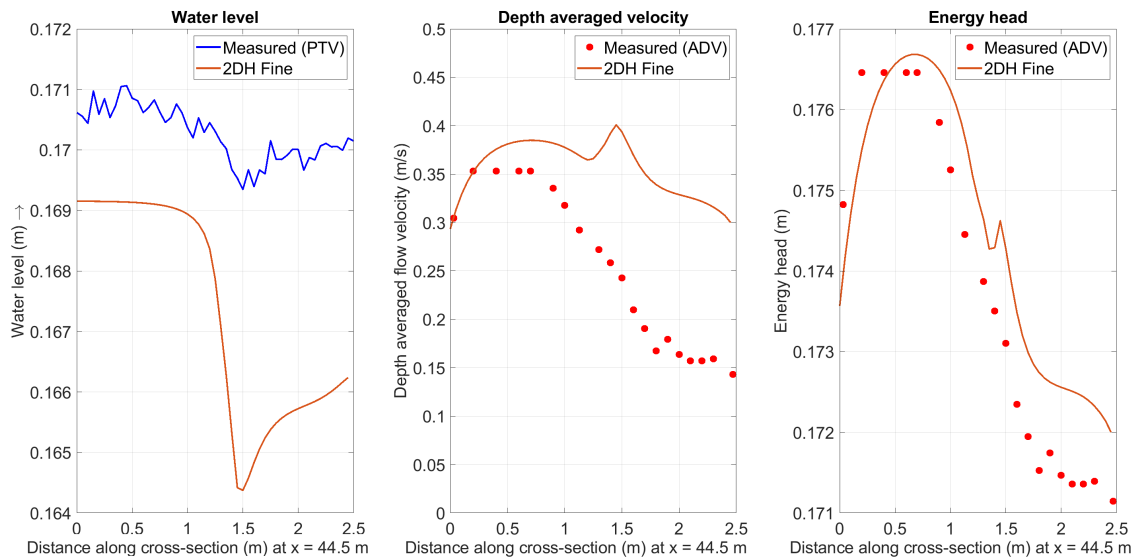


Figure 4.7: 2DH fine grid, groynes included in bed topography. Water level, depth averaged flow velocity and energy head along the cross-section at $x = 44.5$ m. For the h160 case.

4.4.3. Conclusions 2DH models

Both the coarse and the fine grid 2DH models underestimate the resistance of the groynes for strong submerged groynes. The energy losses are too small for both the sub-grid weirs as groynes and the groynes that are included in the bed topography. Both models perform equally well for emerged groynes and just submerged groynes. For stronger submergence the performance of the coarse-grid model with the sub-grid weirs is better than the fine grid model. When the groynes are part of the bed topography only the advection scheme influences the energy losses via the conservation of momentum and energy. There are no parameters that influence the losses over groynes so:

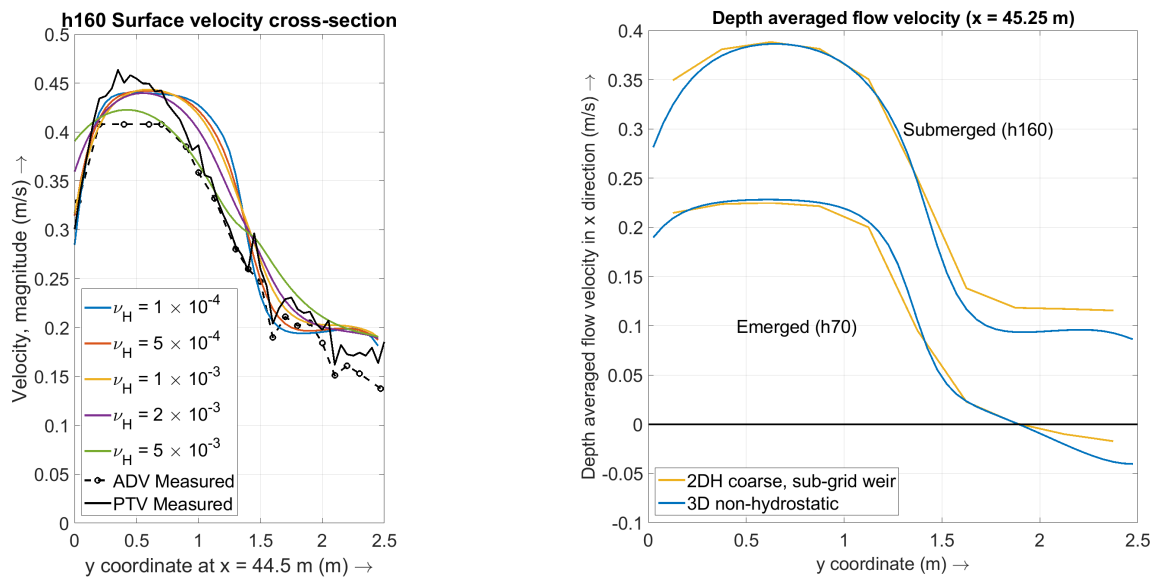
- A 2DH model where the groynes are represented only in the bed topography is not suited to simulate a laboratory experiment with very smooth groynes.
- Discharge distribution between the groyne fields and main channel is off. Too much discharge flows over the groynes and through the groyne fields.
- As a consequence, the velocity gradient between the main channel and groyne fields is too small which leads to too little resistance by lateral shear in the mixing layer.

When groynes are represented as sub-grid weir formulations the energy losses underestimated as well. However a possibility lies in including a calibration coefficient to change the rating curve for the used weir formula. Just like in the 2DH fine grid mode the discharge through the groyne fields is too large. The velocity gradient between the main channel and groyne fields is too small which leads to too little resistance.

- A 2DH model where the groynes are represented by sub-grid energy losses offers better performance than a 2DH model where the groynes are represented in the bed topography.
- It offers flexibility to include an additional calibration parameter.
- However, in practice this calibration parameter is very difficult or impossible to determine.

4.5. 3D and 2DV modelling

In the 3D models groynes are included in the bed topography but there is also an option for sub-grid weirs (Deltares, 2014). The same cases and boundary conditions are modelled as in the 2DH simulations. That is with the measured discharge as upstream boundary or with the measured water level as boundary condition. The 3D model resolves velocity gradients in the vertical and can resolve non-hydrostatic pressures. The horizontal eddy viscosity is determined by calibrating the water level for the emerged groyne cases. Also the effect of the eddy viscosity on the mixing layer width at the surface is compared directly with the BAW data results from Section 3.6. For the h160 case detailed vertical velocity profiles along the cross-section are available at $x = 44.5$ m and some vertical profiles at 44.75 m, 45.5 m and 45.75 m. For an overview of these measurements see Figure 3.15. The goal of the 3D non-hydrostatic models is to get insight in the 3D flow patterns because they resolve the full 3D momentum equation and therefore incorporate all aspects of the flow that introduce resistance.



(a) Influence of the horizontal eddy viscosity on the surface velocity for the h160 case. A value of $1 \cdot 10^{-3} \text{ m}^2/\text{s}$ is used

(b) Flow velocity in the 2DH coarse model with sub-grid weirs and 3D non-hydrostatic model. In the middle of the groyne field at $x = 45.25$ m.

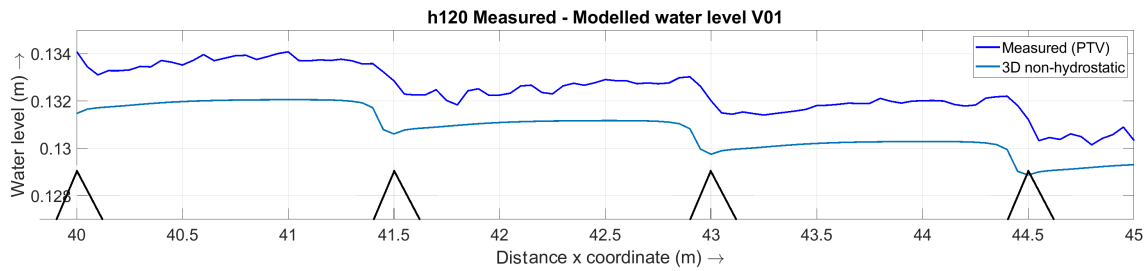
4.5.1. 3D Non-hydrostatic: Delft3D

Both the emerged and submerged cases are modelled with the 3D non-hydrostatic Delft3D model. The horizontal eddy viscosity is used as calibration parameter to calibrate the water level for the emerged cases (h60, h70 and h80). The sensitivity to the horizontal eddy viscosity (ν_H) of the mixing layer for the h160 case is tested. For the ν_H value that was found in the calibration the width of the mixing layer and the maximum gradient are found to match the measured mixing layer width and gradient, see Figure 4.8a.

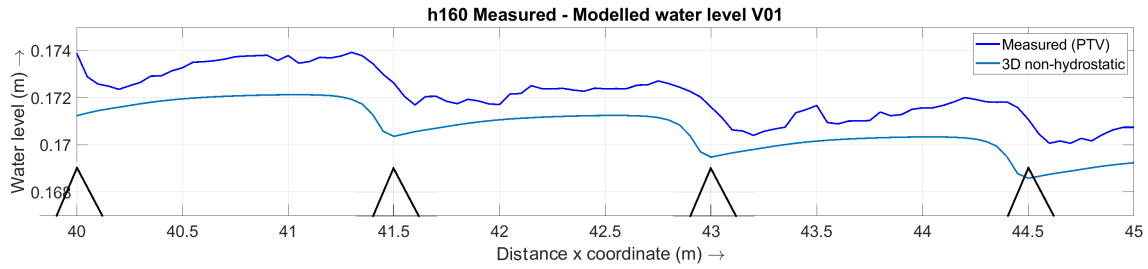
In the 3D non-hydrostatic simulations with the measured discharge as upstream boundary condition the resulting upstream water levels are too low, i.e. the water level slope is too small. See Figure 4.3 and Figure 4.4a. This means that the energy losses due to the groynes are too small. This effect is larger for high water levels however less pronounced compared to the 2DH simulations. The water level drop and subsequent set up over groynes correspond very well with the PTV data, see Figure 4.9.

In Figure 4.9 it stands out that the location of the lowest water level on top of groyne is consequently some 15 cm downstream from the modelled location. The location of the local minimum in the 3D model is just on top of the groyne crest. This implies that the streamlines are already horizontal on top of the groyne in the 3D model. No further drop in water level is possible. This implies that the modelled separation zone is as high as the groynes while in BAW experiment the effective height is higher than the groyne height.

This has consequences for the velocities as well. Because the drop in water level is too small, the increase



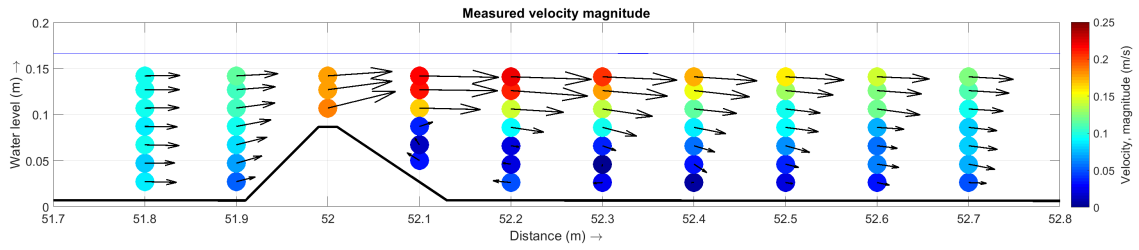
(a) h120 Measured and 3D non-hydrostatic modelled water level detail



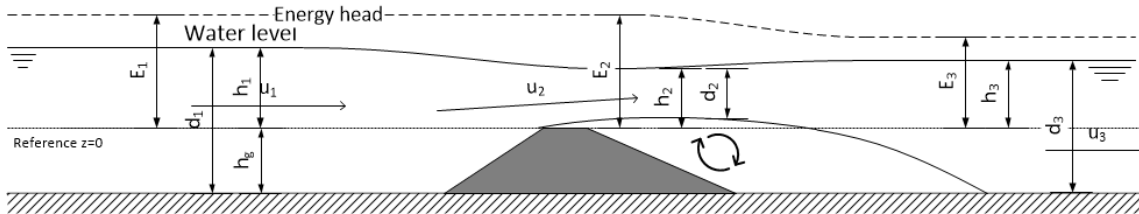
(b) h160 Measured and 3D non-hydrostatic modelled water level detail

Figure 4.9: Water level detail through groyne fields at $y = 2.25$ m. In the PTV data it is visible that the water level set up is larger for a larger water depth. And that in the 2DH fine model the water level set up only happens at the downstream slope of the groyne.

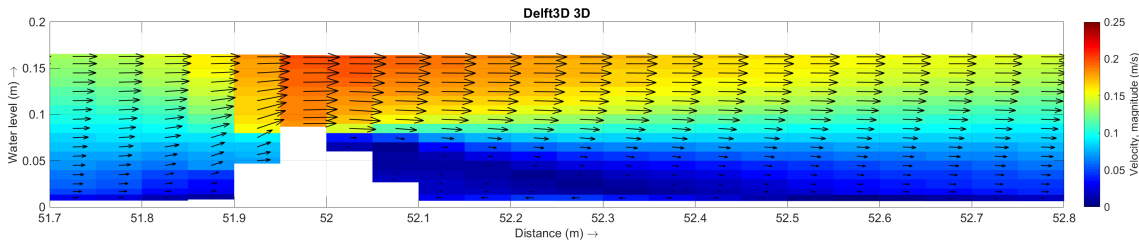
in velocity is also too small. This can be clearly seen in Figure 4.10a. The result is that the modelled deceleration of the flow is smaller than the actual deceleration. Because the energy losses due to flow expansion directly depend on deceleration of the flow the 3D non-hydrostatic model underestimates the energy losses.



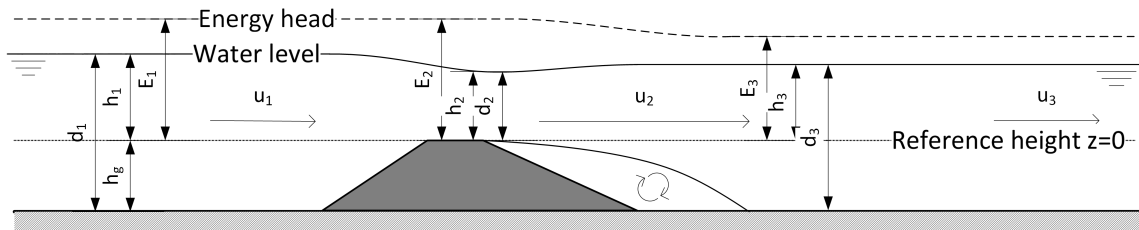
(a) PTV measured velocity just upstream and in the groyne field of the groyne at $x = 52$ m



(b) Schematic drawing of flow separating from the leading edge of the weir, analogous to the measurements



(c) Model velocity in recirculation cell in 3D non-hydrostatic Delft3D



(d) Schematic drawing of flow separating from the downstream edge a weir, analogous to the Delft3D 3D non-hydrostatic model

Figure 4.10: Comparison modelled velocity details with measured velocity details for the h160 case. Also the analogy with the schematic drawing is made to indicate the shortcomings of the 3D model.

The consequence of this is that the modelled maximum surface velocity is lower than the measured one. This can be seen for both the h120 (Figure 4.11a) and h160 case (Figure 4.11b). The underestimation of the surface velocity is stronger for the h160 case than the h120 case. For both the h120 and h160 case the location of the peak is shifted in the same way as mentioned when the water levels were discussed. The surface velocity peak in the model results is right on top of the groyne crest while in the PTV measurements it is around 2 times the groyne height (around 15 cm) downstream. Furthermore it is clearly visible that the modelled surface velocity in the groyne field stays high for too long. Also it decelerates not as much as the measurements show, see Figure 4.11. Together the too low maximum surface velocity and the too high minimum surface velocity generate too little energy losses in the 3D non-hydrostatic model.

Because the 3D model resolves gradients in the vertical the cross-sectional velocity profile can be directly compared with the ADV measurements from the h160 case as discussed in Section 3.6.2, see Figure 4.12. At two locations ($x = 44.5$ m and $x = 44.75$ m) the ADV measurements are compared with the 3D non-hydrostatic model. The first location is along the cross-section over the groyne crest and the second is in the separation zone. What can be seen is that the modelled velocities are higher almost everywhere. This is because for the

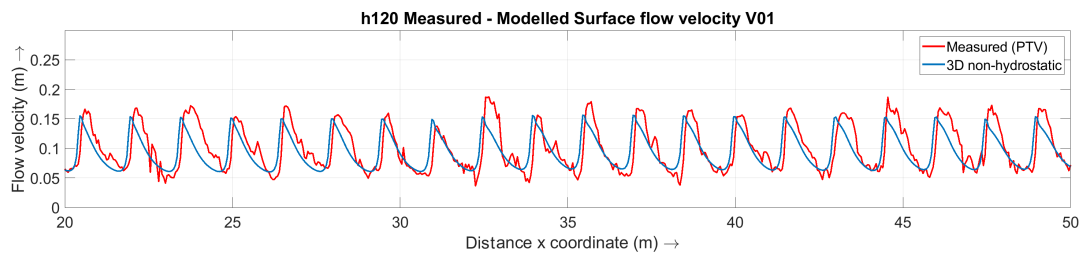
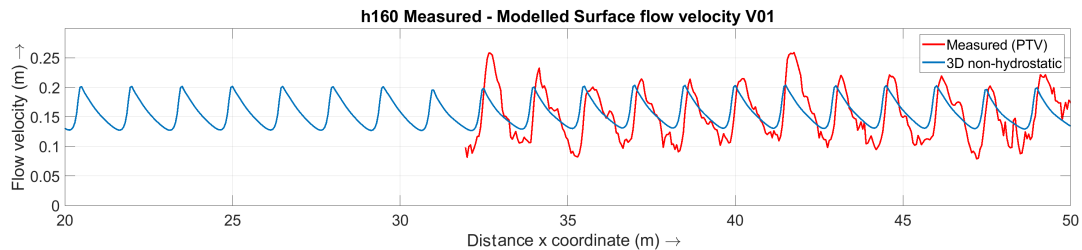
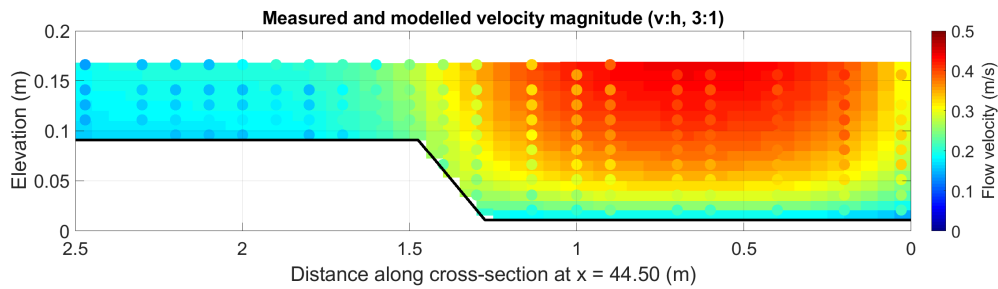
(a) h120 Measured and modelled surface velocity at $y = 2.25$ m.(b) h160 Measured and modelled surface velocity at $y = 2.25$ m.

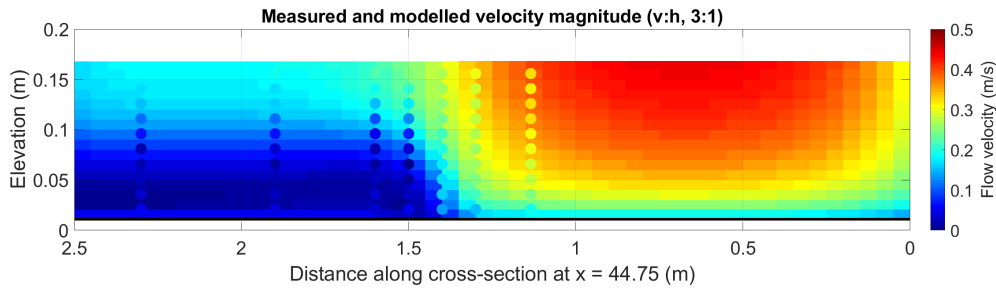
Figure 4.11: PTV measured and 3D non-hydrostatic modelled surface velocity through the groyne fields. The modelled maximum velocity is too low and shifted upstream. The modelled minimum is higher compared to the measured value, especially for h160. The modelled velocity difference is therefore smaller than in reality leading to an underestimation of the energy losses.

model with a total discharge as boundary the water level is too low and for the model with the correct water level as boundary condition the discharge is higher than measured, both leading to higher flow velocities. Furthermore the modelled velocity on top of the groyne is too high and increases from the crest to the surface. While the measurements show a more constant flow velocity with the maximum near the crest, see Figure 4.12a.

In the separation zone the flow velocities near the bed in the groyne field are directed upstream. What stands out is that the vertical location of the horizontal axis around which the velocities change direction is modelled too low, see Figure 4.12b. This indicates that the modelled separation zone is lower than the actual separation zone. Based on the PTV measurements of the surface velocity and water levels it is expected that for stronger submergence (h160, h200) the effects increases.



(a) h160 Measured and modelled vertical velocity profile at $x = 44.5$ m. The dots are the ADV measurements and the background are the simulated values with the 3D non-hydrostatic model.



(b) h160 Measured and modelled vertical velocity profile at $x = 44.75$ m. The dots are the ADV measurements and the background are the simulated values with the 3D non-hydrostatic model.

Figure 4.12: ADV measurements (dots) compared with the 3D non-hydrostatic model. The 3D model overestimates the velocity because the energy losses are too little. The vertical velocity profile on top of the groyne crest does not show the maximum value near the crest but near the surface. And in the separation zone the horizontal axis around which the flow direction reverses is too low in the 3D model.

The discharge distribution between the groyne field and main channel is slightly off in the 3D non-hydrostatic model. Too little energy losses are caused by the groynes so too much discharge flows through the groyne fields and too little through the main channel.

Sub-grid weirs can be used in combination with a 3D model too. This means that the energy losses are computed sub-grid and added to the momentum equation. In the same way as implemented in 2DH. In 3D gradients in the vertical are resolved. This means that when the sub-grid weir extends over multiple computational layers flow separation is modelled. Effectively the flow then accelerates and decelerates twice. First sub-grid and then over the existing separation zone, see Figure 4.13. This leads to an overestimation of the energy losses and therefore the resistance. The consequence is that the modelled water level at the upstream boundary is too high.

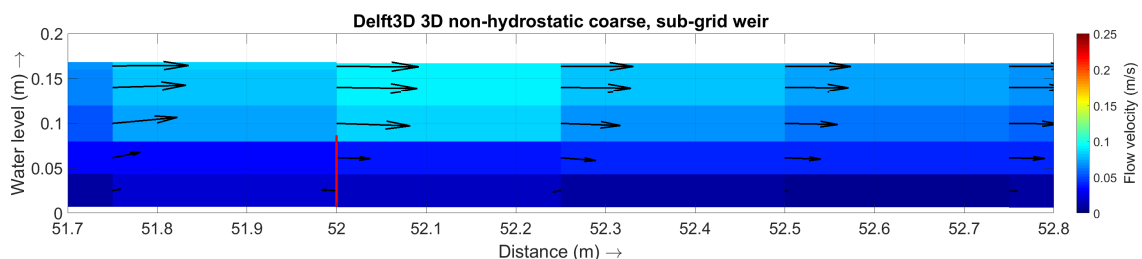
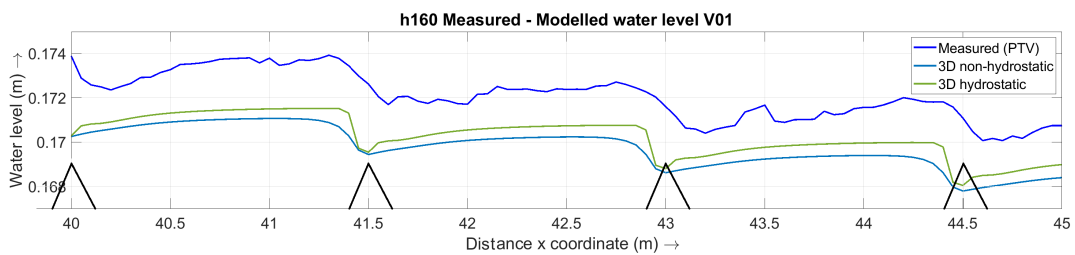


Figure 4.13: 3D coarse model velocity detail over a sub-grid weir. Because the sub-grid weir extends over 2 computational layers the flow effectively accelerates and decelerates twice.

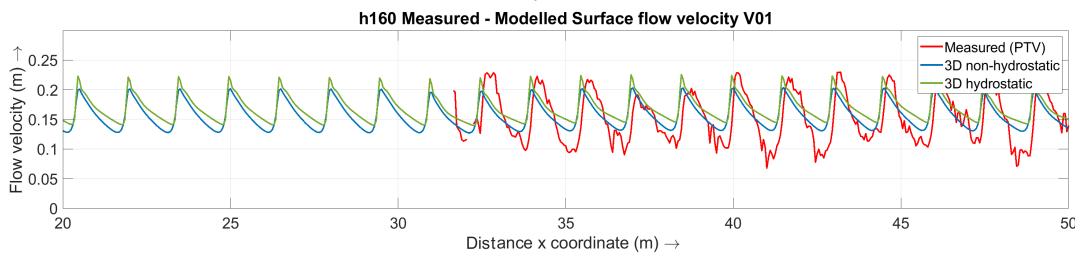
Making use of sub-grid weirs in 3D does not give reasonable results when the sub-grid weir exceeds the height of a computational layer.

4.5.2. 3D Hydrostatic: Delft3D

In the hydrostatic model the vertical momentum equation is reduced to the hydrostatic pressure relation. The pressure only increases with increasing water depth. This means that no underpressure zone is formed at the groyne crest and in the separation zone. Consequence is that the flow can accelerate more over the groyne compared to the non-hydrostatic cases. This leads to a larger drop in water level over the groyne. But also the set up in groyne field is larger, see Figure 4.14a. Leading to a very similar water level slope as in the non-hydrostatic case. The deeper water level drop leads to higher maximum flow velocities over the groynes. However also the minimum surface velocities in the groyne fields are higher, see Figure 4.14b. It appears that the energy loss due to the flow expansion is coincidentally very similar. However the discharge distribution between the main channel and groyne fields is less accurate than the non-hydrostatic model, see Table 4.3. The hydrostatic model overestimates the discharge that flows through the groyne field more than the non-hydrostatic model. Because there are significant vertical accelerations in the flow velocity the hydrostatic model is not suited to model the BAW experiment.



(a) h160 Measured and modelled water level detail at $y = 2.25$ m.



(b) h160 Measured and modelled surface velocities at $y = 2.25$ m.

Figure 4.14: PTV measured and 3D modelled (Delft3D) water levels and surface velocities. In the 3D hydrostatic model the water level drop is steeper and larger. Consequently the maximum surface velocity is larger but the minimum in the groyne fields is higher.

The comparison between the 3D hydrostatic and 3D non-hydrostatic Delft3D models shows a small difference in the location of the reattachment point, which is a measure for the length of the separation zone. Contrary to what Jongeling (2005) and Mosselman (2018) described, the flow reattaches closer to the groyne in the hydrostatic model than in the non-hydrostatic model, see Figure 4.15. The difference in the length is small, only 5 cm on a separation zone length of 45 cm. This is due the fact that the flow decelerates less in the groyne fields in the hydrostatic model, thereby underestimating the energy losses which leads to more discharge through the groyne fields. The higher flow velocities lead to the flow reattaching closer to the groyne, see Figure 4.15.

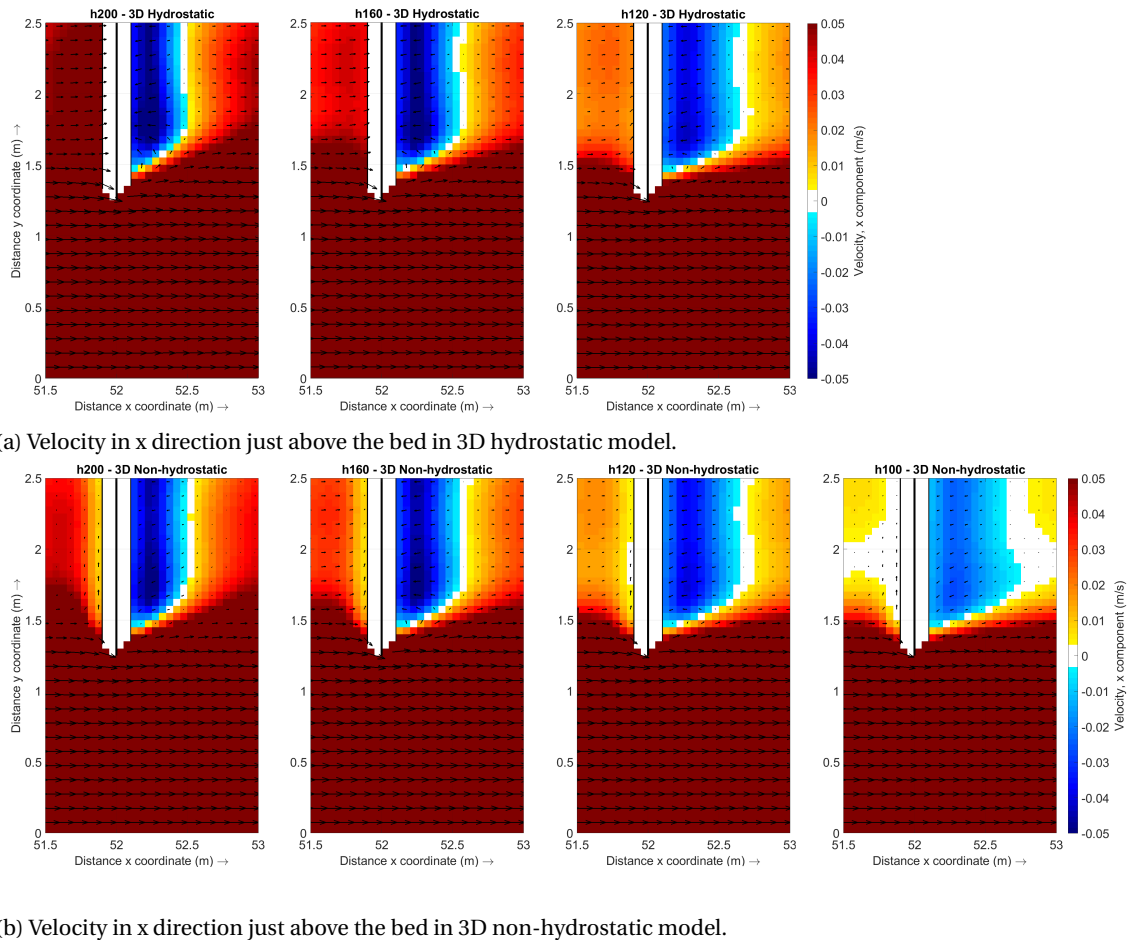


Figure 4.15: The length of the separation zone decreases with increasing water depth and subsequent increase in flow velocities in the groynes field. The figure shows the x component of the flow velocity just above the bed in the 3D hydrostatic and non-hydrostatic model.

4.5.3. 3D Non-hydrostatic: Finel

Finel is a fully three-dimensional non-hydrostatic flow model based on the Finite Element Method (FEM), which is suitable for the simulation of (shallow) water flow and transport processes in rivers and coastal areas. It employs the complete Navier-Stokes equations without a-priori assumptions regarding the vertical pressure distribution (Labeur, 2009; Labeur and Wells, 2012), which makes the model suitable for simulating flows with significant 3D effects like vertical separation. The use of an unstructured mesh (consisting of triangular and tetrahedral elements) offers a lot of flexibility for the incorporation of complex geometries in a numerical grid. This also makes local grid refinement rather easy, both in horizontal and vertical direction (the local vertical element resolution can be adapted in a flexible way).

The 3D results given by Finel are similar to those by Delft3D (non-hydrostatic). In terms of 3D hydrodynamics, both models should give the same results if sufficient mesh resolution is present (apart for some model-specific numerical parameters and design differences). As described in Section 4.1, local grid refinement is applied in the vicinity of the groynes; furthermore, within the scope of the Finel computations carried out, only discharges are applied on behalf of the upstream boundary condition (Delft3D sometimes applies upstream water levels as well).

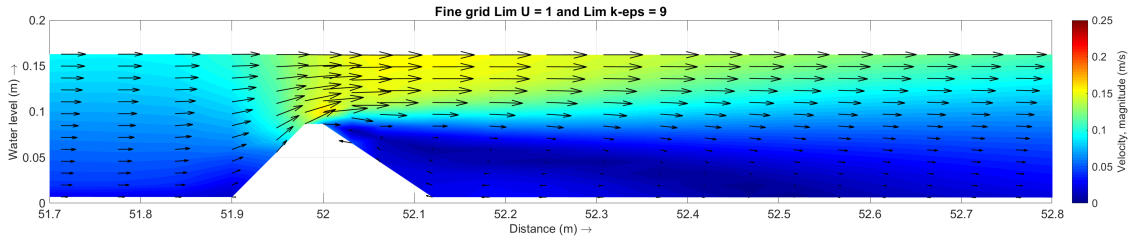
When the default settings within Finel are used, the flow over the groyne separates at the downstream edge of the groyne crest. Hence, the same discrepancy between measurements and model results (as found within default Delft3D results above) will occur here, see Figure 4.17b.

In order to improve the above default performance of the 3D model, a number of adaptations have been implemented with respect to the flux limiters that act on the momentum balance and the $k-\epsilon$ turbulence model. Adaptive flux limiters that allow local numerical "overshoots" near the bed level have been added to Finel by Harmen Talstra. The strict requirement that no such overshoots are allowed by the flux limiter is be-

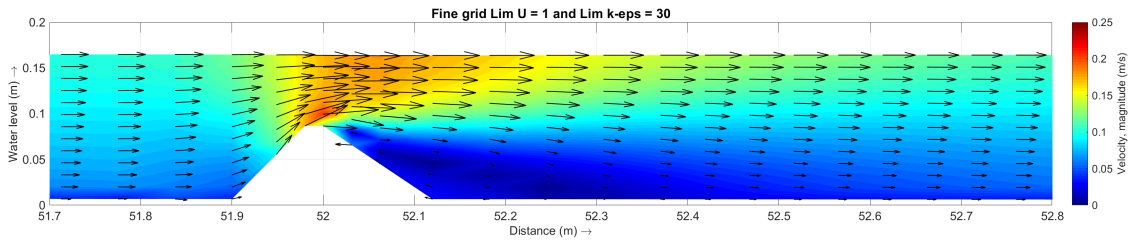
ing relaxed locally near the bottom, which results in steeper bottom boundary layer gradients (especially for the horizontal flow velocity and the turbulent kinetic energy dissipation ϵ). This improves the vertical velocity profile on top of the groyne crest, see Figure 4.16, but also along the flat bed in the main channel. (This flux limiter-induced improvement turns out to be especially important for high-resolution 3D models in which horizontal and vertical resolution are in the same order of magnitude; for coarser horizontal mesh resolution in shallow water ($\Delta x \gg \Delta z$), the default flux limiter within Finel yields good results without adaptations.)

The separation zone length is strongly influenced by the applied flux limiters as well, see Figure 4.16b. Because the acceleration of the flow over the groyne is larger when the adapted flux limiters are used, the energy loss per groyne will become larger. It is observed that the over-all model performance is improved.

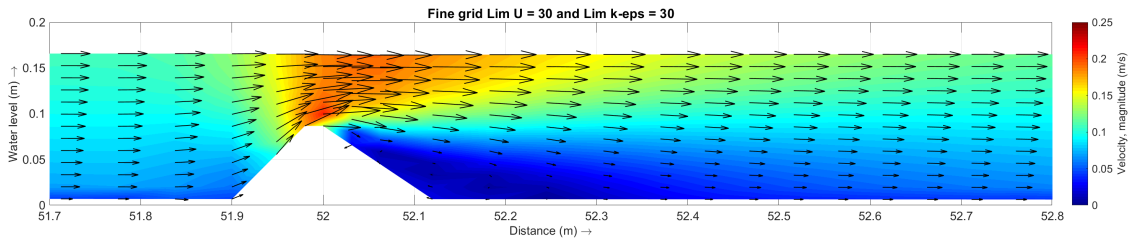
Limiters in Finel



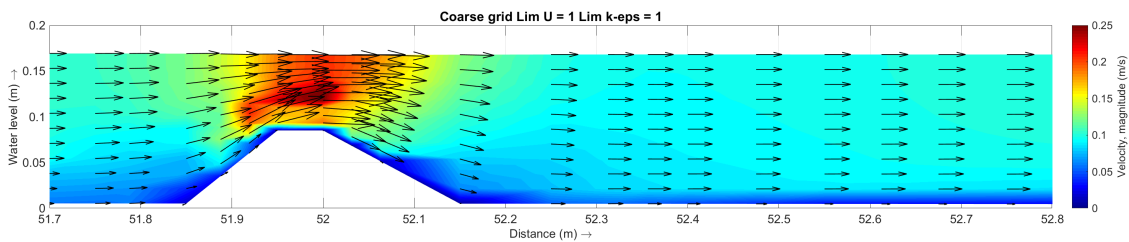
(a) Modelled velocity detail in Finel with: Limu=1 and Limeps=9



(b) Modelled velocity detail in Finel with: Limu=1 and Limeps=30



(c) Modelled velocity detail in Finel with: Limu=30 and Limeps=30



(d) Modelled velocity detail in Finel with coarse grid and: Limu=1 and Limeps=1

Figure 4.16: Comparison of velocity details applying different flux limiter settings within Finel. Legend: lim = 1 is no limiter; lim = 9 is the standard slope limiter in Finel; lim = 30 is the relaxed slope limiter.

4.5.4. 2DV and 1D: Delft3D: Groyne vs. weir comparison

To check if the insufficient energy losses resolved by the 3D non-hydrostatic model are due to the grid size a 2DV model with a grid size of 1 cm by 0.5 cm (x by z) is used. The specific discharge over the centre of the groynes from the 3D non-hydrostatic simulation are used as upstream boundary and the downstream boundary is the measured water level. Four submerged cases (h100, h120, h160 and h200) are modelled, see Figure 4.18 for the h120 and h160 cases.

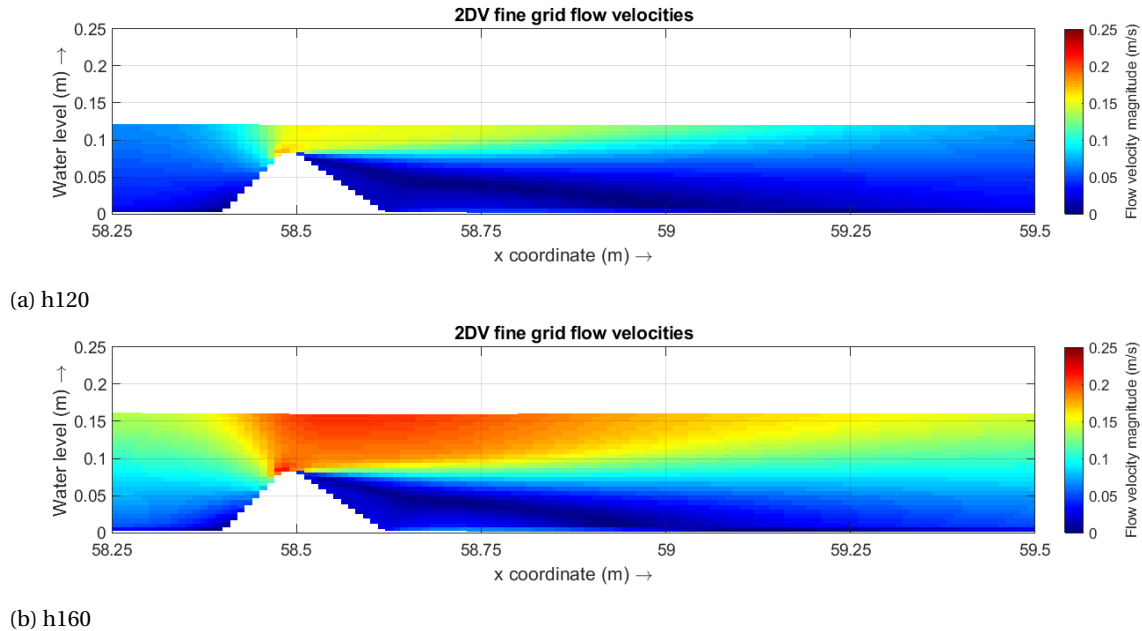
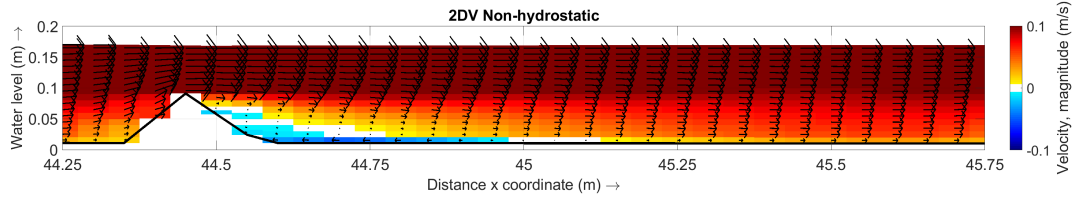


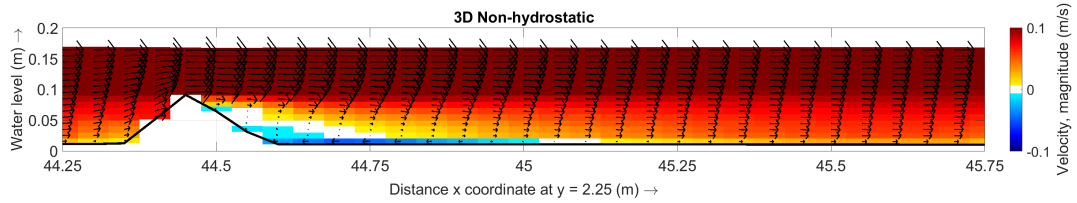
Figure 4.18: 2DV non-hydrostatic, super fine grid modelled vertical velocity profiles for two submerged cases (h120 and h160). Upstream discharge boundary based on specific discharge determined by the 3D non-hydrostatic model and downstream measured water level boundary.

The vertical velocity profile right on top of the groyne crest shows a larger maximum near the groyne crest. This is a slight improvement compared to 3D non-hydrostatic model. However the location of the maximum surface velocity is still too close to the groyne crest. The streamlines are already horizontal just after the crest, see Figure 4.17e. So local grid refinement to 1 cm alone is not sufficient to capture the flow that separates from the groyne crest accurately. Further refinement at the crest could improve the performance (Moss, 1972; Lamballais et al., 2010). This is not tested during this thesis work.

Also a 2DV model with a grid with a resolution of 5 cm (in x direction) is used to directly compare a groyne with a weir. The upstream boundary conditions for the 2DV are taken from the discharge that flows over the groyne at $x = 44.5$ m and $y = 2.25$ m in the 3D non-hydrostatic model. This allows for a direct comparison of the flow over a weir and the flow over a groyne with the same discharge. A the 2DV weir shows a slightly higher resistance. The vertical velocity profile over the weir and over the groyne does not show a significant difference and neither do the flow velocities in the separation zone, the separation zone length and the underpressure, see Figure 4.19 and 4.20. This is true for $1.75 \text{ m} < y < 2.5 \text{ m}$. For $y < 1.75 \text{ m}$ the separation zone becomes smaller until it is vanished at the tip ($y = 1.3 \text{ m}$), see Figure 4.15.

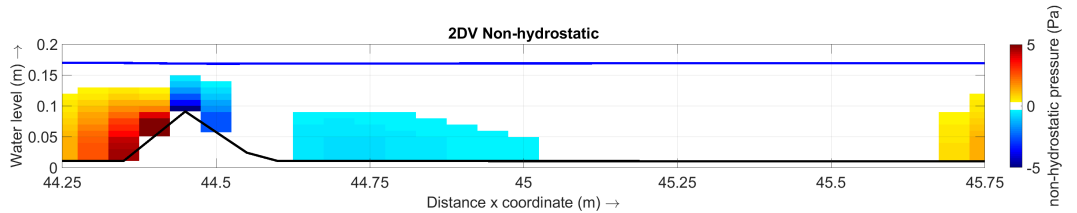


(a) Weir: Velocity in the separation zone behind the weir for the h160 case.

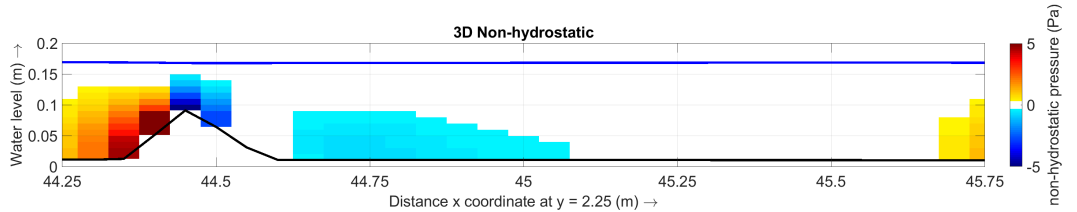


(b) Groyne: Velocity in the separation zone behind the groyne at y= 2.25 for the h160 case.

Figure 4.19: The non-hydrostatic pressure distribution shows no significant difference between the 3D groyne and 2DV weir model when the same specific discharge is used. The blue line represents the water level.



(a) Weir: Non-hydrostatic pressure in the separation zone behind the weir for the h160 case.



(b) Groyne: Non-hydrostatic pressure in the separation zone behind the groyne at y= 2.25 for the h160 case.

Figure 4.20: The length of the separation zone shows no significant difference between the 3D groyne and 2DV weir model when the same specific discharge is used.

The water level over the whole length shows only a minor difference at the first groyne (see Figure 4.21, which is because the energy losses over the first groyne in the 2DV weir model are smaller as the logarithmic vertical velocity profile at the upstream inflow boundary is based on a lower discharge than the 3D groyne model for the h120 case. For higher water levels (h160 and h200) the maximum difference in the upstream water level is 2 mm.

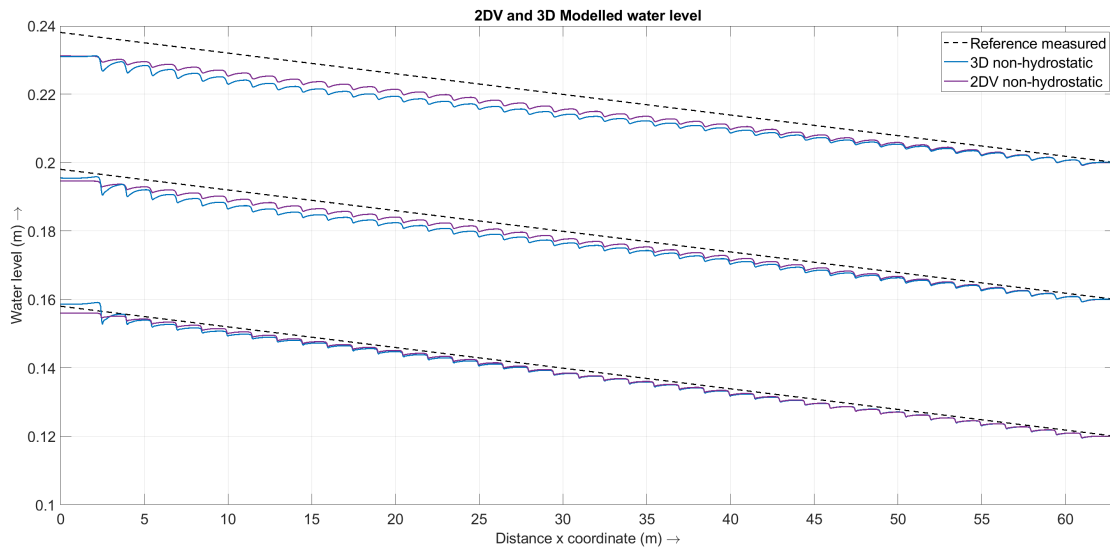


Figure 4.21: 3D non-hydrostatic vs. 2DV weir groyne comparison. Modelled water level in longitudinal section over the groynes and weirs for the different water depth conditions (h120, h160 and h200). Both the groynes and the weirs are resolved in the bed topography.

The same analysis is done to compare the 2DH coarse-grid with sub-grid groynes model with a weir model. This weir model is only a 1D representation of the groyne fields. The discharge that is applied at the upstream boundary is taken from 2DH coarse-grid model. So the same effect is visible as in the 3D groyne and weir comparison, the first weirs have a slightly lower losses because the discharge does not have to redistribute. Again no significant difference between the 2DH sub-grid groynes and the 1D weirs is visible, see Figure 4.22.

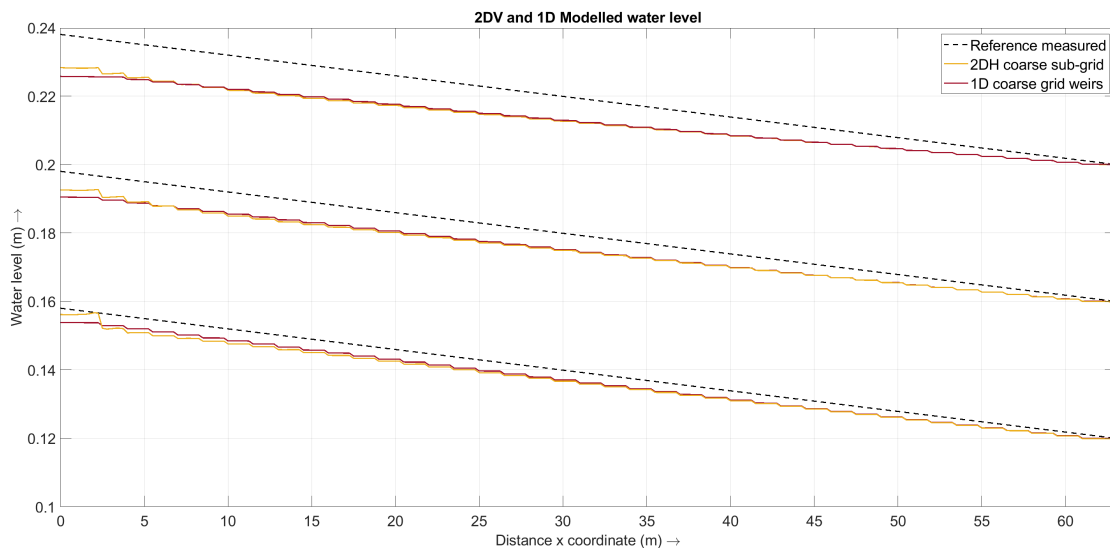


Figure 4.22: 2DH coarse-grid sub-grid groynes vs. 1D sub-grid weir groyne comparison. Modelled water level in longitudinal section over the groynes and weirs for the different water depth conditions (h120, h160 and h200). Both the groynes and the weirs resolved as sub-grid energy losses.

4.5.5. Conclusions 3D models

The 3D models in which the groynes are included in the bed topography underestimate the energy losses due to the groynes. This means that the resistance is underestimated leading to an underestimation of the water level or overestimation of the discharge capacity. When sub-grid weirs are used in a coarse 3D model and the sub-grid weir exceeds the height of one computational layer the resistance is overestimated leading to too much energy losses. This is because the flow effectively accelerates and decelerates twice. Thereby dissipating energy twice.

The 3D non-hydrostatic fine grid models perform better than the 2DH models, especially when looking at the discharge distribution between the main channel and the groyne field. The limitations of the 3D models are modelling the separation at the upstream edge of the groyne crest and the deceleration in the groyne field. Because the models do not capture the leading edge separation and corresponding upward directed streamlines at the groyne crest the separation zone height is smaller than measured. The modelled separation zone starts at the downstream edge of the groyne crest and thus extends over the height of the groyne only. The consequence is that the flow does not accelerate as much as in reality. In the 3D non-hydrostatic models the flow velocity over the separation zone in the groyne fields stays high longer than measured and has a higher minimum than measured. This together with the underestimation of the maximum velocity lead to a velocity difference that is too small. As the energy loss in a separation zone is determined by the velocity difference an underestimation of this difference leads to an underestimation of the energy losses.

In order to improve the performance of the 3D models the resolution near the crest could be increased. However, the effect of this measure is limited: the vertical velocity profile on top of the groyne is modelled more accurately, yet the minimum flow velocity within the groyne fields is not influenced by this measure. In order to induce stronger flow deceleration in the groyne fields, flux limiters (which prevent over- and undershoots of the modelled velocity and turbulence model quantities) can be adapted, e.g. in the manner described in Section 4.5.3 (acceptation of near-bed overshoots). This has been tested in Finel, which has shown promising results.

Summarising:

- A 3D non-hydrostatic model where groynes are included in the bed topography gives the most accurate results concerning the energy losses induced by submerged groynes.
- The discharge distribution between the main channel and groyne fields is a lot better than in the 2DH models.
- Still the modelled discharge through the groyne fields is slightly too high.
- Flow separation at the upstream edge of the groyne crest is important but not resolved by the fine grid Delft3D model.
- Deceleration of the flow after the groyne is too low.

To improve the models the following two improvements appear promising:

- Local grid refinement near groyne crest. Both in vertical and horizontal direction.
- Adaptive flux limiters for the flow velocity and energy dissipation.

4.6. Conclusions on numerical models

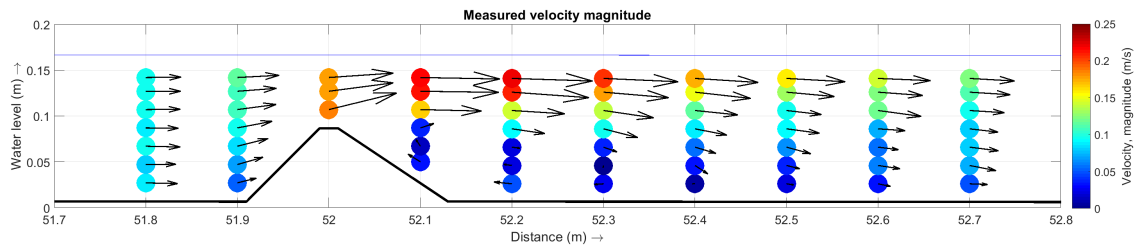
For the geometry of the groynes as used in the BAW experiment the following conclusions can be drawn with regard to 2DH and 3D numerical modelling:

- The resistance in the numerical models is underestimated, i.e. the energy losses are too small leading to a too low water level.
- 2DH fine grid model with groynes included in the bed topography is not suitable for strongly submerged groynes.
- 2DH coarse model with sub-grid weirs performs better than the 2D fine-grid model when considering the water level but worse when the discharge distribution is considered.
- 3D non-hydrostatic model performs the best. It is, however, not perfect because the leading edge flow separation is not modelled correctly when the grid is too coarse and flux limiters are too strict.
- All used models have the same deficiency, that is that the actual height of the separation zone is not well resolved.
 - In the sub-grid weir formula the flow carrying cross-section should be smaller to increase the velocity maximum, analogous to a submerged sluice gate (onderspuier).
 - In the 2DH model with groynes resolved in the bed topography no additional parameters can be altered.
 - In the 3D non-hydrostatic models the grid can be optimised together with the flux limiters for the velocity and energy dissipation.
- The horizontal mixing layer is sensitive to horizontal eddy viscosity. The resistance depends on the value of the horizontal eddy viscosity.

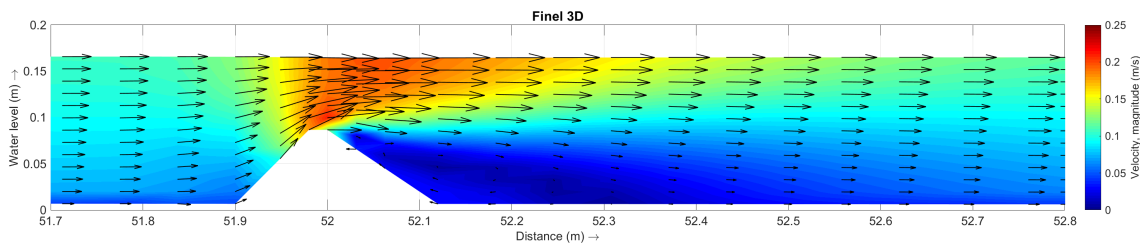
The numerical models show no significant difference between the flow over a groyne and a weir when same specific discharge flows over a section of a groyne that is away from the tip this results in the same energy losses as when that discharge would flow over a weir. In this flume lay-out the length over which the groyne has a 2DV character is 0.75 m from the side wall. This is 3/4 of the length of the horizontal crest. With increasing water depth only a minor deviation from this length is found, around 5 cm. Both the sub-grid and bottom topography implementation of the weirs and groynes give very similar results. Although the sub-grid weirs and groynes in the 2DH coarse and 1D coarse models have less energy losses compared to the 3D and 2DV models.

Based on the available data and descriptions found in literature it appears that the 3D non-hydrostatic models resolve the observed and measured flow patterns well. Thereafter comparing the numerical models it becomes clear that discharge through the groyne field is overestimated by the 2DH models. As a consequence the influence of the mixing layer is underestimated which decreases the energy losses.

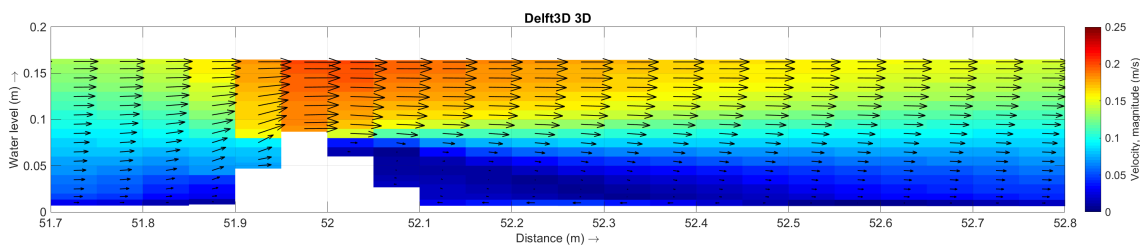
The implication of these findings are that when modelling a river reach that consists of floodplains, groynes and a main channel the influence of lateral shear due to mixing layers is influenced by the discharge distribution between the parts of the cross-section. So when the discharge through the groyne fields is overestimated the velocity gradient between the main channel and groyne fields is underestimated. At the same time the gradient between the floodplains and the groyne fields can be overestimated.



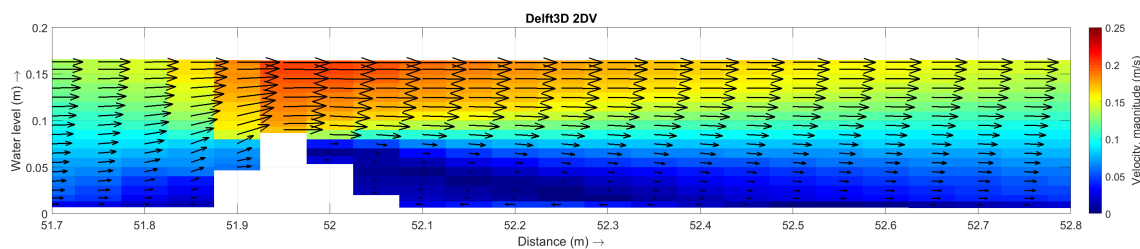
(a) Measured velocity in recirculation cell (Baron and Patzwahl, 2013)



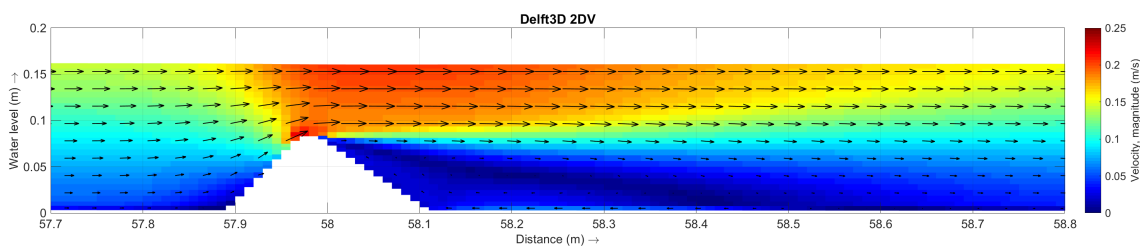
(b) Model velocity in recirculation cell in 3D non-hydrostatic Finel



(c) Model velocity in recirculation cell in 3D non-hydrostatic Delft3D



(d) Model velocity in recirculation cell in 2DV Delft3D



(e) Model velocity in recirculation cell in 2DV Delft3D super fine grid (1 cm)

Figure 4.17: Comparison modelled velocity details with measured velocity details.

Groyne adaptations

As stated in Chapter 2 numerical models are used to evaluate if measures to improve navigability and flood safety are feasible. In the Room for the River programme the effects or measures are presented in water level decrease for a given design flood discharge. So to investigate the effectiveness of measures numerical models are used. Based on these models decisions are made to spend money on projects. To be able to make good decisions the accuracy of the model is important. To investigate the performance of the models, both in the 2DH coarse-grid and in 3D model, groynes are lowered.

No experimental data is available for the modified groynes. So only a comparison is made between the models (2DH vs. 3D) and between lowering and streamlining (3D only). The comparison between the models gives an indication of the reliability of the models when evaluating the effectiveness of measures as groyne lowering and streamlining.

Lowering of the groynes is modelled with the 2DH coarse-grid model including sub-grid weirs and in 3D non-hydrostatic Delft3D models. Streamlining cannot be modelled by the sub-grid implementation in Delft3D. So only a comparison can be made between different downstream slopes in the 3D non-hydrostatic model. The grid used for the 3D non-hydrostatic model has a horizontal resolution of 5 cm, so the geometry of the groyne crest cannot be changed.

The goal is to see if the 2DH and 3D models perform differently and if so if the effect of lowering is either over- or underestimated.

5.1. Lowering

Lowering of groynes gives a positive effect, i.e. in submerged conditions the energy loss due to the groynes decreases and therefore the upstream water level is lowered, see Figure 5.2.

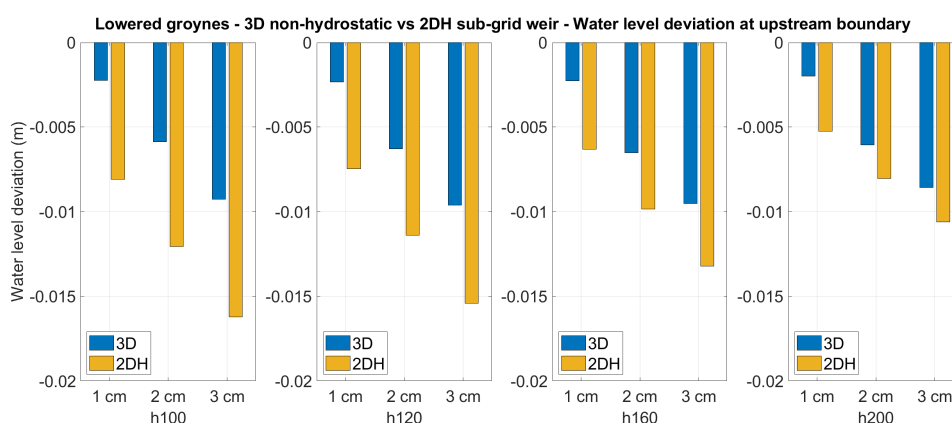
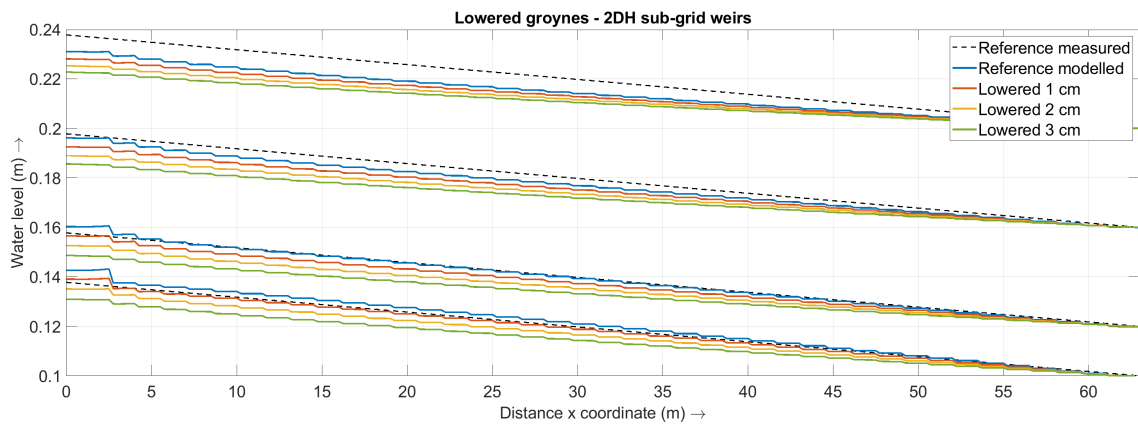
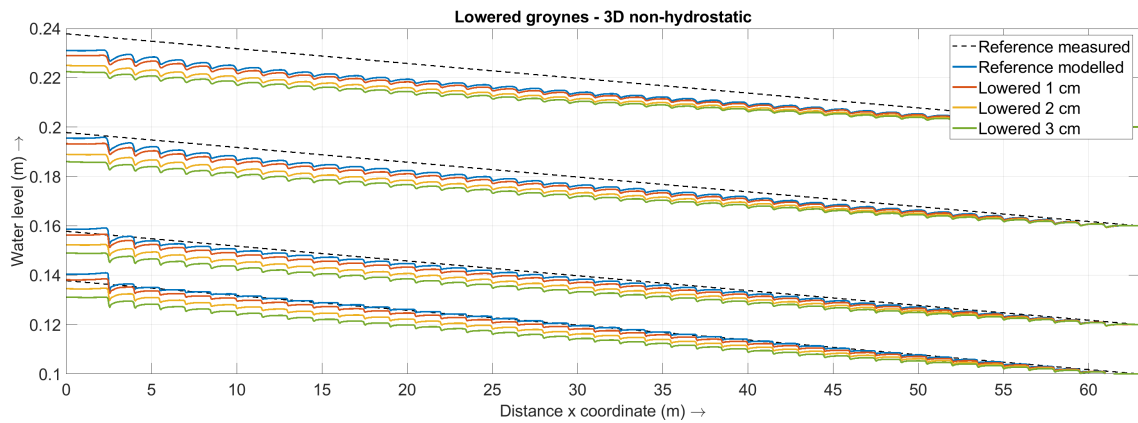


Figure 5.1: Comparison of the upstream water levels for the different lowered groynes. The 2DH coarse model predicts a much larger effect of the lowering of groynes than the 3D non-hydrostatic model. However for increased discharge the difference becomes smaller.

The results of the 2DH and 3D simulations are directly compared, see Figure 5.1. The coarse 2DH model with sub-grid weirs predicts a stronger effect of the lowering than the 3D non-hydrostatic model.



(a) Effect of lowered groynes on water level for with a constant discharge.



(b) h160 Measured and 2DH fine grid modelled water level detail

Figure 5.2: Water levels along the longitudinal section at $y = 2.25$ m in for lowered groynes. Modelled in 2DH with a coarse grid and sub-grid weirs (5.2a) and in 3D with groynes included in the bed topography (5.2b)

The discharge distribution between the main channel and groyne fields changes. More discharge flows over the groynes and through the groyne fields. Because the groynes are lower the flow carrying area increases, therefore flow velocity stays higher in the groyne fields, see Figure 5.3. The energy loss due to the deceleration is thus smaller than in the reference case. Also the velocity gradient in the horizontal mixing layer decreases and therefore energy losses due to lateral momentum exchange decrease as well. Both these effects decrease the energy losses due to submerged groynes which is beneficial for the discharge capacity.

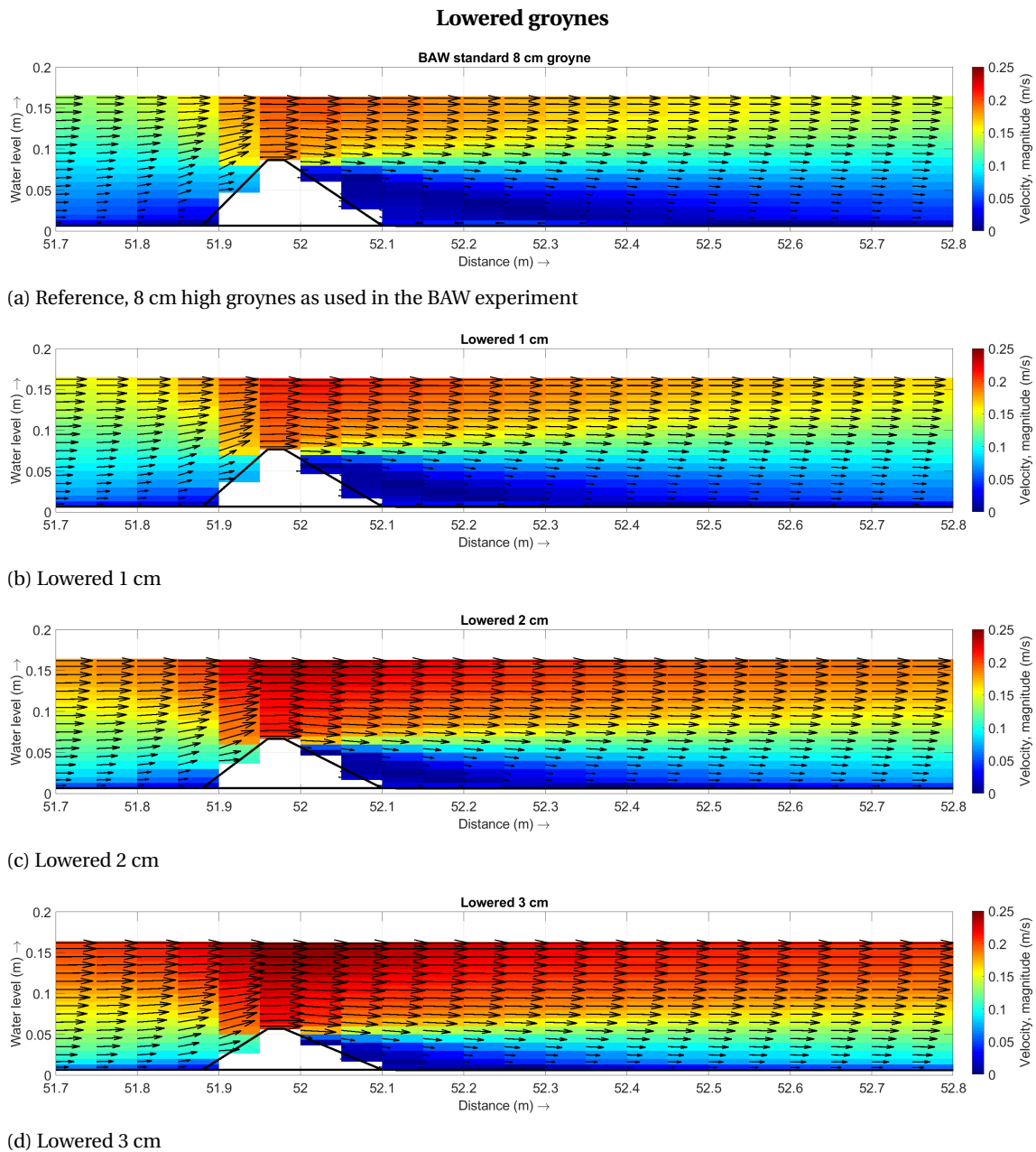


Figure 5.3: Magnitude and direction of the flow velocity modelled with the 3D non-hydrostatic model along $y = 2.25$ m. For the h160 case with the groynes used in the BAW experiment and lowered groynes.

The 2DH coarse model gives a much larger effect of the lowering of groynes than the 3D non-hydrostatic model. So compared to the 3D model the 2DH model overestimates the effect of lowering of groynes. Because the 3D non-hydrostatic model simulates a much more accurate discharge, distribution between the main channel and the groyne field, than the 2DH coarse model it is likely that the sub-grid weir formulas overestimate the effect. In this experimental setup the groynes extend over almost half the cross-sectional width and the groyne fields are equally deep as the main channel. The effectiveness of groyne lowering is therefore higher than in reality.

5.2. Streamlining

When groynes are streamlined the geometry of the groyne is changed. The leading edge of the crest is curved and the downstream slope angle is decreased. The effect is that the streamlines at the leading edge are less

curved and flow separation occurs further downstream or not at all. By decreasing the slope angle of the downstream slope the separation can be prevented completely. For slopes smaller than 1:8 (V:H) no flow separation occurs, see Bloemberg (2001); Wirken and Bladel (2004). Because the height of the groynes is the same the discharge distribution between the main channel and groyne fields does not change as much as when the groyne are lowered. The energy loss due to deceleration over the groynes decreases because the flow does not separate at the downstream edge. Thus no recirculation cell is formed, see Figure 5.4.

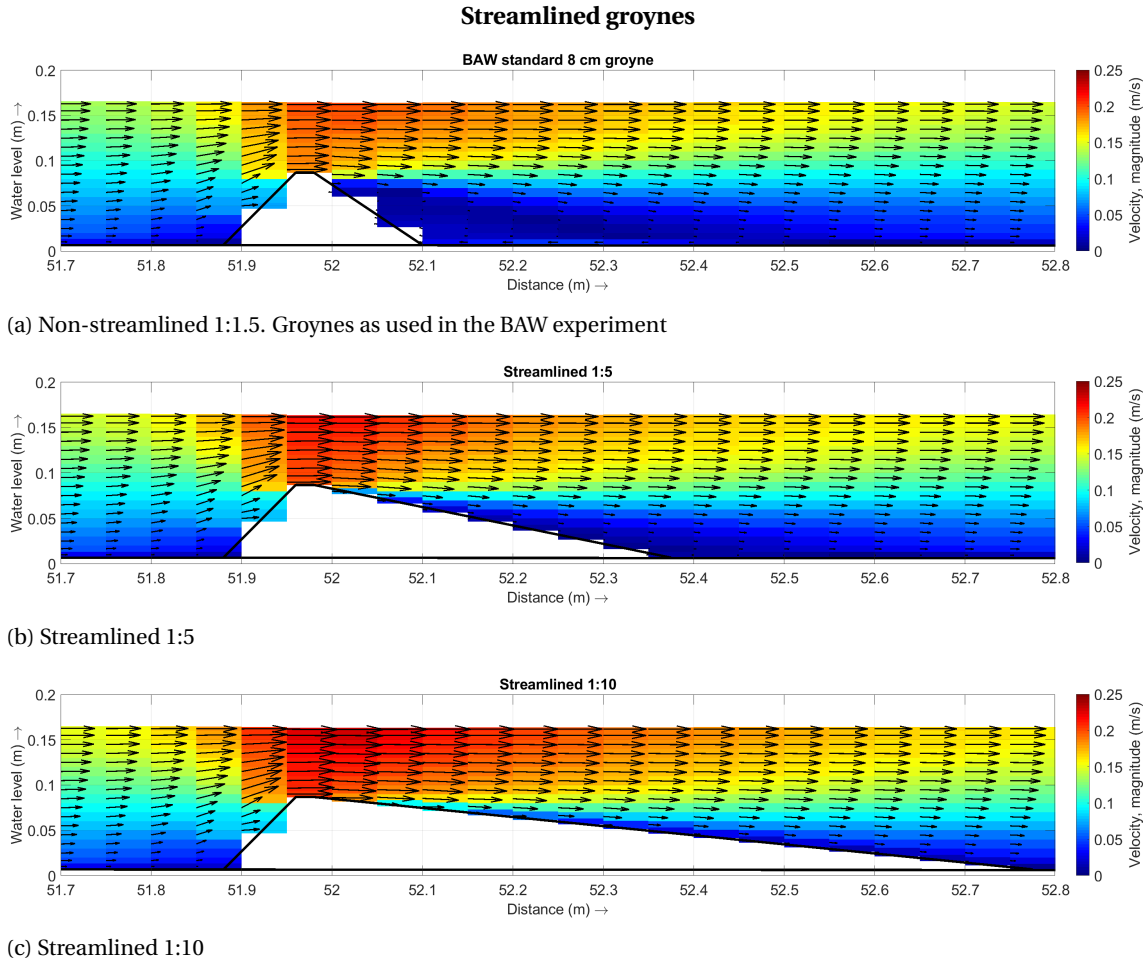


Figure 5.4: Magnitude and direction of the flow velocity modelled with the 3D non-hydrostatic model along $y = 2.25$ m. For the h160 case with the groynes used in the BAW experiment and streamlined groynes.

From the 3D non-hydrostatic model results it is clear that the effect of streamlining the downstream slope from 1:1.5 to 1:5 (V:H) has the same effect on the upstream water level as lowering the groynes with 1 cm, see Figure 5.6. A small separation zone still occurs on the downstream slope. When further streamlining the downstream slope to 1:10 (V:H) no flow separation occurs but only a marginal reduction of the resistance is achieved, see Figure 5.5.

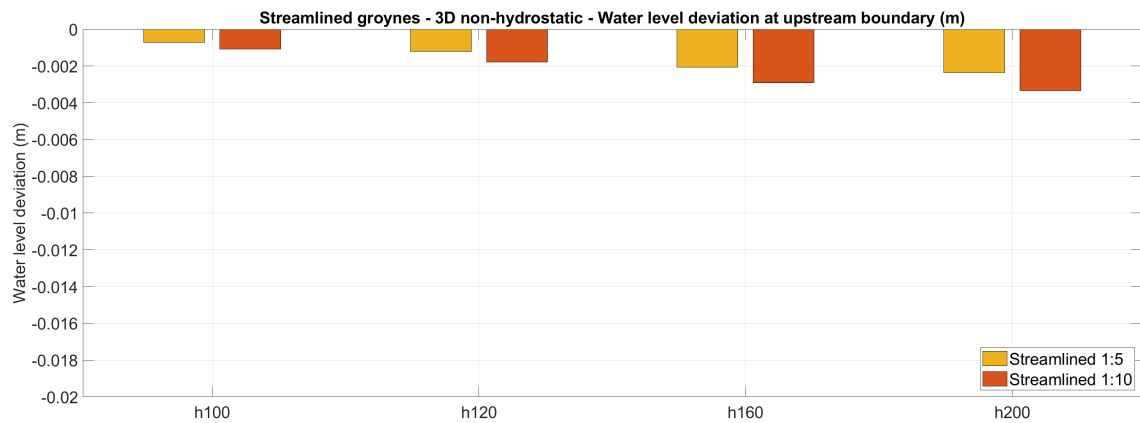


Figure 5.5: Effect of streamlining groynes on the water level. Modelled in Delft3D with the 3D non-hydrostatic model. The Effect of streamlining the downstream slope to 1:5 (V:H) is visible. The effect of further streamlining decreases.

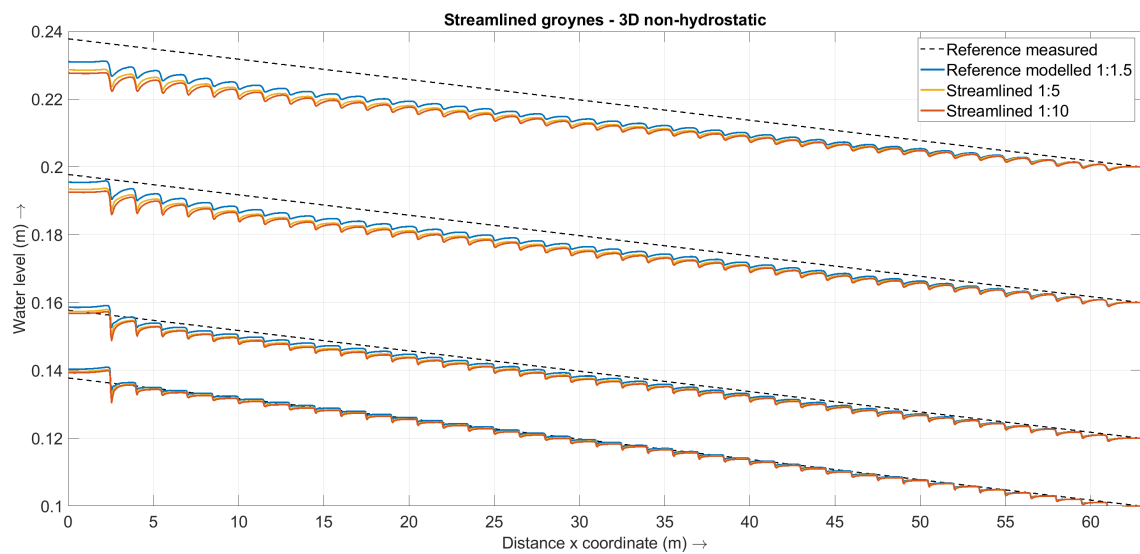


Figure 5.6: Effect of streamlining groynes on the water level. Modelled in Delft3D with the 3D non-hydrostatic model. The Effect of streamlining the downstream slope to 1:5 (V:H) is visible. And is stronger for increasing water depths.

5.3. Conclusions on groyne adaptations

Lowering and streamlining both decrease the energy losses and thereby the resistance. The water level therefore is lower for the same discharge compared to when the reference groynes are used. The 2DH coarse-grid model with sub-grid weirs results in a larger effect of lowering groynes. For a water depth of 10 cm and a lowering of 1 cm the 3D model calculates a lowering of the upstream water level of 0.2 cm while the 2DH model with sub-grid weirs results in a 0.8 cm lower water level at the upstream boundary. For very strong submergence (h200) the results of the 3D non-hydrostatic model and the 2DH model are closer to each other. Still for a lowering of 1 cm the difference in the upstream water level differs by more than a factor of 2.5 for the case with a water depth of 16 cm.

These results indicate that the effect of groyne lowering is overestimated when using sub-grid weirs. This large effect is explained by the larger discharge that flows through the groyne fields compared to the 3D model in the reference case. When the groynes are lowered more discharge flows through the groyne fields. In the reference case with the 8 cm high groynes the energy loss that is modelled with the sub-grid weirs is already lower than modelled with the 3D model. So when a larger fraction of the discharge flows through the groyne fields the larger the underestimation of the energy dissipation by the sub-grid weirs.

The effect of lowering becomes relatively smaller for larger depths. The effectiveness of streamlining however increases for larger discharges. The first lowering of 2 cm is the most effective. The effect of a 3 cm lowering based on the upstream water level is not 1.5 times as effective. see Figure 5.7. An optimal groyne design therefore could be lowered and streamlined groynes using the material from the crest to streamline the downstream slope.

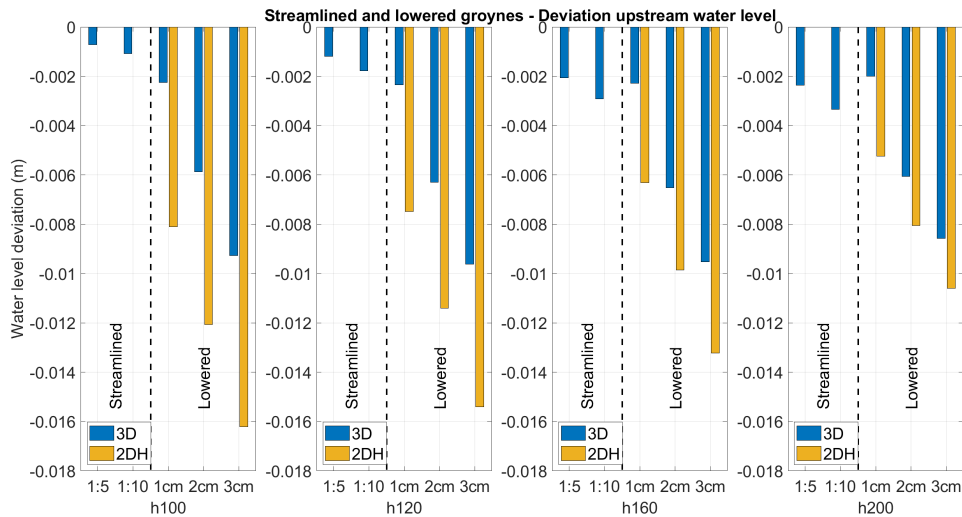


Figure 5.7: Effect of streamlining and lowering on the upstream water level.

It should be noted that in this lay-out the relative effectiveness of streamlining and lowering is larger than when a more realistic river section would be used. Because the groynes cover a large part of the cross-sectional width, no floodplains are included and the groyne fields are deeper than in reality. Above all the slope angle of the bed in the experiment is 6 times steeper than the bed slope of the River Waal. Hence in these experiments the fraction of the discharge that is influenced by the groynes is larger than in reality and the blocking effect of the groynes is exaggerated.

Implications on schematic cross-section of the Waal

The influence of groynes in this experiment are overestimated compared to a realistic river cross-section due to the following factors:

- Steeper slope of the flume than in the River Waal
- No floodplains in the BAW experiment
- Groyne fields are much deeper than in the river Waal
- Groyne spacing is smaller
- The slope angles of the groynes are steeper than real groynes

These factors all amplify the effects of groyne lowering and streamlining. In order to relate the results on the small scale to the real-scale the geometry are be up-scaled by a factor 75 to be able to relate the water depth of 16 cm to a value of 12 m which is close to the design flood water depth of approximately 13.5 m. See Table 5.1 for the relevant parameters.

Table 5.1: Up-scaled geometry of the BAW experiment with a factor 75.

	BAW Experiment	Upscaled (75 times)
Water depth (m)	0.16	12
Width (m)	2.5	187.5
Bed slope (-)	0.0006	0.0006
Discharge (m^3/s)	0.092	4481.68
Velocity (m/s)	0.295	2.5548
Froude number (-)	0.2355	0.2355

Only the bed slope is not accounted for by this Froude scaling. By applying the same scaling to the effects of groyne lowering the effect on the upstream water level of 1 cm would relate to a difference of 75 cm. Over a length an up-scaled length of 4725 m with 40 groynes this is too much. The influence of the bed slope and the groyne spacing as applied in the BAW experiment exaggerate the effect, so no absolute value can be given.

6

Discussion

Analysing the data from the BAW experiment and subsequently modelling the set up with different numerical models provides a lot of insight in the flow over and around groynes. However choices in the laboratory and numerical set up impose limitations on the applicability of the conclusions to full-scale situations and a different geometrical layout.

6.1. BAW groyne experiment: Materials and geometry

The experiment as conducted by the BAW resulted in high-density data which on its own already gives insight in the flow over and around groynes. In order to analyse the PTV data the data is projected on a grid. The measurement points from each particle track are averaged within a 5 cm by 5 cm area. This averaging method is used to compare the data with the numerical results easily. The influence of the area over which is averaged has been checked with a 1 cm and 2cm grid. The smaller the grid the more scattered the results but the location of the maximum drop in water level and maximum surface velocity did not vary significantly.

The averaging removes fluctuations in flow velocity and water level within a grid cell. By doing this only a time averaged view of flow properties is observed. Turbulent fluctuations are not derived from this data.

The geometry used in the BAW experiment has consequences for the applicability of this research to a full scale river with groynes. Some would lead to an increasing resistance of the groynes while others decrease the resistance compared a full-scale river reach. The experiment considers a straight flume whilst in reality low land rivers have a meandering character. Thus in reality the flow over groynes is not always perpendicular to the crest. This can have an effect on the length of the groyne which is affected by the mixing layer.

The geometry of the groyne influences the location of flow separation and hence the energy loss and discharge that flows over the groyne. In the BAW experiment it can be seen that for the submerged groynes the flow separates from the leading edge of the groyne. In practice groyne crests do not have such sharp edges as they are constructed with irregularly placed natural rocks or sometimes with a round crest of regularly placed smooth concrete blocks. Also the slope angles of the groynes from the experiment (1:1 and 1:1.5) are steeper than in reality (1:1.5 to 1:5 for both upstream and downstream slope).

The surface of the groynes in the BAW experiment consist of smooth concrete. This is smoother material than the rocks used in reality (see Figure 6.1). The roughness of the groynes in the experiment is thus smaller than that of the main channel and groyne fields. Whereas in reality the river bed and groyne fields have a sandy bed and the groynes are made of large rocks.

The groyne fields have the same depth as the main channel in the BAW experiment. And the bed level of the main channel is horizontal. In reality the groyne fields are sedimented and have a higher and sloping bed level (see Figure 6.1).

The groynes have a length of 1.2 m and the flume has a total width of 2.5 m. This means that the area that is blocked by groynes is a significant part of the cross-section. Together with the fact that the groyne fields are equally deep as the main channel the influence of groynes could be larger than in reality when groynes are around 60 m in a main channel that is 250 m wide. Moreover the cross-section of a real river has floodplains that contribute to the discharge that decreases the relative importance of the discharge over groynes.

Beside these choices regarding the geometry of the groynes the bed slope used in the experiment is $6.0 \cdot 10^{-4}$ m/m. This is a factor of 6 steeper than the average bed slope in the branches of the Dutch rivers.



Figure 6.1: The River IJssel (left) during extremely low discharge in November 2018 and the BAW flume (right). The difference in bed level of the groyne field can clearly be seen. Also the difference in bed roughness between the groyne and groyne field can be seen.

In general the mentioned properties of the experiment increase the importance of groynes. This makes it easier to model groynes, determine their effect on the resistance and compare different numerical models. However the consequence is that quantitative conclusions based on deviations between the modelled and measured water levels and discharge capacities are overestimated compared to a more realistic river cross-section including floodplains and realistic groyne geometry and material.

6.2. Numerical models: Limitations and modelling choices

The set-up of a numerical flow model requires a number of choices and restriction with respect to maximum allowable computational time and the required level of detail for analysis. In this study Delft3D and Finel have been used to model the described BAW groyne experiment. In Delft3D a structured grid is used whereas Finel applies an unstructured (and locally refined) triangular finite element mesh.

The fine grid used in Delft3D (both for 2DH and 3D simulations) has a horizontal resolution of 5 cm by 5 cm. The exact geometry of the groynes cannot be followed in full detail as the groyne crest is 2 cm wide. Due to the staggered grid approach employed by Delft3D, the actually modelled groyne geometry contains one velocity point half-way the crest width while the water level points are defined along the edges of the crest. Within Finel the velocity, water level and turbulence model quantities are calculated in the same nodes (co-located grid); this approach, in combination with the use of a locally refined unstructured mesh, allows for a more accurate high-resolution representation of the experimental set-up.

As for the coarse 2DH model set-up within Delft3D, this model does not feature the actual groyne shapes in the bed topography; instead, a sloped flat bed is used in combination with sub-grid weir parametrisations at the cell interfaces.

The calibration of the 2DH and 3D models on the case without groynes (V00) resulted in different bed roughness. Although the flume walls are made of glass, wall roughness turned out to be not negligible to get a fitting relation between the discharges and water levels for the uniform V00 case.

The calibration of the water level and discharge in the case with emerged groynes (V01) turned out to be very sensitive to the horizontal eddy viscosity. But also the modelling of submerged groynes is sensitive to the horizontal viscosity (both in 2DH and in 3D). Because in this experiment the relation between the discharge and the water level is known for a range of water depths and with and without groynes, the horizontal eddy viscosity can be used as calibration parameter. In reality it is not possible for 2DH real-scale river models to calibrate separately on bed roughness and horizontal eddy viscosity, because in reality groynes are always present. In the numerical models the eddy viscosity could be increased to widen the mixing layer between the main channel and the groyne field, thereby increasing the resistance. For the 2DH coarse and 3D models this results in a correct water level slope for that specific discharge but then the discharge distribution between the main channel and the groyne field is changed. In that case the model would be correct for the wrong reasons.

The limitations in grid resolution (given by e.g. computational effort requirements), both in vertical and horizontal directions, also put a limit on the accuracy of the model. As it turns out, the vertical velocity profile above the groyne crest strongly depends on the vertical resolution. The horizontal resolution in the vicinity of

the groyne also has a strong influence on the location of flow separation. For example, the Finel results show no separation if the resolution near the crest has been chosen too coarse.

The length of separation zone is slightly different (5 cm) for hydrostatic and non-hydrostatic computations. However, when the flux limiter within Finel is adapted in the way described in section 4.5.3, the flow decelerates over a shorter distance and thus the separation zone size is decreasing in length. This has been tested using Finel, see Figure 4.16.

Both in Finel and in Delft3D the measured discharge is imposed over the full width of the upstream boundary. This means that the discharge distribution between the groyne field and main channel takes some distance to adapt. When at the upstream boundary a water level is imposed the discharge flows into the model domain uniformly (over the width). In reality at the inflow boundary the discharge is not uniformly distributed over the width due to additional roughness elements (diameter 2 cm) that change the inflowing discharge distribution, see Figure 6.2. This means that in the experiment the losses over the first couple of groynes are not larger than the following groynes. This means that the model introduces a small addition loss over the first 5 groynes.



Figure 6.2: Upstream inflow boundary with increased roughness to distribute the discharge between the main channel and groyne field.

In the 3D models the discharge over the first five groynes is larger than over the subsequent groynes. This means that at these groynes the energy losses are slightly larger than over the 35 following groynes. In the 2DH fine-grid model where groynes are included in the bed topography also five groynes are needed for the distribution of discharge to adapt. The 2DH coarse-grid model with sub-grid weirs shows the same behaviour. However when increasing the calibration parameter for the energy loss by the sub-grid weir the losses over initial groynes is much larger than subsequent weirs. This is because the same discharge leads to a larger energy loss.

6.3. Scale effects and real geometry

The simplifications made in the experimental set up increase the influence of groynes compared to an actual river cross-section. Most important is the fact that in reality the groynes are a smaller part of the cross-section, i.e. the total discharge influenced by the groynes is smaller in reality. Therefore the effect of streamlining and lowering can not be directly up-scaled.

The energy losses in the separation zone due to deceleration are smaller when the groyne height is smaller with respect to the bed level in the groyne field. Also the geometry of the groynes in the experiment increases the losses compared to real groynes. The discharge capacity of groyne fields with sub-grid weirs is overestimated for strongly submerged groynes. This could be due to the upward directed leading-edge separation with a smaller effective flow carrying cross-section just downstream of the groyne leading to larger energy losses than when the flow would separate horizontally, at the downstream edge of the groyne crest.

In a real river section with less steep and rough groyne side slopes, or even streamlined crests, the effect of a larger separation zone could be less. In Delft3D the sub-grid weirs use the upstream energy head and downstream water level to calculate the discharge and iteratively the energy loss for flow velocities below 0.25 m/s, as occur in the BAW experiment. In real scale the flow velocities over the groynes can exceed flow velocities of 0.5 m/s (de Goede, 2012). In that case a table look-up function called "Tabellenboek" is used.

This Tabellenboek is based on data from weir experiments. In the transition between 0.25 m/s and 0.5 m/s a weighted average is used.

Due to the floodplains an additional mixing layer between the groyne field and the floodplains forms decreasing the length over which the lateral influence is negligible. Because this is not modelled in this research the influence on the resistance and subsequently water levels and discharge capacity is not known.

Conclusions and recommendations

7.1. Conclusions

What is the 3D flow structure over and around the groyne in highly submerged conditions?

Most of the discharge flows through the main channel (Q_{mc}), but part of the discharge flows over the groynes (Q_{gf}). The flow over the groynes accelerates over the upstream slope (1), leading to a pressure higher than the hydrostatic pressure, and separates from the leading edge (2). At the crest the pressure is lower than hydrostatic and the streamlines are directed upward (2). Downstream a separation zone is formed that is higher than the groyne (3). In the separation zone a recirculation cell is formed, where the pressure is slightly lower than hydrostatic. The length of this zone is constant from the side wall up to the place where the tip starts having influence (4). In this geometry that is at 3/4 of the length of the groyne crest. From that point towards the tip the separation zone shortens until it vanishes at the tip (5). The length of this zone depends on the flow velocity on top of the recirculation zone. The higher the velocity the closer the reattachment point is to the groyne. The flow near the surface is directed into the groyne field (6). The higher the water level the smaller the flow velocities directed into the groyne field are. The mixing layer (7) between the main channel and groyne fields becomes wider for increasing water levels. Near the bottom the flow is directed into the groyne field (8). The flow near the bottom hits the groyne and deflects towards the side wall, away from the main channel. Only over a small part of the tip the flow deflects to the main channel to flow around the tip and then flow towards the recirculation zone. In the recirculation zone the lateral component of the flow is directed towards the main channel up to a point close to the tip where it is virtually stagnant.

The part where the length of the separation zone is constant behaves the same as a weir (grey area). The specific discharge over the length is constant. It has the same energy losses as a weir, an equally long separation zone and the same flow velocities. In the region of influence of the groyne tip the separation zone length and the underpressure decrease to zero at the bottom of the groyne tip, in the main channel.

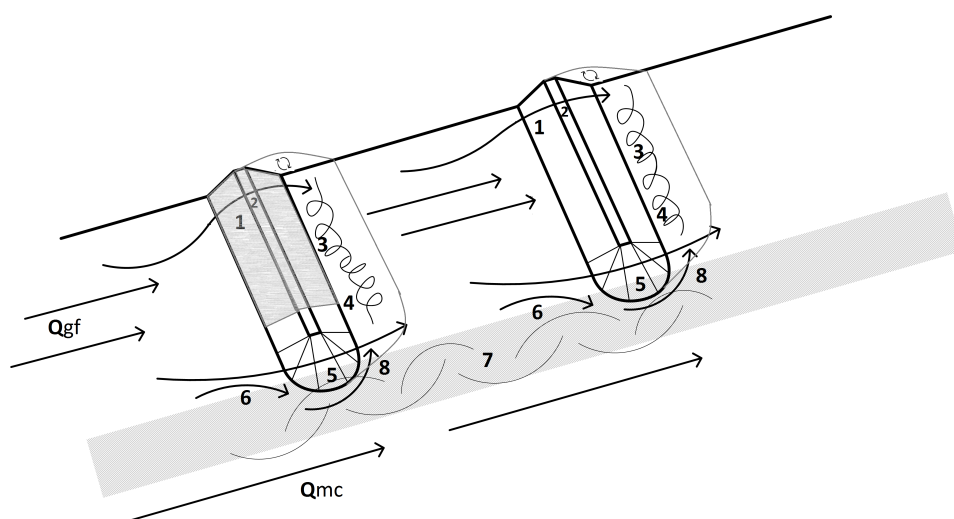


Figure 7.1: Schematic drawing of flow over and around submerge groynes

What processes influence energy losses over a groyne?

The processes that influence the energy losses over a groyne are the mixing layer and the deceleration losses. In the groyne field the flow velocity is lower than in the main channel. This results in a lateral gradient in the velocity, in this mixing layer mass and momentum is transferred laterally. In the mixing layer energy is also dissipated by the eddies that shed from the groyne tip. Due to the mixing layer the discharge over the groyne near the tip is larger than closer to the side wall. Near the tip the energy loss is smaller compared to the region near the wall where the 2DV character is dominant. This is because the deceleration of the flow velocity is smaller, leading to less deceleration losses. In the area where the groyne behaves as a weir the energy loss is only due to the deceleration losses besides the energy losses due to bottom friction.

Streamlining and lowering of groynes decreases the energy losses, because both the deceleration losses and losses due to the mixing layer decrease. Despite the increased fraction of the discharge that flows through the groyne fields when groynes are lowered the velocity deceleration is less. At the same time the gradient in the mixing layer becomes smaller, also leading to less energy loss as well. For streamlined groynes the flow does not separate from the crest, so no recirculation zone forms and therefore the deceleration losses decrease.

How well are these processes represented in numerical models?

The limitations of the 2DH and 3D non-hydrostatic models have become clearer during this research because of the direct comparisons that have been made with the measured and modelled cases. This comparison showed that the 2DH model with groynes represented in the bed topography produces too little energy loss for high submergence, leading to too much discharge flowing over the groynes. The 2DH coarse sub-grid model performs better but the 3D non-hydrostatic model performs the best. However, all models have too little resistance when the groynes are strongly submerged. This contradicts the idea that weirs would overestimate the resistance when compared to groynes.

The 3D non-hydrostatic models capture the processes very well. However due to a too coarse grid (in the vertical and horizontal) and too strict flux limiters for velocity and the energy dissipation (ε) the leading edge separation that occurs in this laboratory experiment is not captured in Delft3D. This leads to too little deceleration losses and subsequently to much discharge flowing through the groyne fields also decreasing the dissipation in the mixing layer. This can be improved by locally refining the grid near the groyne and changing the flux limiters to allow for more overshoots in the velocity and turbulence quantities in the numerical solutions.

In the 2DH model in which the groynes are included in the bed topography the energy losses are underestimated because no vertical separation can be captured. This makes such a model not suitable to model steep gradients in bed levels such as groynes. To be able to use 2DH models with a coarse grid and steep bottom features that are too small to be represented in the grid a sub-grid energy loss is directly added to the momentum equations based on the water level difference on top of the crest and downstream of the crest. The way this is implemented in Delft3D results in too little energy losses. Subsequently the discharge and velocity in the groyne fields are too high, further underestimating the energy losses in the mixing layer. When the horizontal eddy viscosity would be calibrated on a case with strong submergence the water level would be correct but for the wrong reason. The mixing layer would be smeared out too much and the discharge distribution between the groyne field and the main channel would get worse. In this case, where the separation zone is higher than the groyne, the flow velocity on which the energy loss is based should be larger. A formula for a submerged sluice gate could improve the 2DH coarse model with sub-grid weirs, because the net flow carrying area (vena contracta) is smaller than the water depth above the sub-grid weir.

The size of the separation zone and the location and magnitude of the local maximum flow velocity in the groyne field depend on the grid resolution and also (if adjustable by the model user) on flux limiters for velocity and turbulence model properties (k, ε). Within the context of Finel, the adaptation of flux limiters for high-resolution model geometries has shown potential to improve the velocity profile along flow separation regions near groynes (even though this may come at the expense of the length of the separation zone in the present case).

How well are groyne adaptations modelled by the numerical models?

The modifications of groynes in the form of streamlining and lowering decrease the energy losses over groynes. They thereby lower the upstream water level or increase the discharge capacity. Both in 3D non-hydrostatic and in 2DH numerical models this effect is clearly visible. The simulation of lowered groynes shows the positive effect on the upstream water levels both in 2DH and in 3D. However the effect of lowering is significantly larger in the 2DH model with sub-grid weirs compared to the 3D non-hydrostatic model.

The 2DH model with the sub-grid weir formulations overestimates the discharge through the groyne fields, leading to a higher depth averaged velocity in the groyne fields than in the 3D model. This implies that even in the calibrated case the discharge distribution between the main channel and groyne field is off. For the upstream water level this has no direct consequence. However, when studying the adaptation of groynes the effect of measures is overestimated. As mentioned above, the 3D model is thought to perform better when the influence of the vertical recirculation zone decreases. With groynes streamlined to 1:5 the recirculation cell is significantly smaller and with 1:10 it is non-existent. Also for lowered groynes the recirculation cell becomes smaller. This gives more confidence in the 3D non-hydrostatic model results as the influence of the leading edge separation is thought to decrease.

7.2. Recommendations

To quantify the effect of groyne lowering or streamlining more accurately, than by using 2DH coarse models that include sub-grid weirs as groynes, 3D non-hydrostatic models with a fine grid should be used. When this is not feasible the 2DH model including the sub-grid energy losses has to be compared with 3D non-hydrostatic simulations for a smaller river reach to quantify the difference. To improve the used weir formula a comparison has to be made between the performance the various available sub-grid weir formulations for a particular set-up of which sufficient data is available. This to compare energy losses, water levels and if possible, the discharge distribution between the main channel and the groyne field.

To obtain data like that a laboratory experiment with adaptable groynes and a realistic cross-section should be carried out.

Because a schematised geometry of both the groynes and river cross-section is used the conclusions are limited to this particular situation. In order to gain more insight in the implications and effects of groyne adaptations and modelling choices in real life the following steps have to be taken:

- Investigate how strong the effect of vertical flow separation is with a more realistic geometry (with less deep groyne fields and rough groynes with milder up- and downstream slopes).
- Determine relative importance of groynes in a realistic cross-section which includes floodplains.
- Compare for this more realistic set-up the performance of 2DH models, with and without sub-grid weirs, with 3D non-hydrostatic simulations.
- Compare the available range of different weir formulas (given in literature as well as by existing model implementations), by implementing them within one single numerical framework (like Delft3D, WAQUA or Finel) in order to make a one-to-one comparison of their results.
- Model the BAW experiment on a real life scale to determine if the sub-grid implementation and groynes that are included in the bed topography behave the same in an up-scaled case.
- Investigate role of flux limiters for separating flows to improve 3D modelling.
- Investigate if in reality the flow separates at the leading edge of a groyne crest, or if streamlines are directed upwards on top of the groyne.

Bibliography

- Albers, L. (2016). Monitoring van de eilandkribben in de IJssel bij Deventer. B.Sc. thesis, University of Twente.
- Ali, S. (2013). *Flow over weir-like obstacles*. PhD dissertation, Technische Universiteit Delft.
- Ali, S. and Uijtewaal, W. S. J. (2013). Flow Resistance of Vegetated Weirlike Obstacles during High Water Stages. *Journal of Hydraulic Engineering*, 139(3):325–330.
- Anlauf, A. and Hentschel, B. (2007). Untersuchungen zur Wirkung verschiedener Bühnenformen auf die Lebensräume in Bühnenfeldern der Elbe. *Wasserstraßen-Verkehrswege und Lebensraum in der Kulturlandschaft*, pages 94–100.
- Azinfar, H. and Kells, J. A. (2009). Flow resistance due to a single spur dike in an open channel. *Journal of Hydraulic research*, 47(6):755–763.
- Baron, M. and Patzwahl, R. (2013). Influence of numerical schemes in representing flow over and around groynes. In *Proceedings of the XXth TELEMAC-MASCARET User Conference*, pages 13–17.
- Bloemberg, G. (2001). Stroomlijnen van zomerkaden. master thesis, Technische Universiteit Delft.
- Bouwmeester, J. (1987). Flexibele waterbouwkundige constructies. *Collegediktaat f4*.
- Busnelli, M. (2002). Numerieke simulatie van de stroming rondom kribben met het CFX-5 model. Technical report, Witteveen+Bos.
- de Goede, E. (2012). Validatie van Villemonte overlaatformulering in WAQUA met praktijkmetingen, 1204153-001-ZWS-0001. Technical report, Deltares.
- Deltares (2014). Delft3D Flow: User manual. Technical report, Deltares.
- Deltares (2018). Programmable electromagnetic liquid velocity meter. Technical report, Deltares.
- Francis, J., Pattanaik, A., and Wearne, S. (1968). Observations of flow patterns around some simplified groyne structures in channels. *Proceedings of the Institution of Civil Engineers*, 41(4):829–837.
- Fritz, H. and Hager, W. (1998). Hydraulics of Embankment Weirs. *Journal of Hydraulic Engineering*, 124:963–971.
- Han, L. (2015). *Recirculation zone developing downstream of an expansion in a shallow open-channel flow*. PhD thesis, INSA de Lyon.
- Heijer, F. d., van Schijndel, S., Sloff, C., Wal, M., van Voorthuizen, J., and Verheij, H. (1997). Effectiviteit van kribben. Q2360.
- Henning, M., Sahrhage, V., and Hentschel, B. (2007). 3D-PTV-Ein System zur optischen Vermessung von Wasserspiegellagen und Fließgeschwindigkeiten in physikalischen Modellen. *Wasserbauliches Versuchswesen*, 1(90):91–100.
- Hentschel, B. (2007). Ein finite-differenzen-verfahren zur strömungsanalyse. *Mitteilungsblatt der Bundesanstalt für Wasserbau*, 1(90):101–106.
- Hüsener, T. (2015). Hydraulisch-morphologische Laboruntersuchungen an Stromregelungsbauwerken. In *Proceedings of the 38. Dresdner Wasserbaukolloquium 2015 „Messen und Überwachen im Wasserbau und am Gewässer“*, pages 79–88.
- Hüsener, T., Faulhaber, P., and Baron, M. (2012). Modifikationen in bestehenden Stromregelungssystemen an Wasserstraßen. In *Proceedings of Wasserbausymposium 2012, 12. - 15. September 2012 Graz, Austria*, pages 395–402.

- Huthoff, F., Barneveld, H., Pinter, N., Remo, J., Eerden, H., and Paarlberg, A. (2013). Optimizing design of river training works using 3-dimensional flow simulations. *Smart Rivers, Paper 31*.
- Jansen, P. P., van Bendegom, L., van de Berg, J., de Vries, M., and Zanen, A. (1979). *Principles of River Engineering: The non-tidal alluvial river*. Pitman, London. Reprint (1984) VSSD, Delft.
- Jongeling, T. (2005). Stroming over een kribsectie: Nadere analyse afvoermetingen Wirken & van Bladel. Q4052, WL|delft hydraulics.
- Jongeling, T., Goede, E. d., and van Kester, J. (2010). Stroomlijnen van kribben in WAQUA, memo 1002047-000-ZWS-0012. Technical report, Deltares.
- Klaassen, G. J., van Groen Pieter, Pilarczyk, K., and Hazendon, N. F. (2006). Prijsvraag Kribben van de Toekomst. Technical report, Rijkswaterstaat.
- Kruijt, M. (2013). Resistance of submerged groynes. master thesis, Technische Universiteit Delft.
- Labeur, R. J. (2009). *Finite element modelling of transport and non-hydrostatic flow in environmental fluid mechanics*. PhD dissertation, Technische Universiteit Delft.
- Labeur, R. J. and Wells, G. N. (2012). Energy stable and momentum conserving hybrid finite element method for the incompressible navier–stokes equations. *SIAM Journal on Scientific Computing*, 34(2):A889–A913.
- Lamballais, E., Silvestrini, J., and Laizet, S. (2010). Direct numerical simulation of flow separation behind a rounded leading edge: Study of curvature effects. *International Journal of Heat and Fluid Flow*, 31(3):295–306.
- Mamak, W. C. E. (1964). *River regulation*. Arkady.
- McCoy, A. W. (2006). *Numerical investigations using LES: exploring flow physics and mass exchange processes near groynes*. PhD dissertation, University of Iowa.
- McCoy, A. W., Constantinescu, G., and Weber, L. J. (2008). Numerical investigation of flow hydrodynamics in a channel with a series of groynes. *Journal of Hydraulic Engineering*, 134(2):157–172.
- Moss, W. (1972). Flow separation at the upstream edge of a square-edged broad-crested weir. *Journal of Fluid Mechanics*, 52(2):307–320.
- Mosselman, E. (2018). Modelling in applied hydraulics: More accurate in decision-making than in science? In Gourbesville, P., Cunge, J., and Caignaert, G., editors, *Advances in Hydroinformatics*, pages 741–749, Singapore. Springer Singapore.
- Mosselman, E. and Struikma, N. (1992). Effecten van Kribverlaging. *WL|Delt Hydraulics*.
- Nieuwstadt, F. T., Westerweel, J., and Boersma, B. J. (2016). *Turbulence: introduction to theory and applications of turbulent flows*. Springer.
- Nikuradse, J. (1933). Strömungsgesetze in rauhen rohren: Forschung auf dem gebiete des ingenieur-wesens. *Fachgebiet Maschinenbau, Ausgabe B*, 4(361).
- Ogink, H. and Driegen, J. (1984). Vormweerstand van kribben. *WL|Delt Hydraulics*.
- Ouillon, S. and Dartus, D. (1997). Three-dimensional computation of flow around groyne. *Journal of hydraulic Engineering*, 123(11):962–970.
- Platzek, F. W. (2017). *Accuracy and efficiency in numerical river modelling: Investigating the large effects of seemingly small numerical choices*. PhD dissertation, Technische Universiteit Delft.
- Przedwojski, B., Błazejewski, R., and Pilarczyk, K. W. (1995). *River training techniques: fundamentals, design and applications*. A.A. Balkema.
- Rajaratnam, N. and Nwachukwu, B. A. (1983). Flow near groin-like structures. *Journal of Hydraulic Engineering*, 109(3):463–480.

- RWS-WVL (2017). Modelbeschrijving Rijntakken 5^e generatie schematisaties. Versie 2017-01, RWS-WVL & Deltares.
- Sieben, A. (2009). Wanden in de Waal, onderzoek naar de invloed van kribkoppen op de lokale bodemligging, *memo*. Technical report, Rijkswaterstaat.
- Sieben, A. (2011). Overzicht en synthese beschikbare data overlaat proeven, *memo110806 Villemonte verbetering*. Technical report, Rijkswaterstaat RIZA.
- Sijmons, D., Feddes, Y., Luiten, E., Feddes, F. M., and Bosch, J. (2017). *Ruimte voor de rivier: Veilig en mooi landschap*. Uitgeverij Blauwdruk.
- Stelling, G. and Duinmeijer, S. (2003). A staggered conservative scheme for every froude number in rapidly varied shallow water flows. *International journal for numerical methods in fluids*, 43(12):1329–1354.
- Stolker, C. (2005). Stroombeelden bij recht aangestroomde kribben. *WL|Delt Hydraulics*.
- Straatsma, M. and Huthoff, F. (2011). Uncertainty in 2d hydrodynamic models from errors in roughness parameterization based on aerial images. *Physics and Chemistry of the Earth, Parts A/B/C*, 36(7-8):324–334.
- Sukhodolov, A. N. (2014). Hydrodynamics of groyne fields in a straight river reach: insight from field experiments. *Journal of Hydraulic Research*, 52(1):105–120.
- Talstra, H. (2011). *Large-scale turbulence structures in shallow separating flows*. PhD dissertation, Technische Universiteit Delft.
- Uijttewaal, W. and Booij, R. (2000). Effects of shallowness on the development of free-surface mixing layers. *Physics of Fluids*, 12(2):392–402.
- Uijttewaal, W., Lehmann, D., and van Mazijk, A. (2001). Exchange processes between a river and its groyne fields: Model experiments. *Journal of Hydraulic Engineering*, 127(11):928–936.
- Uijttewaal, W. S. J. (2005). Effects of groyne layout on the flow in groyne fields: Laboratory experiments. *Journal of Hydraulic Engineering*, 131(9):782–791.
- Uijttewaal, W. S. J. (2007). Inundated flood plains and the flow over groynes and oblique weirs. *Publs. Geophys. Pol. Acad. Sc., E-7 (401)*, pages 245–254.
- Uijttewaal, W. S. J. and Tukker, J. (1998). Development of quasi two-dimensional structures in a shallow free-surface mixing layer. *Experiments in Fluids*, 24(3):192–200.
- van Banning, G. (2002). Evaluatie stromingsmodellering rondom kribben. Technical report, Alkyon.
- van Broekhoven, R. W. (2007). Het effect van kribverlaging op de afvoercapaciteit van de Waal ten tijde van hoogwater. master thesis, Technischer Universiteit Delft.
- van der Wal, M. (2004). Innovatieve Kribben met Palenrijen Hoofdrapport. Rapport dww-2004-055, RWS DWW.
- van der Wal, M., Akkerman, G., and Stam, J. (2006). Multifunctional river groynes: Providing nautical depth and mitigation of flood levels. In Jan Alphen, J., van Beek, E., and Taal, M., editors, *Advances in Hydroinformatics*, pages 378–384. CRC Press.
- van Leeuwen, K. (2006). Modelling of submerged groynes in 1D hydraulic computations. master thesis, University of Twente.
- van Prooijen, B. C. (2004). *Shallow Mixing Layers*. PhD dissertation, Technische Universiteit Delft.
- Villemonte, J. R. (1947). Submerged weir discharge studies. *Engineering News-Record*, 139(26):54–56.
- Warmink, J., Straatsma, M., and Huthoff, F. (2013). The effect of hydraulic roughness on design water levels in river models. *Comprehensive Flood Risk Management; Klijn, Schweckendiek, Eds.*

- Warmink, J. J., Booij, M. J., Hulscher, S., and van der Klis, H. (2010). Uncertainty in design water levels due to uncertain bed form roughness in the river rhine. In *River Flow 2010: Proceedings of the international Conference on Fluvial Hydraulics*, pages 359–366.
- Wirken, H. and Bladel, S. (2004). Innovatieve kribben: modelonderzoek naar het effect van de hydraulische ruwheid op kribben. afstudeerverslag, Avans Hogeschool Tilburg.
- Wols, B. (2005). Undular hydraulic jumps. master thesis, Technische Universiteit Delft.
- Yan Toe, C. (2018). Issues in Numerical Modelling and Assessing the Flow over Weirs and Groynes. master thesis, Technische Universiteit Delft.
- Yossef, M. F. M. (2002). The effect of groynes on rivers: Literature review. *Delft Cluster*.
- Yossef, M. F. M. (2004). The effect of the submergence level on the resistance of groynes—An experimental investigation. In *Proc., 6th Int. Conf. on Hydroscience and Engineering, Brisbane, Australia*.
- Yossef, M. F. M. (2005). *Morphodynamics of Rivers with Groynes*. PhD dissertation, Technische Universiteit Delft.
- Yossef, M. F. M. (2016). Groynes, an overview of two decades of research. *Deltares*.
- Yossef, M. F. M. (2017). Hydraulic modelling of standard and streamlined groynes, *11201089-000-ZWS-0009*. Technical report, Deltares.
- Yossef, M. F. M. and Visser, T. (2018). Effect of Groyne schematisation on WAQUA model results, *11202188-008-ZWS-0001*. Technical report, Deltares.
- Yossef, M. F. M. and Zagonjoli, M. (2010). Modelling the hydraulic effect of lowering the groynes on design flood level. Research project 1002524-00, Deltares.
- Zagonjoli, M. (2017). Sensitivity analysis on the groyne modelling in WAQUA, *1230071-003-ZWS-0035*. Technical report, Deltares.
- Zagonjoli, M., Platzek, F., and van Kester, J. (2017). Modelling the flow over a groyne and weir in WAQUA, *11200536-008-ZWS-0005*. Technical report, Deltares.



Theoretical roughness

In the V00 case without groynes a uniform flow is assumed. This means that in 2D the Q-h relation can be determined based on the roughness only. This is done by assuming a representative grain size. In the experiments gravel with a diameter between 4 and 8 mm was used. For the 1D analytic calculations and the 2DH numerical modelling representative grain size k_r of 7 mm is used as this gives a very good fit with the measured Q-h relation.

Analytical computation of the bed roughness

The width of the flume is 2.5 m and the slope is $6 \cdot 10^{-4}$ m/m. The situation of smooth side walls and rough walls are compared. Smooth walls mean that the hydraulic radius (R) equals the water depth while with rough side walls R is the wet cross-section (A) divided by the wet perimeter (P). It can be seen that the assumption of smooth side walls does not match the measured Q-h relation. While assuming rough walls gives a good match, especially for the higher water depths ($h > 100$ mm). First it is assumed that the water level slope i_w

Table A.1: Measured depths and their respective discharges in variants V00 and V01 (Hüsener et al., 2012)

Water depth [mm]	40	50	60	70	80	85	100	120	160	200
Discharge V00 [l/s]	17.7	25	33	42	52	57.5	74.5	100	157.8	222

equals the bed level slope i_b . The Chézy coefficient is calculated based on the work of Nikuradse (1933).

$$z_0 = k_r/30 \quad (\text{A.1})$$

With z_0 the Chézy coefficient is calculated.

$$C_{2D} = \frac{\sqrt{g}}{\kappa} \cdot \ln\left(1 + \frac{R}{e \cdot z_0}\right) \quad (\text{A.2})$$

In which κ is the Von Kármán constant with a value of 0.4 and g is the 9.81 m/s².

The resulting Chézy value can be used to calculate the depth averaged flow velocity U .

$$U = C_{2D} \cdot \sqrt{R \cdot i_b} \quad (\text{A.3})$$

Together with the water depth and width of the flume the discharge is calculated.

$$Q = U \cdot B \cdot h \quad (\text{A.4})$$

For the 2DH Delft3D simulation from the z_0 value a value for the Nikuradse roughness height (k_s) is calculated by using the following equation Deltares (2014).

$$k_s = \frac{12 \cdot R}{10^{C_{2D}/18}} \quad (\text{A.5})$$

This gives $k_s = 7.5$ mm.

In the Figure A.1 the calculated roughness and the roughness derived from the data are shown. The resulting Q-h relation is shown in Figure A.2. It is noted that the hydraulic radius should be used instead of the water depth to calculate the roughness.

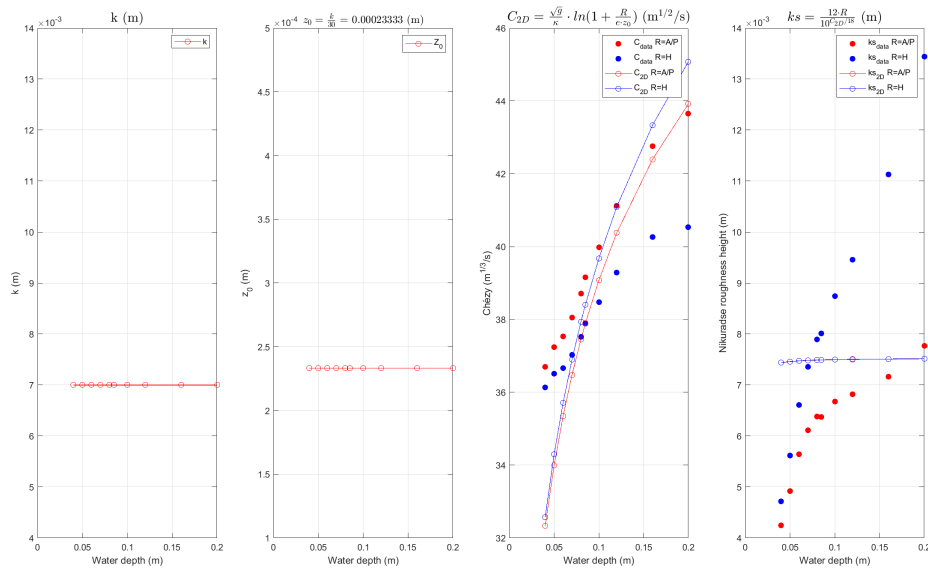


Figure A.1: Calculated and derived roughness with $R = A/P$ and $R = H$

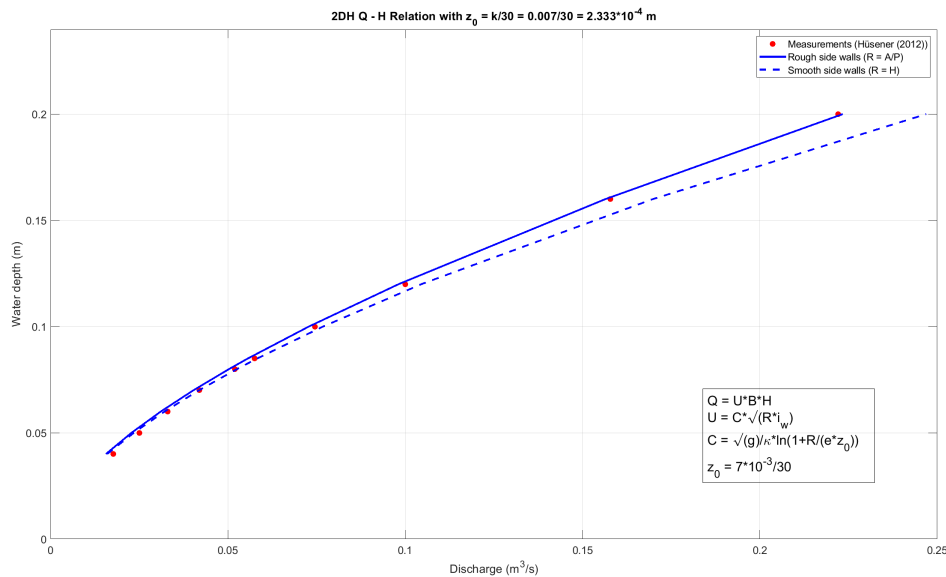


Figure A.2: Measured Q-h relation (red dots) and theoretical Q-h relation

It should be noted that in 3D in Delft3D the Chézy value depends on the layer thickness of the layer closest to the bed (Δz_b). This means that the Chézy value is calculated to determine the velocity in the lowest layer by Equation A.6.

$$C_{3D} = \frac{\sqrt{g}}{\kappa} \cdot \ln\left(1 + \frac{\Delta z_b}{2z_0}\right) \quad (\text{A.6})$$

The velocity in the layers on top of that are subsequently calculated based on the vertical viscosity that is

calculated with the turbulence closure model. This gives that for 3D simulation a slightly different roughness value is needed. It is found that a z_0 value of $3.3333 \cdot 10^{-4}$ m is needed to get the correct Q-h relation.

B

Discharge coefficient analysis

By looking at the lateral differences in discharge that flow over the groynes it can be seen that the region where the separation zone length is constant also a constant specific discharge flows over the groynes. By relating the energy head upstream and downstream of the groyne and the discharge a 1D analysis of the groyne can be made as is often done for weirs. From this analysis it is visible that the in the 2DH coarse-grid model with sub-grid weirs results in a higher discharge coefficient than the 3D non-hydrostatic model. With both models it is visible that from the side wall multiple cells lie on the same point and that near the tip the discharge coefficient increases, see Figure B.1.

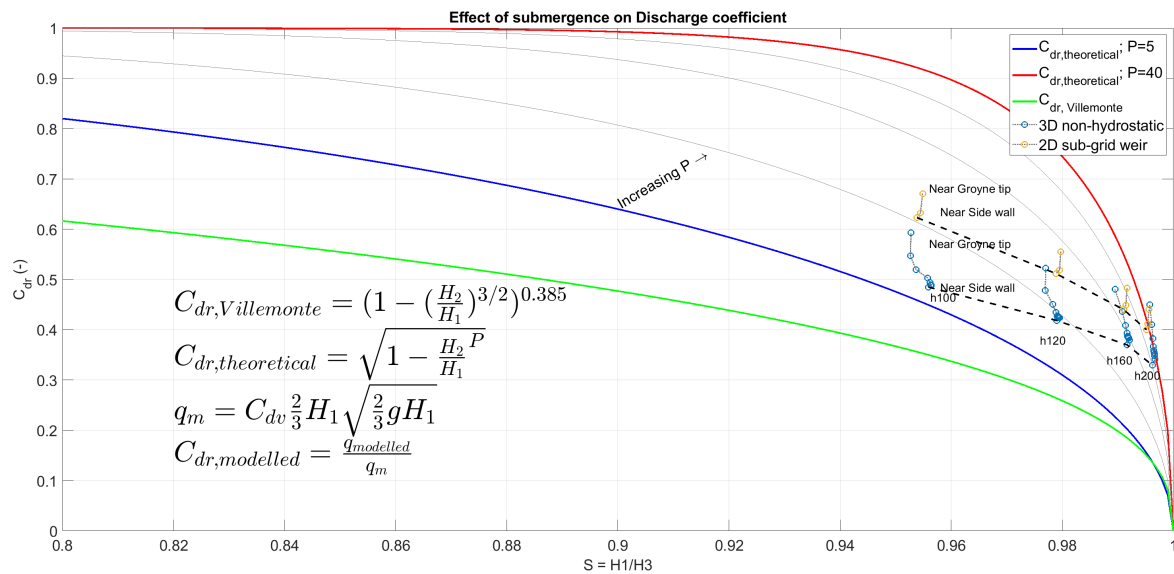


Figure B.1: Effect of submergence on discharge coefficient. Discharge coefficient analysis for the 2DH coarse model and 3D non-hydrostatic model. The discharge over the groynes in the coarse model including sub-grid weirs is larger than the discharge calculated by the 3D model.